



Master's Degree in Environmental Engineering

**Hydrodynamic modeling of the final reach of the
Misa River (Senigallia, Italy): model setup and
calibration**

Advisor:

Prof. Matteo Postacchini

Student:

Jacopo Martinelli

Co-advisor:

Prof. Giovanna Darvini

A.Y. 2020/2021

CONTENTS

ABSTRACT.....	1
1 INTRODUCTION	2
2 DESCRIPTION OF THE AREA.....	3
3 MATERIALS AND METHODS	7
3.1 HEC-RAS description	7
3.1.1 Steady flow analysis.....	7
3.1.2 Unsteady Flow Analysis	14
3.1.3 Program interface	15
3.1.4 Steady simulation.....	25
3.1.5 Unsteady simulation.....	28
3.1.6 Unsteady simulation results	34
3.2 Data used for the model construction.....	38
3.2.1 Data from Civil Protection of the Marche Region.....	38
3.2.2 Data from surveys.....	43
3.2.3 Hydrodynamic data.....	46
4 MODEL CONSTRUCTION	53
4.1 Cross-section removal	54
4.2 Bettolle bridge positioning.....	55
4.3 Bettolle and Ponte Garibaldi 2019 cross-section implementation.....	59
4.4 Boundary conditions	61
4.5 Ponte Garibaldi runoff estimation	63
4.6 Senigallia wastewater treatment plant discharge analysis	67
4.7 Digital terrain models implementation	69
4.8 Walls implementation.....	80
4.9 DTM Bettolle cross-section – Civil Protection 2019 Bettolle cross-section comparison.....	81
4.10 Bridges implementation.....	84
4.11 Bathymetry implementation	85
5 MODEL CALIBRATION	88
5.1 Roughness selection.....	90
5.2 Other calibration parameters.....	92
6 DISCUSSION.....	94
6.1 Aggregated data comparison at Ponte Garibaldi	108
7 CONCLUSIONS	110

8 REFERENCES 112

9 ACKNOWLEDGEMENTS..... 114

ABSTRACT

This thesis is devoted to the implementation and the subsequent calibration of a hydraulic model concerning the last stretch of the Misa River through the use of the HEC-RAS software. Firstly, by means of cross-section data coming from the Civil Protection of the Marche Region survey made in 2001, a preliminary steady simulation aimed at verifying the correctness of the model has been performed. In order to increase the reliability of the model, updated cross-sections relative to Bellolelle and Ponte Garibaldi derived from the Civil Protection 2019 survey, along with flow data retrieved by the use of Bettollelle rating curves and the tidal data, have been used to carry out different unsteady simulations for selected time periods. Afterwards, through the use of digital terrain models coming from the Ministero dell'Ambiente e della Tutela del Territorio e del Mare Lidar surveys, a bi-dimensional model of the Misa River has been constructed, being the data belonging to the DTMs more recent and more detailed if compared to those coming from the Civil Protection 2001 survey. The model calibration has been carried out by acting on different parameters, among which the Manning coefficients, the contraction/expansion coefficients in correspondence of bridges and the setting of both the levees and the main channel banks. Finally, the results of simulated events relevant to different years coming from the calibrated model, have been compared with the data measured by the Civil Protection instrumentation for both the Bettollelle and Ponte Garibaldi cross-sections.

1 INTRODUCTION

The aim of this work lies on the construction and the calibration of a hydraulic model of the Misa River, which is a river that flows through the Marche Region and that ends in Senigallia municipality. The implementation of a river hydraulic model results to be very important for both a scientific and a practical point of view, since it can be used as starting point for further analysis relative to the river. As an example, this model has been used to study the effects deriving from the presence of river bars, which occasionally arise at the Misa River mouth. The construction of a hydraulic model requires different data, such as cross-sections coming from field surveys, river discharges, tidal ranges, bathymetric surveys etc. The accuracy of these data is fundamental to obtain precise outputs from the software, thus the most updated information must always be considered. This thesis is developed by using the HEC-RAS software, which is the most used open-source software dedicated to the modeling of mono and bi-dimensional natural and anthropic channel networks. It allows to conduct different types of analysis, such as steady simulations, unsteady simulations (thus with a change of flowrate over time), sediment transport and water quality analysis. The present work focuses in particular on simulations which are carried out with the aim at calibrating the previously constructed river model. The calibration procedure is a very important phase in the realization of a hydraulic model, since a well calibrated model allows to get reliable forecast of even future events, which may be decisive in avoiding possible catastrophic phenomena (e.g. floods).

2 DESCRIPTION OF THE AREA

The Misa River flow path, which owns a length of 45 kilometers, is entirely comprised in the province of Ancona and its catchment has an extension of approximately 383 km² with discharges of about 400, 450, and 600 m³s⁻¹ for return periods of 100, 200, and 500 years, respectively (Brocchini et al., 2017).

The Misa River flows into an estuary which is a partially enclosed coastal body of brackish water with one or more rivers or streams flowing into it, and with a free connection to the open sea (Pritchard, D. W., 1967). Estuaries characterize a transition zone between the river environments and maritime environments and are subject both to marine influences such as tides, waves and salt water intrusion and to riverine influences such as flows of freshwater and sediment. The mixing of seawater and freshwater provides high levels of nutrients both in the water column and in sediment, making estuaries among the most productive natural habitats in the world (McLusky, D. S., Elliott, M., 2004). Estuaries are typically classified according to their geomorphological features or to water-circulation patterns. Following the water-circulation classification, the Misa River estuary is characteristic of a salt-wedge estuary (Kennish, 1986), in which the river forcing dominates over both marine actions in winter (in particular during storms) and tidal influence. Another definition of an estuary is given by the place where the tide overlaps with the current of a stream, and, following this definition, the Misa River estuary is classified as microtidal, with tidal excursion not larger than 50 cm (Postacchini et. al., 2020).

The Misa River is bounded by the Cesano river watershed north-westward, by the Esino river watershed south-eastward and by the Sentino stream (an Esino river tributary) sub-basin southward.



Figure 1. Misa River location.

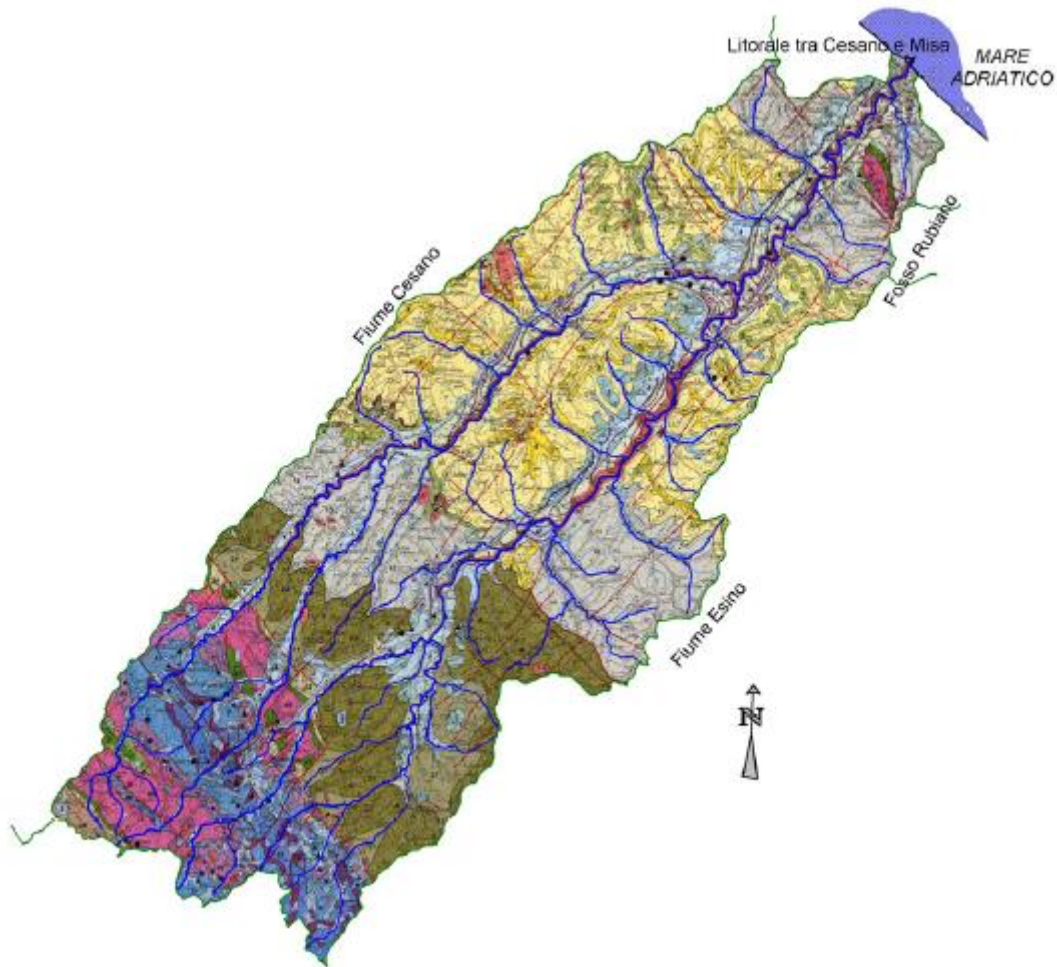


Figure 2. Misa River catchment.

The Misa River watershed is enclosed between the following municipalities: Arcevia, Barbara, Belvedere Ostrense, Castelleone di Suasa, Corinaldo, Genga, Mergo, Montecarotto, Ostra, Ostra Vetere, Poggio San Marcello, Rosora, Sassoferrato, Senigallia, Serra dei Conti, Serra San Quirico, Trecastelli (Castelcolonna and Ripe).

The Misa River, which is of Apennine origin, is born on the south-west slopes of the Arcevia's anticlinal, more precisely in Colle Ameno (793 m.a.s.l.) close to San Donnino village in Genga municipality. After travelling through Genga, Arcevia, Serra De'Conti, Ostra Vetere, Ostra and lastly Senigallia in SW-NE direction, where the river flows into the Adriatic Sea within an estuary bounded by two reinforced concrete jetties, which stick out on the shoreline longitudinal profile for about 250 – 300 m.

The main Misa River left tributary is the Nevola River, which, in turn, generates from the confluence between the Fenella stream and the Acquaviva one, and joins the Misa River at about 9 km before its end, thus ensuring a remarkable increase of both solid and liquid flows. The Nevola River, along with the Acquaviva stream, point in the same direction as the Misa River (SW-NE).

The Misa River, as the vast majority of the Marche Region rivers, is characterized by a torrential regime, i.e. with poor or null flows during dry periods and very high flows (in the order of magnitude of hundreds of cubic meters of water per second) during rainy periods depending on the geological, geomorphological, lithological and climatic characteristics of the watershed. Specifically, the Misa River basin is composed of around 85% of clayey rocks, thus owning a low permeability degree, whereas, for what concerns the most inner area, is made up of calcareous rocks having a secondary permeability deriving from the rocks fracturing. This lithology leads to a fairly high runoff coefficient, from which the poor subsoil infiltration derives from and that allows for very fast meteoric water discharges along the slopes and relatively short times of concentration.

The natural Misa River, at times, is characterized by a meander-like shape flow path and it is strongly influenced by a remarkable number of anthropic structures, in particular by several roads which cross the river channel transversally. Moreover, the Misa River is also crossed by numerous transversal and longitudinal river bank protections. For what concerns the former, they include 23 bridges and 2 traverses, the vast majority of whom are located upstream of Pianello di Ostra, thus implying a strong vertical erosion. As regards the latter, they consist of 2,337 m of protecting walls (including stone gabions, concrete cubes, concrete slabs, reinforced concrete Jersey barriers), 318 m of bank strengthening using soft approaching (bioengineering) and 403 m of cliffs (gigantic calcareous boulders, concrete hexapods and tetrapod).

The Misa River hydrographic basin is significantly asymmetric, and the left tributaries, which are more developed than the right ones, predominantly participate to the river discharge.

The geomorphology of the watershed is characterized by narrow and deep valleys in the upstream sections of the river and by an enlargement of the latter moving downstream where there is also the presence of alluvial terraces. Also in this case, the alluvial terraces are greatly developed on the hydrographic left than on the hydrographic right.

The Misa River features a river bed which flows within its own terraces that are characterized by different width and order. From a geological-sedimentological point of view, the alluvial terraces in the middle section of the catchment are made of gravel and calcareous boulders intertwined with gravelly-sandy lenses. On the other side, for what regards the alluvial deposits, they are characterized by an increased clayey fraction.

3 MATERIALS AND METHODS

3.1 HEC-RAS description

HEC-RAS is an open-source software developed by the US Army Corps of Engineers in 1995 at the Hydrologic Engineering Centre (HEC) in Davis, California, and it is one of the most famous software for the modeling of mono and bi-dimensional natural and anthropic channel networks (River Analysis System, RAS). The software allows to carry out:

- simulations in steady flow conditions, by considering either sub-critical and/or super-critical and/or mixed regimes. This tool is used to analyze mild slope flows in both single channels and channel networks;
- simulations in unsteady flow conditions;
- simulations devoted to the quantification and classification of solid transport hydrodynamic processes linked to either erosion and/or deposition phenomena;
- water quality simulations, i.e. water temperature analysis and transported material such as dissolved oxygen and organic materials.

The employed software version has been the 5.0.7 which allows to make bi-dimensional hydraulic simulations in unsteady flow environments.

The HEC-RAS 6.0.3 (last version) has been used at the beginning, but then has been deemed necessary to switch back to the previous one due to problems regarding the interpolation phase of some layers. Probably, these errors may be addressed to the fact that the last version was still a beta one, and perhaps some bugs inherent to the interpolation phases had not yet been fixed.

3.1.1 Steady flow analysis

In performing steady flow analysis, the software returns water profiles relative to steady or quasi-steady conditions. These profiles are elaborated by the software moving from one cross-section to the next one (Figure 3) by applying the law of conservation of energy by means of an iterative process referred to as “standard step method”. The following equation represents the law of conservation of energy applied by the software for two consecutive sections (1 and 2):

$$Z_2 + Y_2 + \frac{a_2 V_2^2}{2g} = Z_1 + Y_1 + \frac{a_1 V_1^2}{2g} + h_e$$

where:

Z_1, Z_2 = thalweg of the two cross-sections;

Y_1, Y_2 = water depth (stage) at the two cross-sections;

V_1, V_2 = average velocity of the two cross-sections (total discharge / total flow area);

α_1, α_2 = velocity weighting coefficients of the two cross-sections;

g = gravitational acceleration;

h_e = energy head loss.

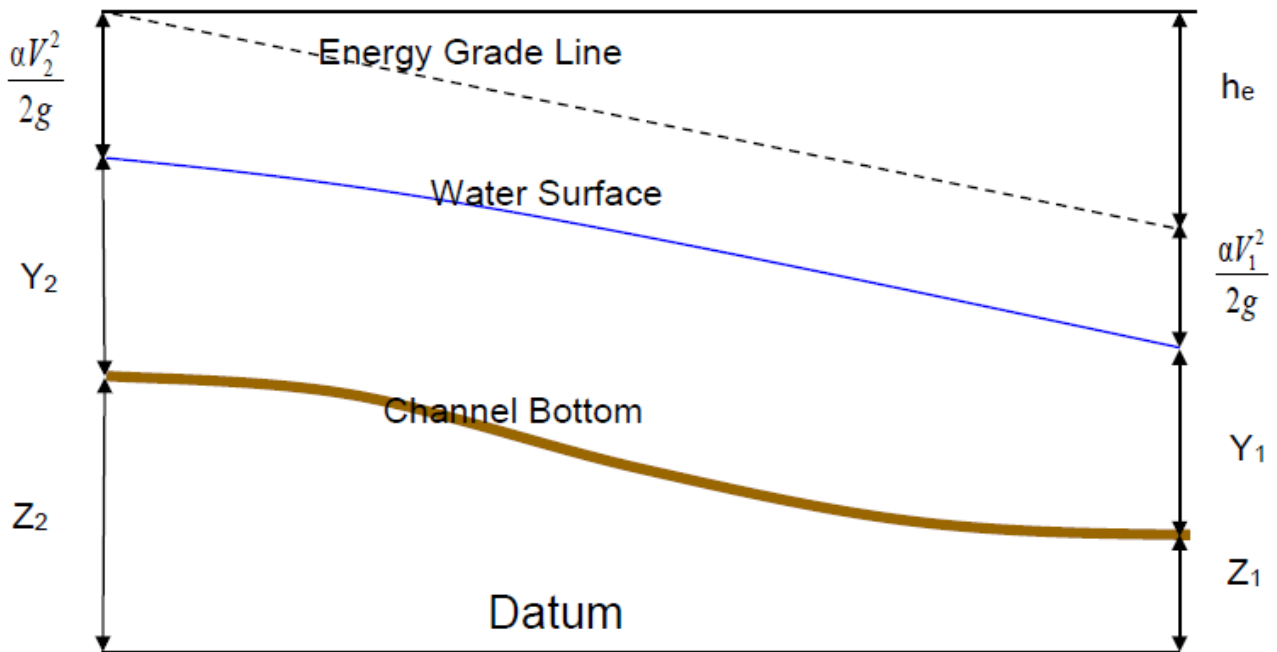


Figure 3. Representation of terms in the energy equation.

The head loss (h_e) between the two cross-sections accounts for both the friction losses (due to roughness) and contractions/expansions losses and it is evaluated by means of the following equation:

$$h_e = L\bar{S}_f + C \left| \frac{\alpha_2 V_2^2}{2g} - \frac{\alpha_1 V_1^2}{2g} \right|$$

where:

\bar{S}_f = representative friction slope (slope of the energy grade line) between the two cross-sections;

C = expansion or contraction loss coefficient;

L = average length of the reach between the two cross-sections weighted with respect to the discharge distribution in the cross-sections, which is evaluated as:

$$L = \frac{L_{lob} \bar{Q}_{lob} + L_{ch} \bar{Q}_{ch} + L_{rob} \bar{Q}_{rob}}{\bar{Q}_{lob} + \bar{Q}_{ch} + \bar{Q}_{rob}}$$

considering that:

L_{lob}, L_{ch}, L_{rob} = cross-sections reach lengths specified for flow in the left overbank, main channel, and right overbank, respectively:

$\bar{Q}_{lob} + \bar{Q}_{ch} + \bar{Q}_{rob}$ = arithmetic average of the flows between sections for the left overbank, main channel, and right overbank, respectively.

Since the cross-sections can be made of different parts, each of them having different roughness coefficients (Manning “ n ”), the total conveyance (flow per unit of head loss per unit of length) must be determined in order to find out the slope of the energy grade line (S_f). This is done within each subdivision through the use of the Manning equation:

$$Q = KS_f^{1/2}$$

$$K = \frac{1.486}{n} AR^{2/3}$$

where:

K = conveyance for subdivision;

n = Manning coefficient for subdivision;

A = flow area for subdivision;

R = hydraulic radius for subdivision (A/P , with P = wet perimeter);

S_f = slope of the energy grade line.

The incremental conveyances are summed up by the software in order to get two final values of the conveyance, K_{lob} , K_{rob} , which stand for left overbank and right overbank, respectively, whereas the main channel conveyance K_{ch} is computed as a single conveyance element (Figure 4).

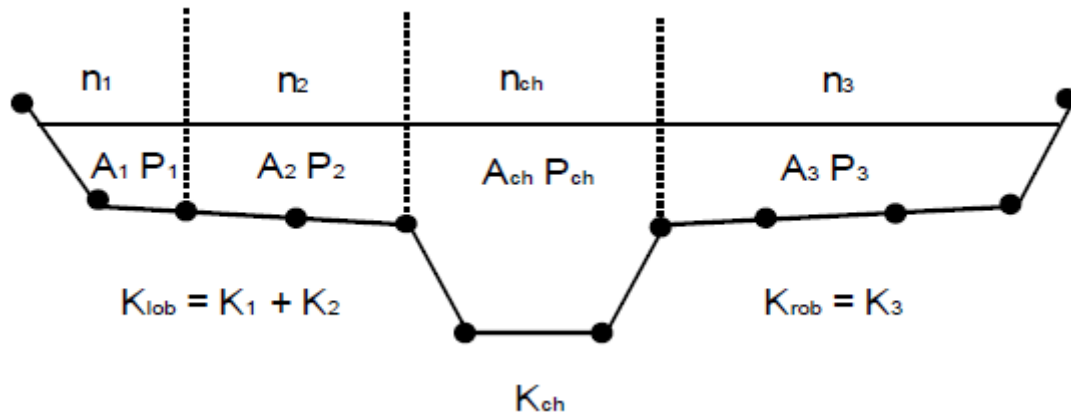


Figure 4. Default conveyance subdivision method.

The total conveyance for the whole section is obtained by summing up all the three subdivision conveyances (K_{lob} , K_{rob} , and K_{ch}).

The just mentioned method is the default one in HEC-RAS for calculating the conveyances throughout the cross-sections, but an alternative procedure is also available. In this case, the conveyance is evaluated between every point in the overbanks (and no more in within subdivision) (Figure 5).

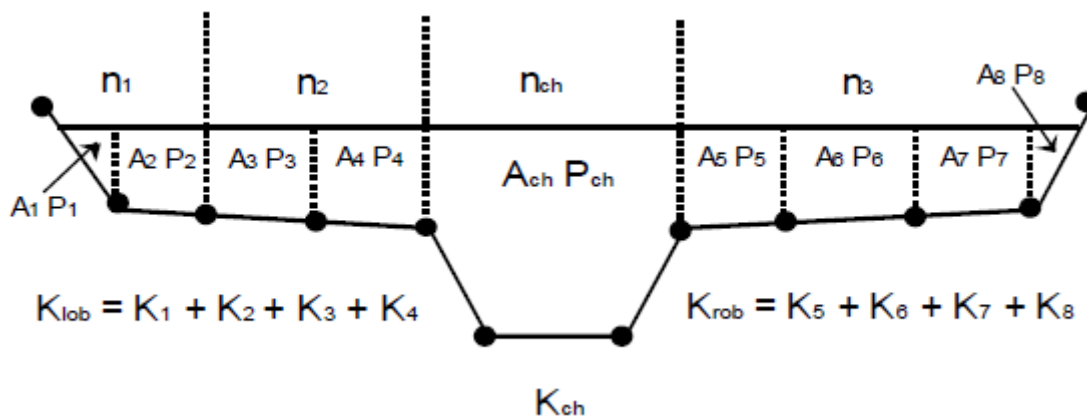


Figure 5. Alternative conveyance subdivision method.

Then, the conveyances are summed up in order to get the total left overbank and right overbank values.

The two methods for computing the conveyance release different results whenever portions on the overbank have ground sections with significant vertical slopes. It is important to know that, in general,

the default approach provides a lower value for the total conveyance considering the same water surface elevation.

Nonetheless, the HEC-RAS default method is more consistent with the Manning equation and the concept of separate flow elements.

The velocity weighting coefficient (α), is evaluated with respect to the conveyances of the left, right and main channel overbanks:

$$\alpha = \frac{(A_t)^2 \left[\frac{K_{lob}^3}{A_{lob}^2} + \frac{K_{ch}^3}{A_{ch}^2} + \frac{K_{rob}^3}{A_{rob}^2} \right]}{K_t^3}$$

where:

A_t = total flow area of cross section;

A_{lob} , A_{ch} , A_{rob} = flow areas of left overbank, main channel overbank and right overbank, respectively;

K_t = total conveyance of the cross-section;

K_{lob} , K_{ch} , K_{rob} = conveyances of left overbank, main channel overbank and right overbank, respectively.

In order to calculate the friction loss, that is part of the total head loss which is needed to solve the law of conservation of energy equation, HEC-RAS performs a product between the slope of the energy grade line (S_f) and the average length of the reach between the two cross-sections weighted with respect to the discharge distribution in the cross-sections (L). Since the value of L has been determined previously, the remaining term (S_f) is computed at each cross-section by exploiting the Manning equation:

$$S_f = \left(\frac{Q}{K} \right)^2$$

In HEC-RAS, four different alternatives are proposed for the estimation of the reach friction slope:

- Average Conveyance Equation

$$\bar{S}_f = \left(\frac{Q_1 + Q_2}{K_1 + K_2} \right)^2$$

- Average Friction Slope Equation

$$\bar{S}_f = \frac{S_{f1} + S_{f2}}{2}$$

- Geometric Mean Friction Slope Equation

$$\bar{S}_f = \sqrt{S_{f1} \times S_{f2}}$$

- Harmonic Mean Friction Slope Equation

$$\bar{S}_f = \frac{2(S_{f1} \times S_{f2})}{S_{f1} + S_{f2}}$$

where the subscripts 1 and 2 refer to the two subareas the river cross-section is divided into. The Average Conveyance Equation is that used by the software as default, unless differently specified.

The last parameter needed for the evaluation of the head loss (h_e) is the contraction/expansion coefficient, which stands for the contraction or expansion to which the flow is subjected due to changes in the cross-section, since the latter provoke an additional energy loss within the reach. In order to take into account this energy loss, the contraction/expansion values must be added to each cross-section. Considering a sub-critical flow regime, if the change in the cross-section is mild, values of 0.1 and 0.3 for the contraction/expansion coefficients, respectively, should be considered. In the case of a sudden change of the cross-section (typical bridge sections), higher values of the contraction/expansion coefficients should be assumed, in particular 0.3 for the contraction and 0.5 for the expansion. In the presence of abrupt transitions, these values should be even higher, such as 0.6 for the contraction and 0.8 for the expansion. The value of these coefficients cannot be greater than 1, and, on the other way round, if there is the presence of identic cross-section or anytime this further energy loss does not want to be taken into consideration, both coefficients can be set to 0.

In the case of super-critical flows, lower values of contraction/expansion coefficient should be adopted, because, since the dynamic head ($\alpha V^2/2g$) varies exponentially, to small stages variations correspond high variations of the total head, with the consequent overestimation of the head losses. For this reason, considering super-critical flows with a mild cross-section variation, suitable contraction/expansion coefficient values are 0.01 and 0.03, respectively. In the case of sudden geometry variation, typically, vales of 0.05 for the contraction coefficient and 0.2 for the expansion coefficient are usually recommended.

The software considers the presence of a contraction whenever the downstream flow velocity is higher than the upstream one. On the contrary, if the upstream velocity is greater than the downstream one, the program considers the presence of an expansion.

In order to run the simulation, the boundary conditions must be added following these indications: downstream for sub-critical flow, upstream for super-critical flow and both upstream and downstream for mixed regime. It is possible to select between different types of boundary conditions, such as water surface elevation, critical depth, normal depth and rating curves.

The HEC-RAS computation procedure to evaluate the unknown water surface elevation is based on the following iterative procedure:

1. Assumption of a water surface elevation at the first cross-section (the most upstream one) or, in case of supercritical flows, in the downstream cross-section;
2. In relation to the water surface elevation assumed in the previous point, determination of the corresponding total conveyance and velocity head;
3. With the values found in the step 2, calculation of the friction loss \overline{S}_f and development of the head loss equation h_e ;
4. Once the values of the point 2 and 3 are known, these are used to find out a new value of the water surface elevation by using the law of conservation of energy equation;
5. The two values of the water surface elevations (the assumed and the calculated ones) are compared and if the difference between them is less than 0.003 m, the iterative procedure ends up, on the other hand, if the difference is higher than 0.003 m, the iterative procedure continues until the latter value is satisfied.

It is important to highlight that, in those cases where the water surface elevation passes through the critical state, the application of the law of conservation of energy is no longer applicable, since it can be applied only for sub-critical flow regimes. Some examples where the law of conservation of energy cannot be applied are the following: significant variation in the channel bed slope, hydraulic jumps, overflows, presence of bridge piles and junctions.

To get over these issues, it is necessary to consider the momentum equation, and a way to account for it is by the implementation of an unsteady flow analysis.

3.1.2 Unsteady Flow Analysis

In order to carry out an unsteady flow analysis, both the principle of conservation of mass (continuity equation) and the principle of conservation of momentum (momentum equation) must be considered. The former states that for a control volume the net rate of flow into the volume must be equal to the rate of change of storage inside the volume, whereas, the latter, states that for a control volume the net rate of momentum entering the volume (momentum flux) plus the sum of all external forces acting on the volume must be equal to the rate of accumulation of momentum:

Continuity equation:

$$\frac{\partial A_T}{\partial t} + \frac{\partial Q}{\partial x} - q_l = 0$$

Momentum equation:

$$\frac{\partial Q}{\partial t} + \frac{\partial QV}{\partial x} + gA \left(\frac{\partial z}{\partial x} + S_f \right) = 0$$

where:

Q = channel flow;

A_T = total flow area (it is the sum of the active area and the off-channel storage area);

q_l = lateral inflow per unit length;

A = cross-sectional area;

g = gravitational acceleration;

S_f = friction slope;

V = average flow velocity;

$\frac{\partial z}{\partial x}$ = water surface slope.

The two equations are simultaneously solved by the program by applying the finite difference method, which allows the equations to be rewritten as finite differences, so that avoiding the consideration of the partial derivatives. In this way, it is possible to pass from a differential equation system with partial derivatives to an algebraic equation system.

3.1.3 Program interface

The HEC-RAS main window (Figure 6) is structured in three sections, where at the top there is the menu bar, while moving downward there are the button bar and the part devoted to the project information.

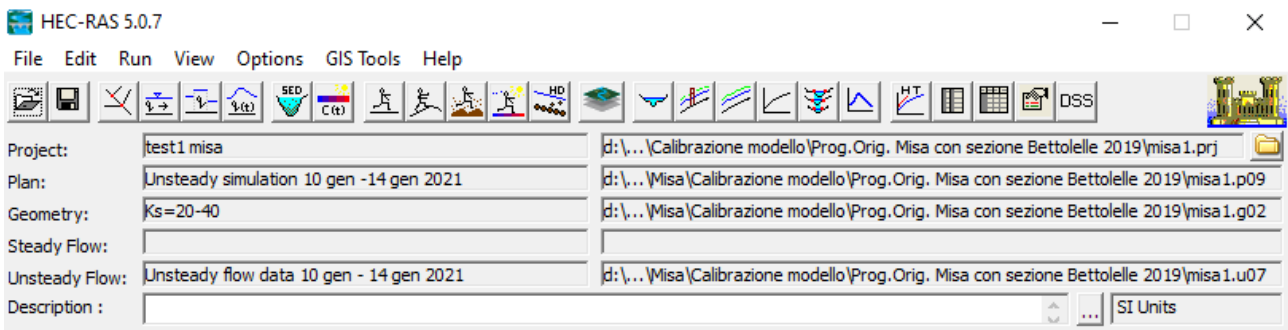


Figure 6. HEC-RAS main window.

The menu bar, is essentially composed of the following options:

- File: option used for file management;
- Edit: option used for entering and editing data;
- Run: option used to perform hydraulic calculations;
- View: option containing a set of tools used to display the model output by means of graphs and tables;
- Options: menu item used to change program setup options;
- GIS tools: option used to enter the HEC-RAS Mapper tool, which allows the creation of terrain models with the subsequent visualization of inundations mapping and flood animations;
- Help: option used to get on-line help.

For what regards the main window button bar, all the functions are illustrated in Figure 7:

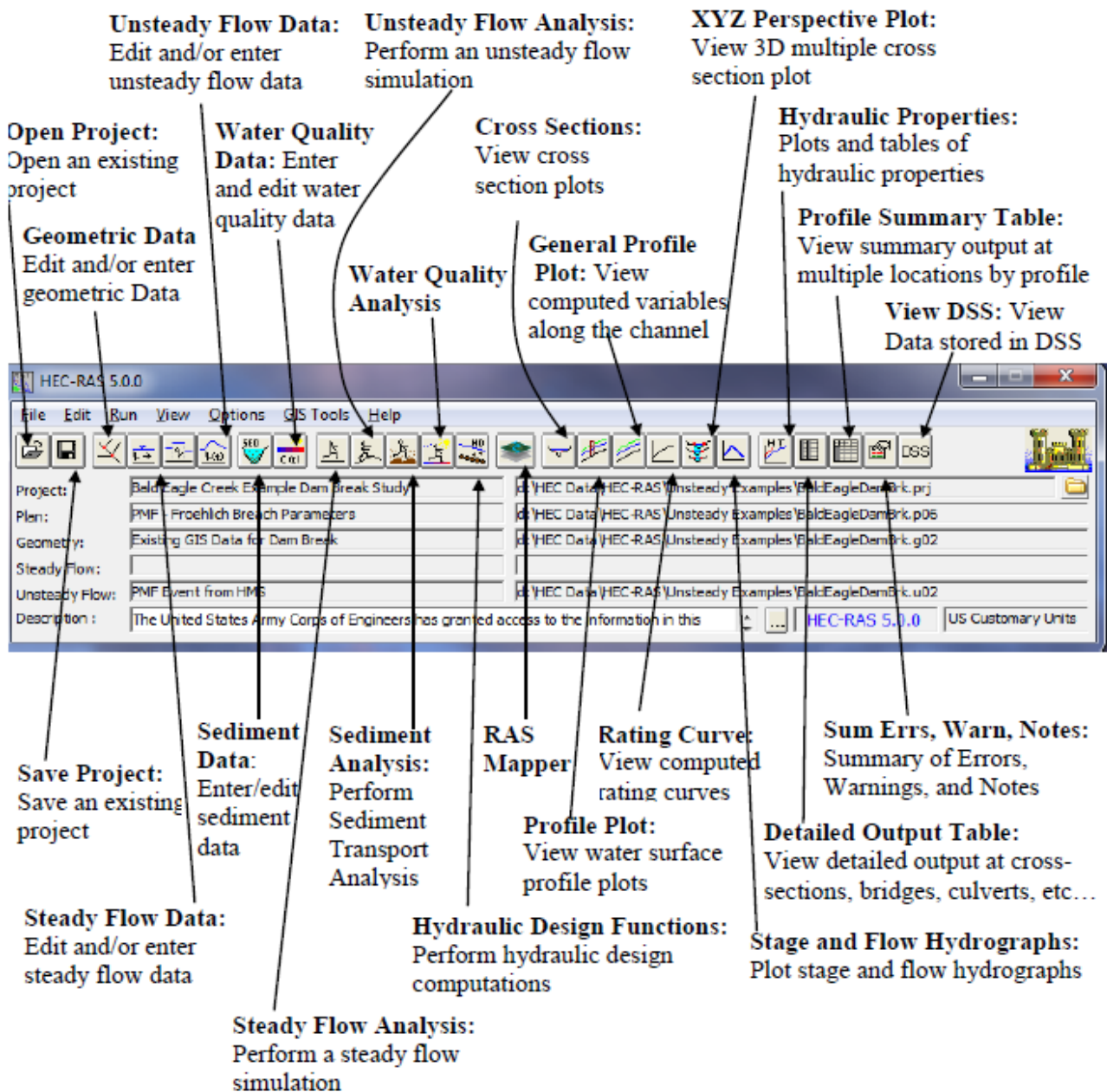


Figure 7. HEC-RAS main window button bar.

When either a new project or an existing one is opened, it is possible to enter the “Geometric Data” button to have an overview of the river path (Figure 8).

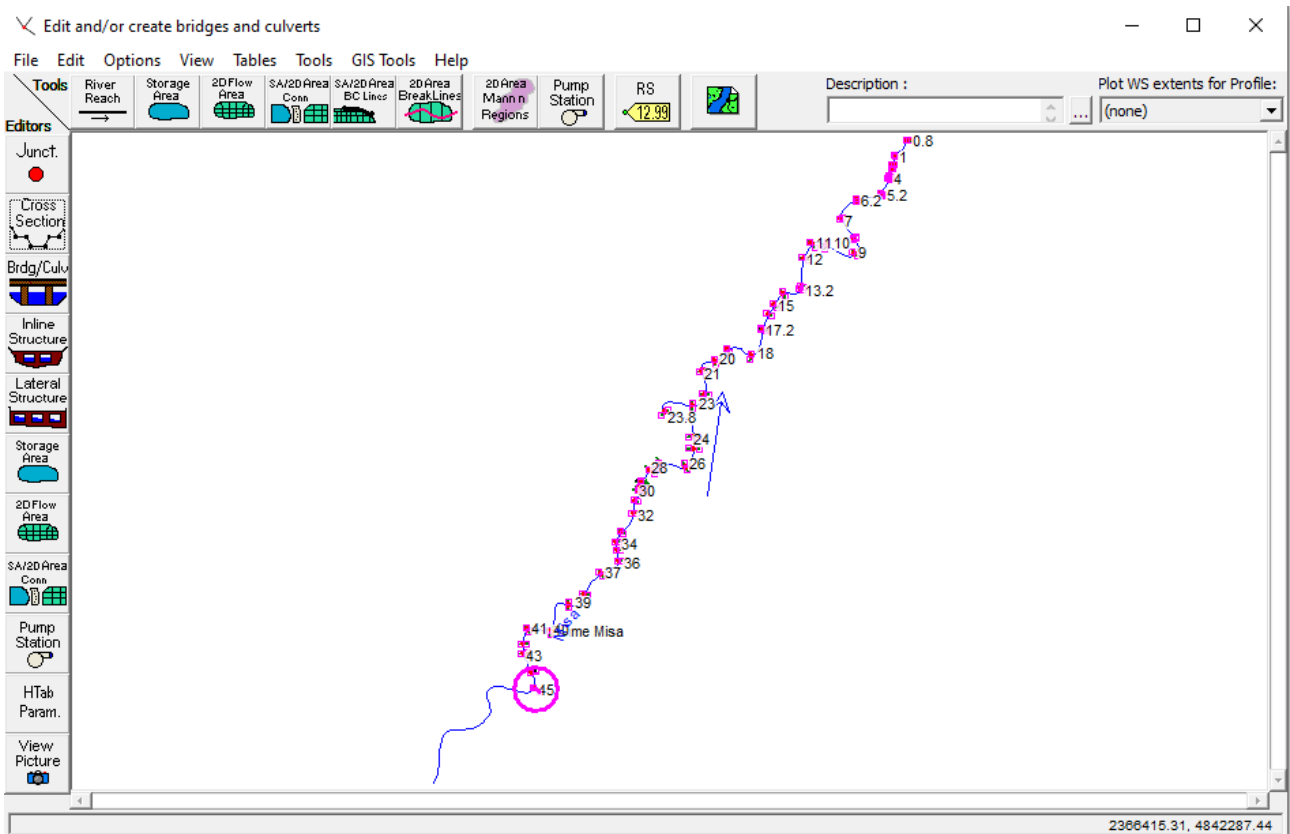


Figure 8. Geometric data window.

In this window, pressing the “Cross section” button, the cross-sections relative to the river are shown in details one by one.

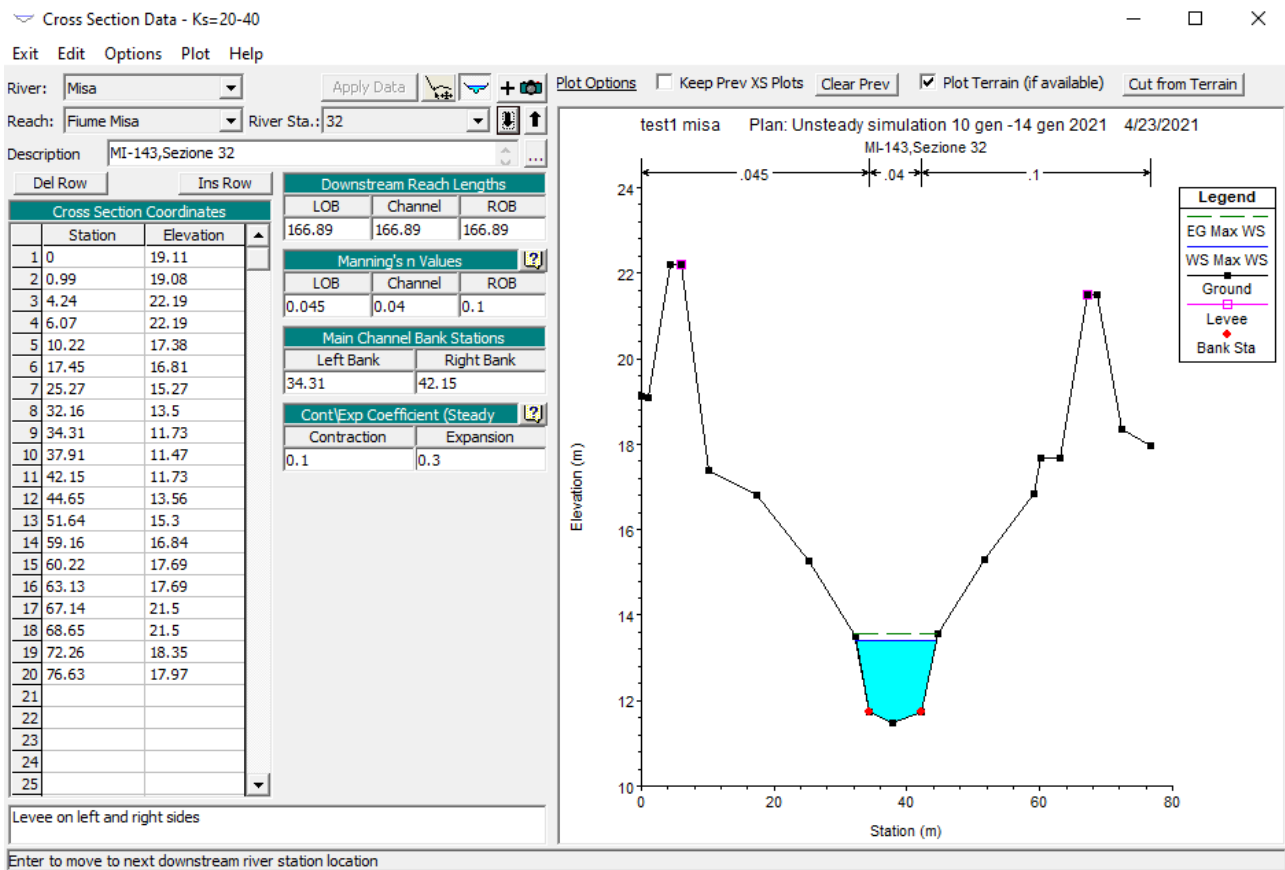


Figure 9. Cross-section data editor.

From the window shown in Figure 9, several details about the selected cross-sections are displayed. In the top part, there are the cross-section general information, such as the name of both the river and the reach, the river station (which has a decreasing numbering moving downstream) and a brief description of the current cross section. Each cross-section is composed of different points, which are defined through the use of the “Cross Sections Coordinates” table. In particular, the station column, indicates the progressive distance that each point has with respect to the origin (along the x-axis), whereas, the elevation column stands for the elevation that each point of the cross-section has with respect to the average sea level. With the table “downstream Reach Lengths” it is possible to define the distance between the cross-section and the following one. Specifically, the terms “LOB” and “ROB” indicate the left-over bank and the right-over bank, respectively, and are used to identify the distance of both the leftmost point and the rightmost point of the cross-section from the following section, while “Channel” indicates the distance between the cross-section thalweg and the following section.

Another important table is that relative to the “Main Channel Bank Station”, where the points of the cross-section belonging to the to the main channel (red points in the figure), and which represent the low flow conditions, are chosen.

From the options menu, it is also possible to add levees to the cross-section along with the ineffective flow areas, which are portions of the cross-section where water has no conveyance.

For what concerns the Manning table, it is possible to insert three different roughness coefficients, one for the left-over bank, one for the main channel and one for the right-over bank.

In particular, the Manning coefficients must be added in relation to the type of both the channel and the flood plains.

Lastly, it is also possible to enter the contraction/expansion coefficients, which are particularly important in presence of bridges.

However, since the number of the cross-sections is significant, another way for inserting these and more parameters in a faster manner is by going to the “Geometric Data” window and entering the “Table” menu where all the cross-section of the river are listed (Figure 10).

Edit Downstream Reach Lengths

River: Edit Interpolated XS's

Reach:

Selected Area Edit Options

	River Station	LOB	Channel	ROB
1	52	257.98	257.98	257.98
2	51	165.51	165.51	165.51
3	50	333.57	333.57	333.57
4	49	531.01	531.01	531.01
5	48	274.01	274.01	274.01
6	47	378.46	378.46	378.46
7	46	330.7	330.7	330.7
8	45.2	9.85	9.85	9.85
9	45.1	Bridge		
10	45	219.09	219.09	219.09
11	44	267.97	267.97	267.97
12	43	123.53	123.53	123.53
13	42	187.75	187.75	187.75
14	41	294.15	294.15	294.15
15	40	525.37	525.37	525.37
16	39	318.83	318.83	318.83
17	38	337.19	337.19	337.19
18	37	298.75	298.75	298.75
19	36	140.02	140.02	140.02
20	35	111.04	111.04	111.04
21	34	148.31	148.31	148.31
22	33	291.36	291.36	291.36
23	32	166.89	166.89	166.89
24	31	135.24	135.24	135.24
25	30	44.23	44.23	44.23
26	29.8	68.61	68.61	68.61
27	29.2	13.85	13.85	13.85
28	29.1	Bridge		
29	29	173.24	173.24	173.24
30	28	143.18	143.18	143.18
31	27	349.34	349.34	349.34
32	26	276.02	276.02	276.02
33	25	150.15	150.15	150.15
34	24	556.81	556.81	556.81
35	23.8	491.45	491.45	491.45
36	23	243.91	243.91	243.91
37	22	307.79	307.79	307.79
38	21	255.18	255.18	255.18
39	20	220.06	220.06	220.06
40	19	339.1	339.1	339.1
41	18	405.17	405.17	405.17
42	17.2	10.6	10.6	10.6
43	17.1	Bridge		
44	17	194.49	194.49	194.49
45	16	136.34	136.34	136.34
46	15	190.19	190.19	190.19
47	14	254.86	254.86	254.86
48	13.2	32	32	32
49	13.1	Bridge		

Figure 10. Downstream reach lengths table.

For what regards the bridge modeling, HEC-RAS calculates the energy losses in three parts. The first part, concerns the losses that occur in the reach immediately downstream of the structure (where an expansion generally takes place). The second part regards the structure itself and this can be modeled

by exploiting several methods. The third part concerns the losses that occur immediately upstream of the structure, where the flow is generally contracting to get through the opening.

To calculate the bridge energy losses, the program needs four cross-sections which should be located in the following way (Figure 11):

- Cross-section 1: sufficiently downstream of the structure so that the flow is not affected by the structure.
- Cross-section 2: a short distance downstream of the bridge.
- Cross-section 3: a short distance upstream of the bridge.
- Cross-section 4: sufficiently upstream of the structure so that the flow lines are approximately parallel and the cross-section is fully active.

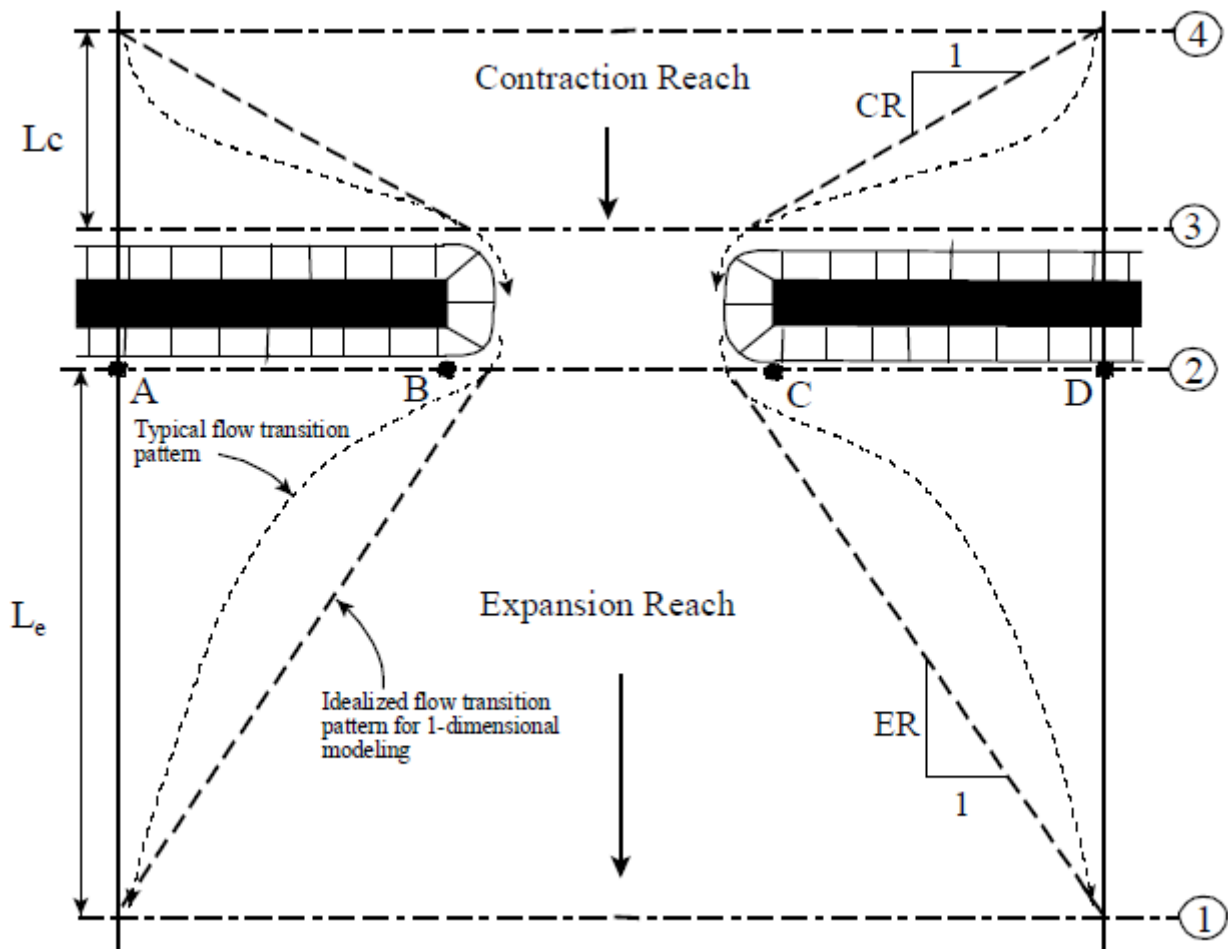


Figure 11. Cross-section location at a bridge.

Other important features to add into the model are the ineffective flow areas. The ineffective flow areas are set in the two sections close to the bridge to keep all the active flow in the area of the bridge

opening until the elevations associated with the left and/or right ineffective flow areas are exceeded by the computed water elevation (Figure 12).

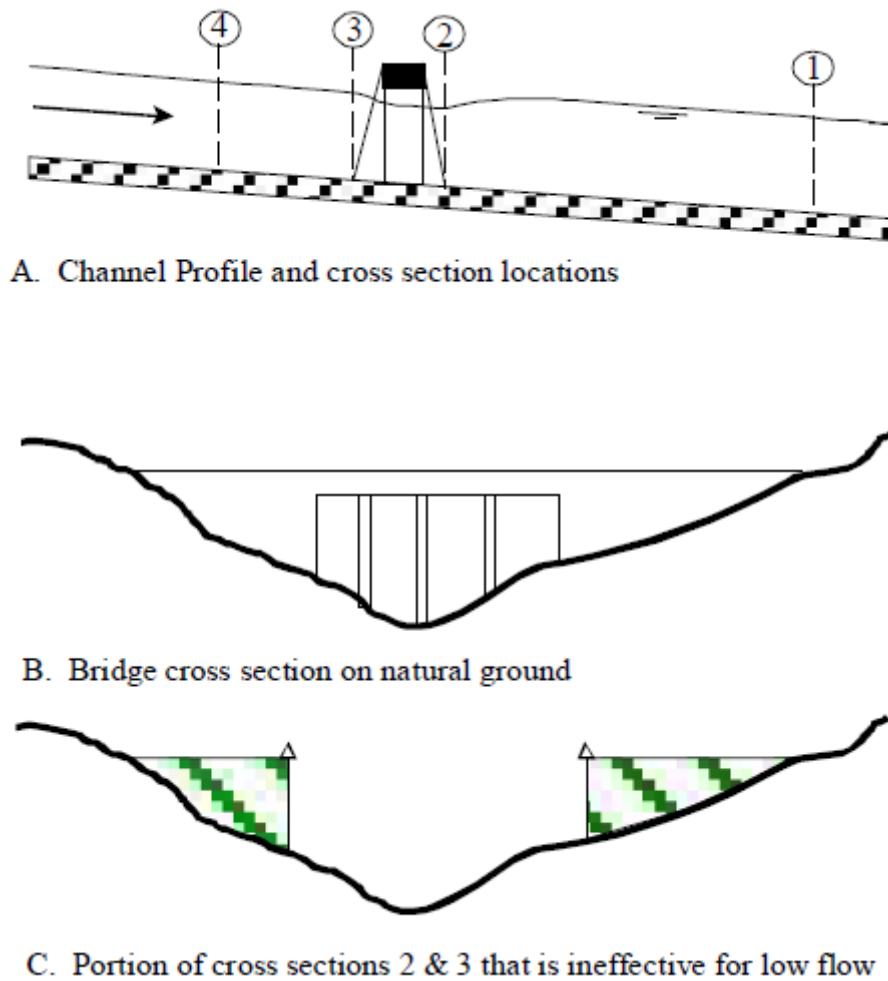


Figure 12 Ineffective flow area.

In low flow conditions, so that when the flow going through the bridge opening is an open channel flow (water surface below the highest point of the low chord of the bridge opening), the software uses the momentum equation to verify the flow regime. If the momentum in the downstream end of the bridge is greater than the critical depth momentum inside the bridge, the flow is considered as completely sub-critical (water surface through the bridge is above the critical depth). On the contrary, if the momentum in the downstream end of the bridge is less than the momentum at critical depth, it is assumed that the constriction will cause the flow to pass through critical depth and a hydraulic jump will occur at some distance downstream. In this last case the flow is considered as super-critical.

The program has also the capability of computing high-flow conditions (flow coming in contact with the maximum low chord of the bridge deck) and in this case, it can use either the energy equation (standard step method) or separate hydraulic equations for pressure and/or weir flow.

From a practical point of view, the inclusion of the bridge into the river geometry is done by using the “Bridge/Culvert Data” button in the “Geometric Data” window (Figure 13).

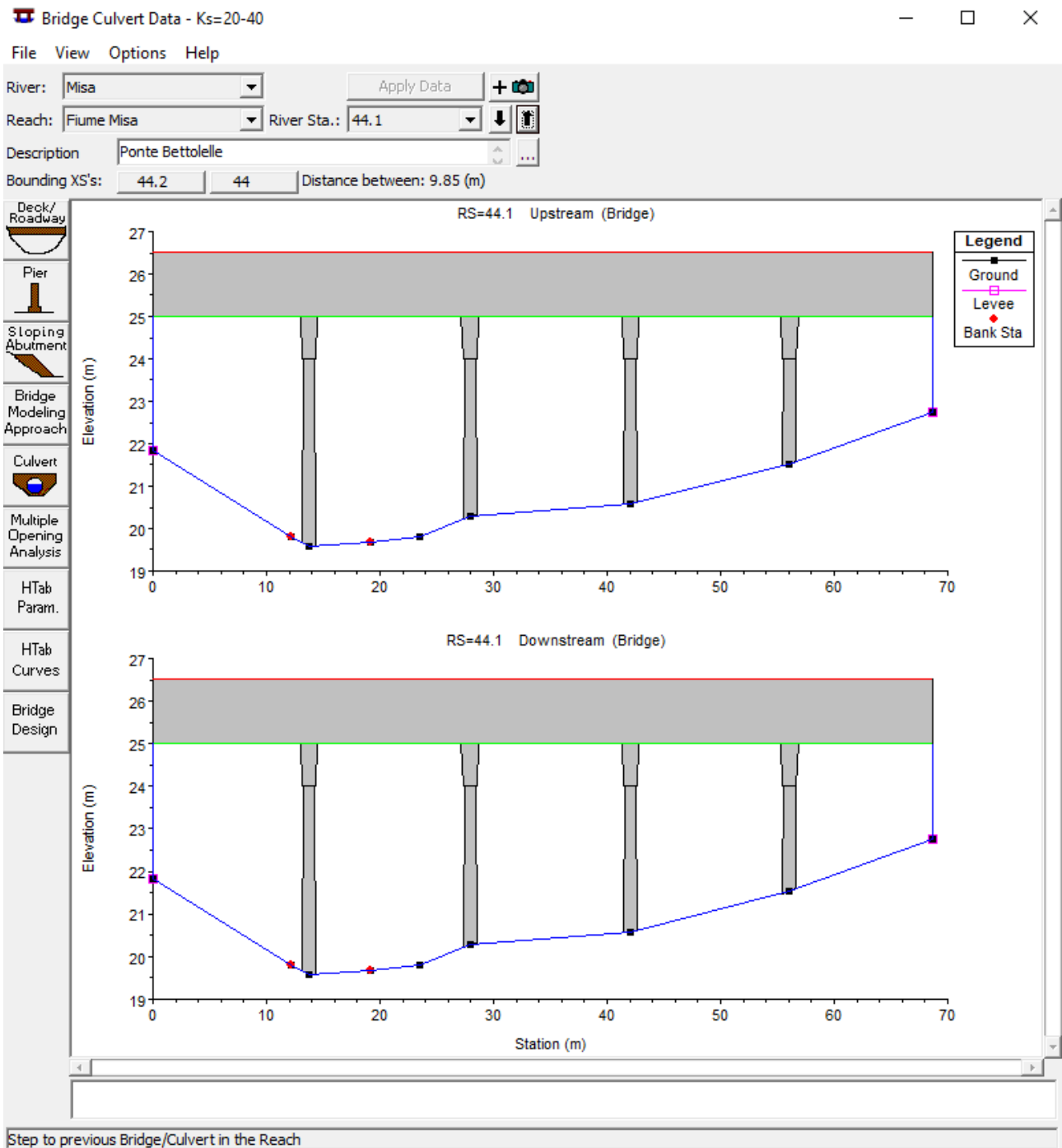


Figure 13. Bridge main window.

In this window, the name of both river and reach is reported, together with the river station. To create a bridge, the first step is to add a new bridge and then select the “Deck/Roadway” button (Figure 14).

Distance	Width	Weir Coef
1.	7.85	1.44

Clear Del Row Ins Row Copy US to DS

Upstream			Downstream			
	Station	high chord	low chord	Station	high chord	low chord
1	0	26.51	25.01	0	26.51	25.01
2	68.73	26.51	25.01	68.73	26.51	25.01
3						
4						
5						
6						
7						
8						

U.S Embankment SS: 0 D.S Embankment SS: 0

Weir Data
 Max Submergence: 0.95 Min Weir Flow El:

Weir Crest Shape
 Broad Crested
 Ogee

OK Cancel

Enter distance between upstream cross section and deck/roadway. (m)

Figure 14. Deck/Roadway window.

Here it is possible to define the distance between the two adjacent cross-sections, the width of the bridge and the weir coefficient (which will be used for weir flow over the bridge deck in the standard weir equation). Then, the bridge is modeled by inserting the values of the station, the high chord and the low chord of the structure in both the upstream and the downstream sections.

As regards to bridge piers, once selected the dedicated button, it is possible to add as many piers as desired from the “Pier Data Editor” by entering the progressive distances of the pier wheelbases for both upstream and downstream sections and, similarly to the deck editor, by inserting the width and the elevation of the single parts of the pile (Figure 15).

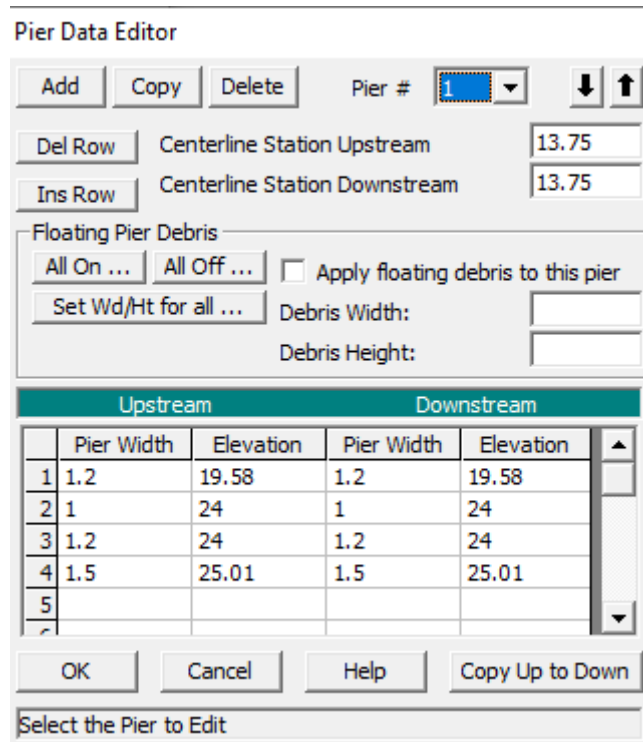


Figure 15 Pier window.

3.1.4 Steady simulation

In order to carry out a steady analysis of the river, it is necessary to add different data such as: flow regime, boundary conditions and discharge information (either peak flows or flow data from a specific instance of time).

The flow regime can be sub-critical, super-critical or mixed and it can be specified in the “Steady Flow Analysis” window (Figure 16).

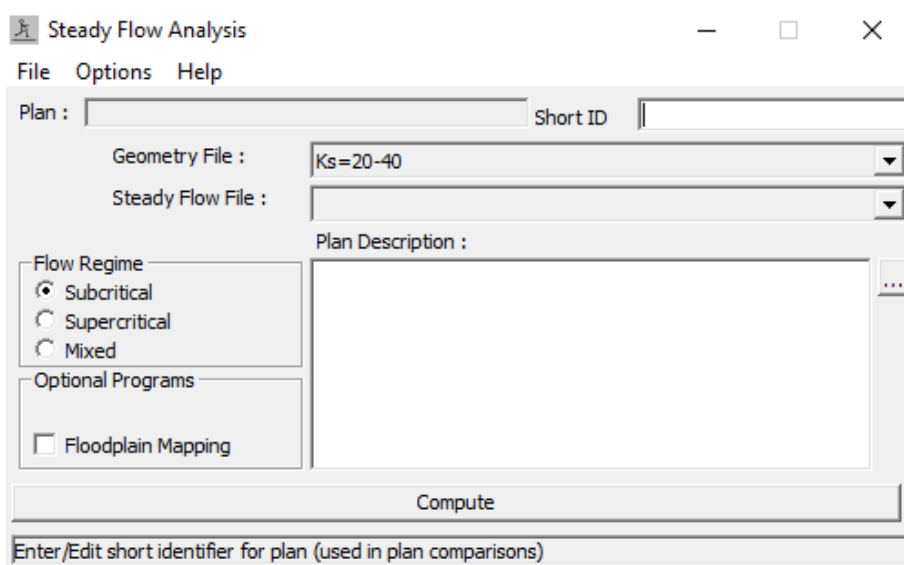


Figure 16. Steady flow analysis window.

In the case of sub-critical regime, the profiles are constrained to critical depth or above, whereas, for a super-critical regime the profiles are constrained to critical depth or below. When the flow regime passes from sub-critical to super-critical, or vice versa, the mixed regime should be selected.

For what regards the discharge, it is entered into the program from upstream to downstream and it must be set in order to compute the water surface profile (Figure 17). This discharge value remains constant along the river until another flow value is encountered in the same reach.

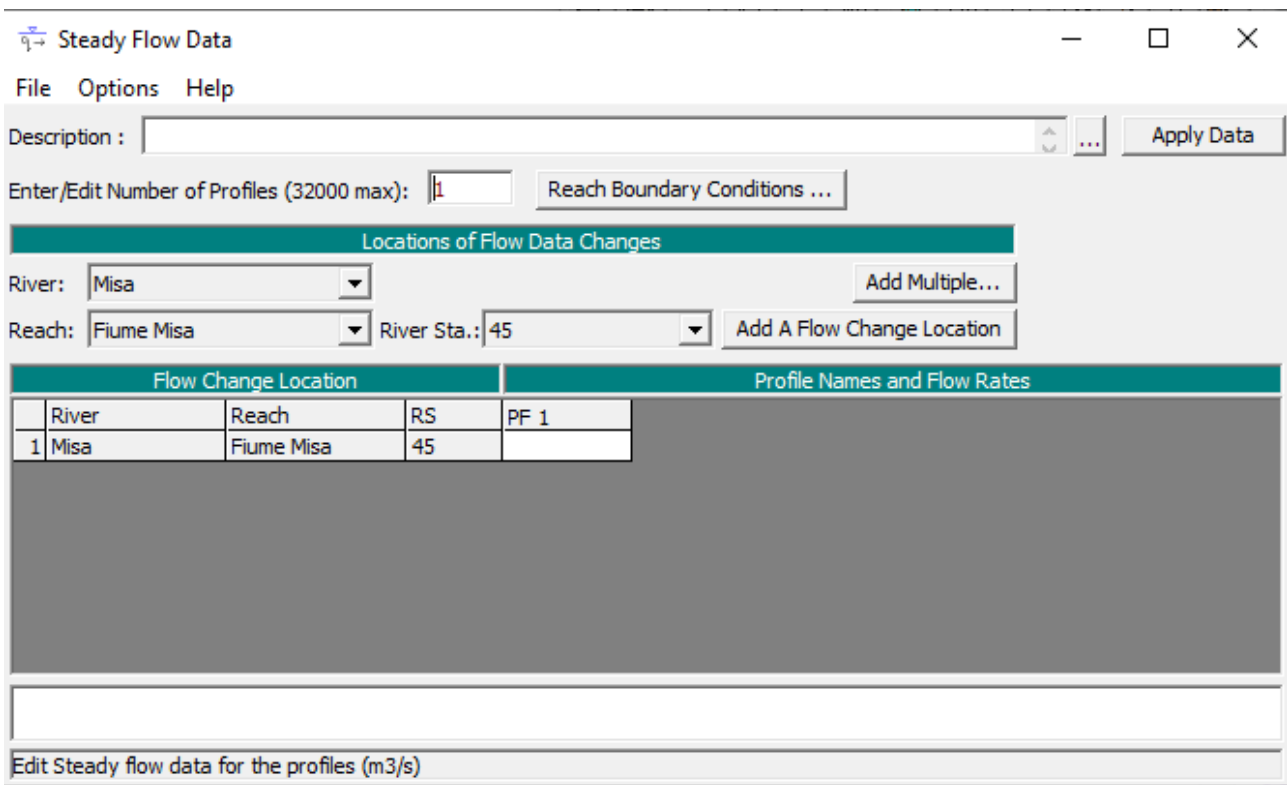


Figure 17. Steady flow data editor.

The boundary conditions are used by the program to establish the starting water surface upstream and downstream of the river. In the case of a sub-critical flow regime, the boundary conditions must be set only at the downstream end of the river, whereas, for super-critical flow regimes the boundary conditions must be set only in the upstream end of the river. If a mixed flow regime calculation is required, the boundary conditions must be set at both the downstream and the upstream river ends.

As shown in Figure 18, there are four types of boundary conditions that can be used:

- Known Water Surface Elevations;
- Critical Depth: where the program calculates the critical depth for each profile;

- Normal Depth: in this case the energy slope (retrieved by the Manning equation) must be added. Anyway, since the average slope of the channel does not significantly differ from the energy slope, it can be used as boundary condition;
- Rating Curve: in this case it is possible to add manually both the elevation and the flow. The elevation is interpolated from the rating curve given the flow through a linear interpolation between the entered points for each profile.

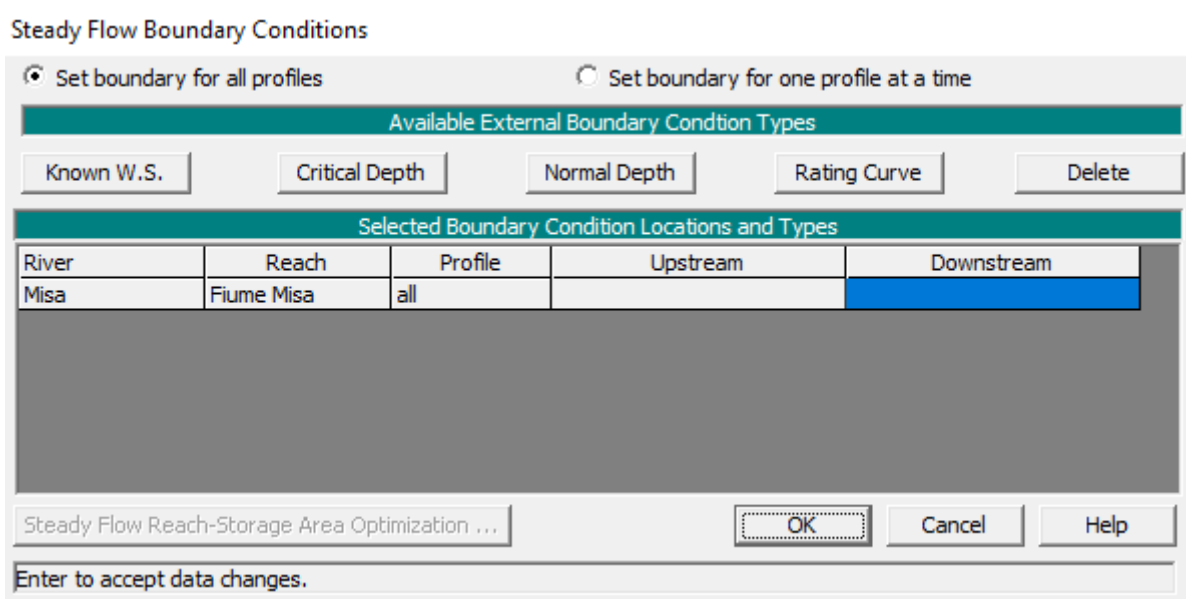


Figure 18. Steady flow boundary conditions.

In those cases in which the water surface elevations at the boundaries are unknown but the program requires the water surface to start the calculations, normal depth or critical depth boundary conditions should be chosen.

3.1.5 Unsteady simulation

To perform an unsteady flow analysis, the first thing to do is the implementation of the boundary conditions (Figure 19).

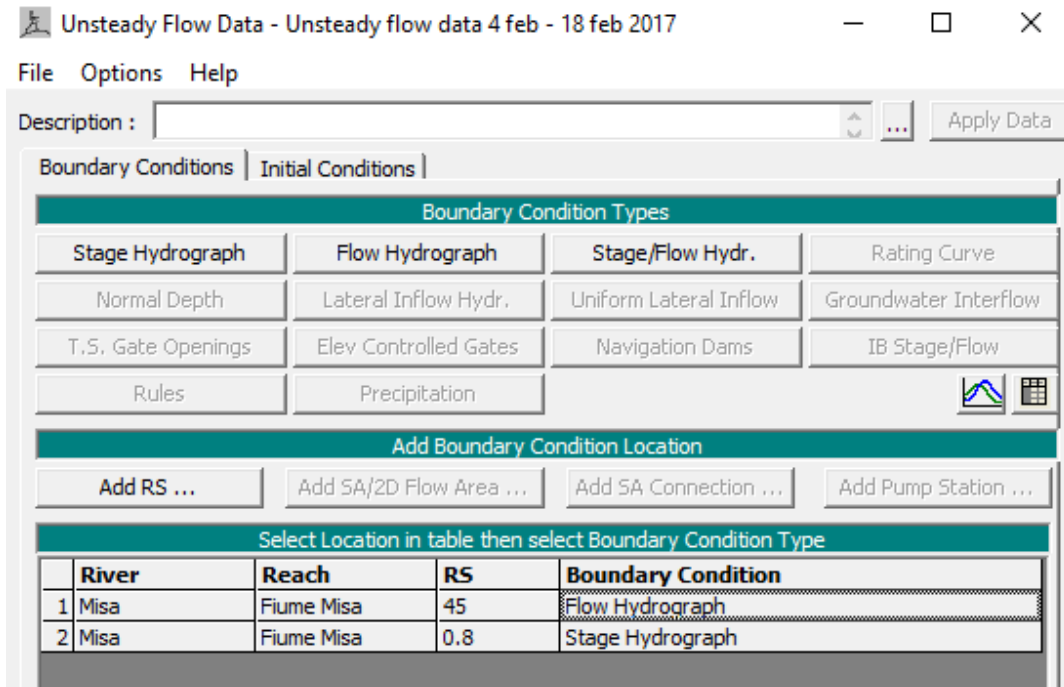


Figure 19. Unsteady flow data boundary conditions.

In this case, differently from the steady simulation, there are different boundary conditions that must be assigned on both the most upstream section and the most downstream one. The most used boundary conditions types are the following:

- Stage Hydrograph: where there is the possibility to add different water elevation values (referred to the average sea level) related to the considered time series;
- Flow Hydrograph: where there is the possibility to add different flow data for the considered time series;
- Stage/Flow Hydrograph: where it is possible to enter both values of stage and flow for the considered time series.

In each of these types of boundary conditions, there is the possibility to set the period of analysis along with the “Data time interval”, which is the interval of time over which the stage/flow data will be inserted into the software. Moreover, since by default the maximum number of insertable values is set to 100, there is the possibility to increase this value up to 50000. Another opportunity is that of filling missed values inside the time series, if any, through the button “Interpolate Missing Values” (Figure 20).

Flow Hydrograph

River: Misa Reach: Misa RS: 39110

Read from DSS before simulation Select DSS file and Path

File:

Path:

Enter Table Data time interval: 30 Minute

Select/Enter the Data's Starting Time Reference

Use Simulation Time: Date: 04FEB2017 Time: 0000

Fixed Start Time: Date: 04FEB2017 Time: 0000

No. Ordinates | Interpolate Missing Values | Del Row | Ins Row

Hydrograph Data			
	Date	Simulation Time (hours)	Flow (m3/s)
1	03Feb2017 2400	00:00	5.266
2	04Feb2017 0030	00:30	5.266
3	04Feb2017 0100	01:00	5.266
4	04Feb2017 0130	01:30	5.428
5	04Feb2017 0200	02:00	5.428
6	04Feb2017 0230	02:30	5.428
7	04Feb2017 0300	03:00	5.594
8	04Feb2017 0330	03:30	5.428
9	04Feb2017 0400	04:00	5.107
10	04Feb2017 0430	04:30	5.594
11	04Feb2017 0500	05:00	5.763
12	04Feb2017 0530	05:30	5.428
13	04Feb2017 0600	06:00	5.266
14	04Feb2017 0630	06:30	5.266
15	04Feb2017 0700	07:00	5.266

Time Step Adjustment Options ("Critical" boundary conditions)

Monitor this hydrograph for adjustments to computational time step

Max Change in Flow (without changing time step):

Min Flow: Multiplier:

Plot Data | OK | Cancel

Figure 20. Flow hydrograph edit window.

Once the hydrograph is added, it is possible to plot it in order to visually check its correctness (Figure 21).

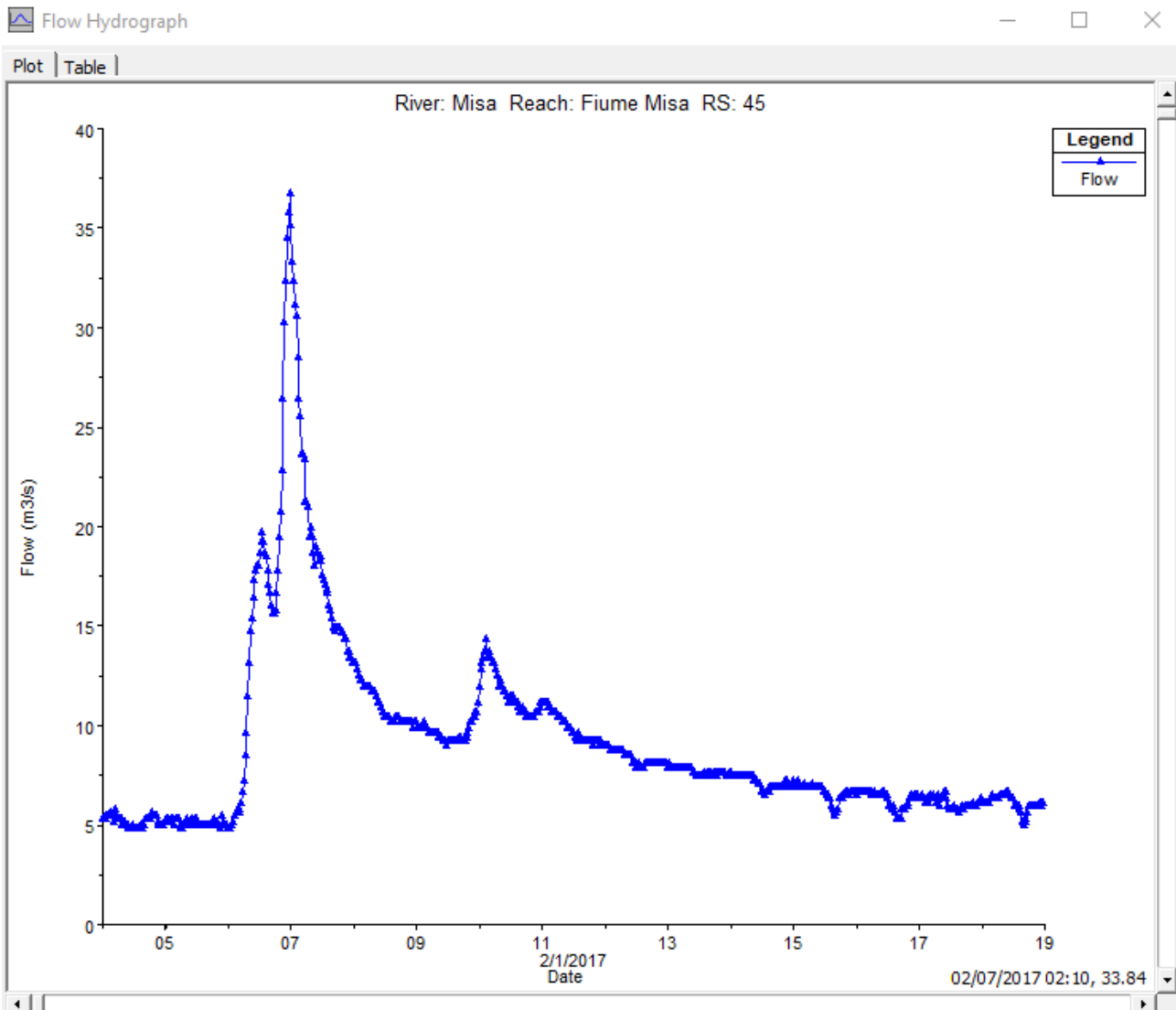


Figure 21. Flow hydrograph graph over time.

There are also other types of boundary conditions that can be applied only as downstream boundary conditions:

- Rating Curve;
- Normal depth: it can be used only for open-ended reaches and it requires to enter the slope of the energy grade line (the slope of the water surface can be used instead of the energy grade line since the two are similar).

In order to simulate an external inflow, that could be, for instance, a waste water treatment plant discharge (as it has been evaluated in this work), further boundary conditions can be applied on each cross-section of the river. In particular:

- Lateral Inflow Hydrograph: this option is used as an internal boundary condition to simulate an external inflow at a specific point along the stream. To implement this boundary condition,

it is necessary to add a new river station (in the cross-section where the external inflow is supposed to be), then the flow hydrograph can be entered;

- Uniform Lateral Inflow Hydrograph: with this option a flow hydrograph can be added and it will be uniformly distributed between two specified cross-sections along the river.

In addition to the already mentioned boundary conditions, other options concerning the groundwater (inflow or outflow depending on the water surface head), gate openings and navigation dams can be implemented into the software.

Once the boundary conditions are set, the unsteady flow data can be saved in order to be immediately recalled.

To run the unsteady simulation, the first step is the definition of a plan which defines both the geometry and the unsteady flow data to be analyzed. Afterwards, it is possible to select the components which will be used for the unsteady flow analysis and that are: a geometric data pre-processor, the unsteady flow simulator and an output post-processor.

The geometric pre-processor is used to process the geometric data into a series of hydraulic properties tables, rating curves and family of rating curves. This option must be run at least once for the first time and it needs to be re-executed only if something in the geometric data changes. The cross-sections are processed into tables of elevation vs hydraulic properties of areas, conveyance and storage. The pre-processor creates hydraulic property tables for both the main channel and floodplain and, for what concerns the latter, differently from the steady simulation, they are worked out as combination of the left overbank and the right overbank properties, summed together in a single set of curves. The unsteady flow option utilizes an arithmetic average between the left and the right overbank reach lengths in order to compute a floodplain reach length. In order to correctly set the hydraulic property table, it is required to enter an interval which will be used for spacing the points in the cross-section table (Figure 22). In particular, this interval should be large enough to capture all possible water surface elevations that may be encountered during the unsteady flow simulations, because, in the case in which the water surface goes above these intervals, the model could be unstable. On the other hand, the interval should be also small enough in order to guarantee a sufficient level of detail to depict changes in area, conveyance, and storage with respect to elevation.

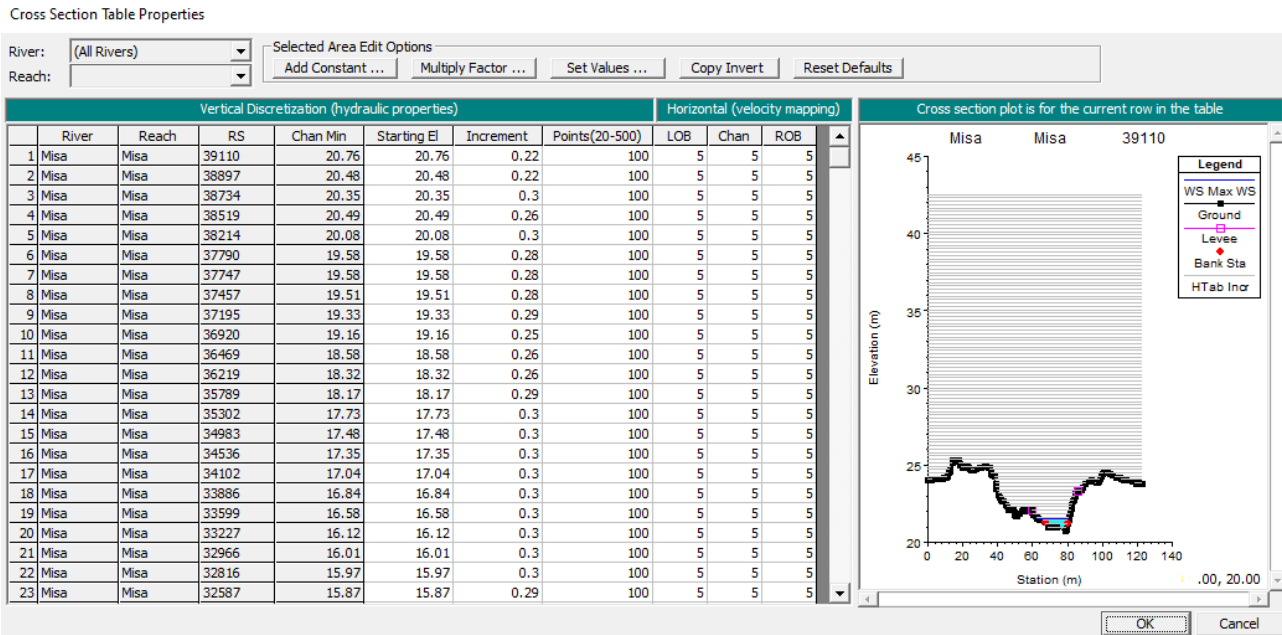


Figure 22. Hydraulic table parameters for cross-sections.

The post-processor provides further hydraulic information if compared to the unsteady flow computation. In general, the unsteady flow computation only calculates stage and flow at all the selected cross-sections, thus, if the post-processor is not run, the outputs of the simulation will only be the stage and flow hydrographs and the inundation mapping. On the other side, if the post-processor is run, all the available plots and tables can be interrogated as for the steady flow simulation.

In order to correctly set up the unsteady simulation, it is required entering both the start and the end of the simulation period from the “Simulation Time Window” in the “Unsteady Flow Analysis”. This time interval can be either equal or less than the time period associated to the “Unsteady Flow Data”.

For what regards the “Computation Setting” table, it is composed of different options such as:

- **Computation Interval:** this represents the simulation timestep. Firstly, it should be small enough to accurately describe both the rise and the fall of the hydrograph. Generally, a good estimate is to consider a computation interval which is equal or less than the time of rise of the hydrograph divided by 20. Secondly, it should follow the Courant condition criteria, i.e., the computation interval should be equal or less than the time required by water to travel from one cross-section to the next. Considering the latter time step, the model will have a high stability although it may require longer time to be run. Additional factors are linked to the presence of bridges and culverts, since the flow transition from unsubmerged to submerged

flow within these structures can lead to an abrupt rise of the water surface upstream of the structure provoking a model instability;

- Mapping Output Interval: this field is used to enter the interval at which it is possible to visualize mapping output within HEC-RAS Mapper;
- Hydrograph Output Interval: this interval must be equal or large than the selected computation interval and is set in order to give a suitable number of points to define the shape of the computed hydrograph without losing information regarding the peaks or volume of the hydrograph;
- Detailed Output Interval: this option allows to set the time interval on which the simulation results will be shown. The selected time interval must always be equal or higher than the computational interval.

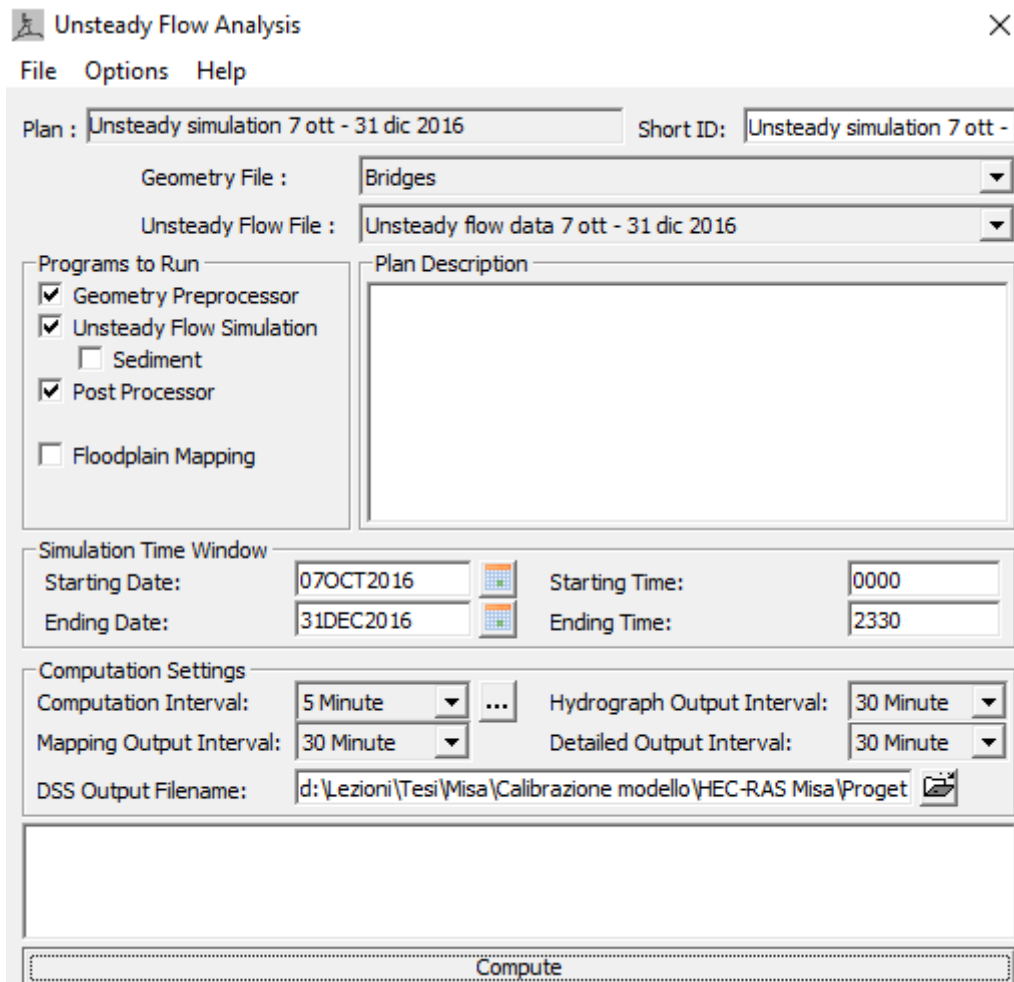


Figure 23. Unsteady flow analysis window.

3.1.6 Unsteady simulation results

Once the simulation has been run, the obtained results can be consulted in different ways. One of these consists in the visualization of the results by means of a table which can be organized in relation to either the desired cross-sections and/or the desired profiles (Figures 24 and 25).

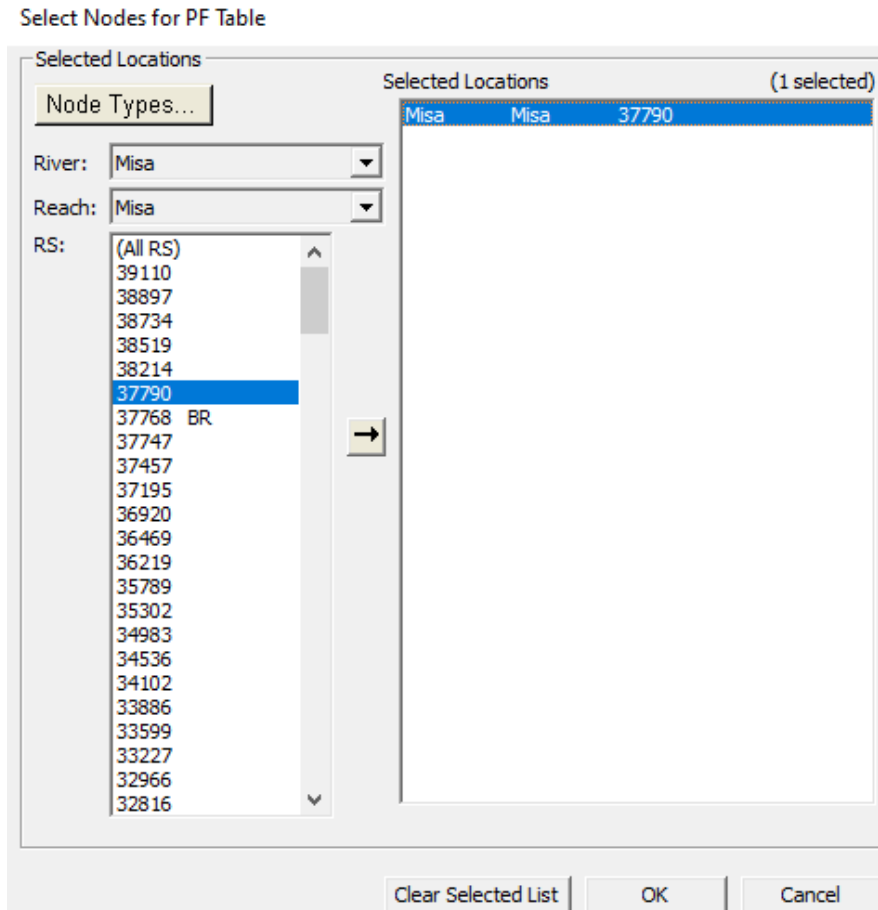


Figure 24. Selection of the cross-section.

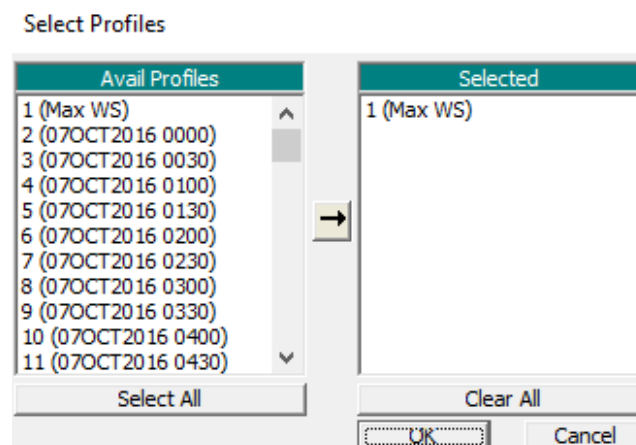


Figure 25. Selection of the profile.

As both the cross-sections and the profiles are selected, all the information concerning the cross-sections, profiles, total flow, minimum channel elevation, water surface elevation, critical water surface, energy grade line elevation, energy grade line slope, channel velocity, flow area, top width and Froude number, are displayed as in Figure 26.

Profile Output Table - Standard Table 1

File Options Std. Tables Locations Help

HEC-RAS Plan: Unsteady simulation 7 ott - 31 dic 2016 Locations: User Defined Reload Data

River	Reach	River Sta	Profile	Q Total (m3/s)	Min Ch El (m)	W.S. Elev (m)	Crit W.S. (m)	E.G. Elev (m)	E.G. Slope (m/m)	Vel Chnl (m/s)	Flow Area (m2)	Top Width (m)	Froude # Chl
Misa	Misa	37790	07OCT2016 0000	4.08	19.58	20.22	19.94	20.25	0.000642	0.87	7.28	17.41	0.37
Misa	Misa	37790	07OCT2016 0030	4.19	19.58	20.22	19.95	20.26	0.000663	0.88	7.34	17.46	0.37
Misa	Misa	37790	07OCT2016 0100	4.22	19.58	20.22	19.95	20.26	0.000665	0.89	7.37	17.48	0.37
Misa	Misa	37790	07OCT2016 0130	4.22	19.58	20.22	19.95	20.26	0.000665	0.89	7.37	17.48	0.37
Misa	Misa	37790	07OCT2016 0200	4.11	19.58	20.21	19.94	20.25	0.000657	0.88	7.26	17.39	0.37
Misa	Misa	37790	07OCT2016 0230	4.08	19.58	20.21	19.94	20.25	0.000655	0.87	7.22	17.36	0.37
Misa	Misa	37790	07OCT2016 0300	4.19	19.58	20.22	19.95	20.26	0.000662	0.88	7.34	17.46	0.37
Misa	Misa	37790	07OCT2016 0330	4.11	19.58	20.21	19.94	20.25	0.000657	0.88	7.26	17.39	0.37
Misa	Misa	37790	07OCT2016 0400	4.30	19.58	20.23	19.95	20.27	0.000670	0.90	7.46	17.56	0.38
Misa	Misa	37790	07OCT2016 0430	4.36	19.58	20.23	19.96	20.27	0.000673	0.90	7.53	17.62	0.38
Misa	Misa	37790	07OCT2016 0500	4.36	19.58	20.23	19.96	20.27	0.000673	0.90	7.53	17.62	0.38
Misa	Misa	37790	07OCT2016 0530	4.25	19.58	20.22	19.95	20.26	0.000673	0.89	7.38	17.49	0.38
Misa	Misa	37790	07OCT2016 0600	4.22	19.58	20.22	19.95	20.26	0.000665	0.89	7.37	17.48	0.37
Misa	Misa	37790	07OCT2016 0630	4.33	19.58	20.23	19.96	20.27	0.000671	0.90	7.49	17.59	0.38
Misa	Misa	37790	07OCT2016 0700	4.47	19.58	20.24	19.96	20.28	0.000670	0.91	7.69	17.76	0.38
Misa	Misa	37790	07OCT2016 0730	4.61	19.58	20.25	19.97	20.29	0.000670	0.92	7.90	17.93	0.38
Misa	Misa	37790	07OCT2016 0800	4.54	19.58	20.24	19.96	20.29	0.000673	0.92	7.78	17.83	0.38
Misa	Misa	37790	07OCT2016 0830	4.50	19.58	20.24	19.96	20.28	0.000672	0.91	7.74	17.79	0.38
Misa	Misa	37790	07OCT2016 0900	4.40	19.58	20.23	19.96	20.27	0.000672	0.90	7.59	17.66	0.38
Misa	Misa	37790	07OCT2016 0930	4.25	19.58	20.22	19.95	20.26	0.000673	0.89	7.38	17.49	0.38
Misa	Misa	37790	07OCT2016 1000	4.22	19.58	20.22	19.95	20.26	0.000665	0.89	7.37	17.48	0.37
Misa	Misa	37790	07OCT2016 1030	4.22	19.58	20.22	19.95	20.26	0.000665	0.89	7.37	17.48	0.37
Misa	Misa	37790	07OCT2016 1100	4.22	19.58	20.22	19.95	20.26	0.000665	0.89	7.37	17.48	0.37
Misa	Misa	37790	07OCT2016 1130	4.22	19.58	20.22	19.95	20.26	0.000665	0.89	7.37	17.48	0.37
Misa	Misa	37790	07OCT2016 1200	4.22	19.58	20.22	19.95	20.26	0.000665	0.89	7.37	17.48	0.37
Misa	Misa	37790	07OCT2016 1230	4.11	19.58	20.21	19.94	20.25	0.000660	0.88	7.24	17.37	0.37
Misa	Misa	37790	07OCT2016 1300	4.19	19.58	20.22	19.95	20.26	0.000662	0.88	7.34	17.46	0.37
Misa	Misa	37790	07OCT2016 1330	4.33	19.58	20.23	19.95	20.27	0.000671	0.90	7.49	17.59	0.38
Misa	Misa	37790	07OCT2016 1400	4.47	19.58	20.24	19.96	20.28	0.000670	0.91	7.69	17.76	0.38
Misa	Misa	37790	07OCT2016 1430	4.39	19.58	20.23	19.96	20.27	0.000672	0.90	7.59	17.66	0.38
Misa	Misa	37790	07OCT2016 1500	4.25	19.58	20.22	19.95	20.26	0.000668	0.89	7.40	17.51	0.38
Misa	Misa	37790	07OCT2016 1530	4.11	19.58	20.21	19.94	20.25	0.000657	0.88	7.26	17.39	0.37
Misa	Misa	37790	07OCT2016 1600	3.88	19.58	20.20	19.93	20.24	0.000638	0.85	7.01	17.17	0.36

Total flow in cross section.

Figure 26. Results table.

Another way to access the simulation results is by checking directly either each cross-section or the entire river profile (Figures 27 and 28), where it is even possible to see an animation of the water surface elevation trend over time.

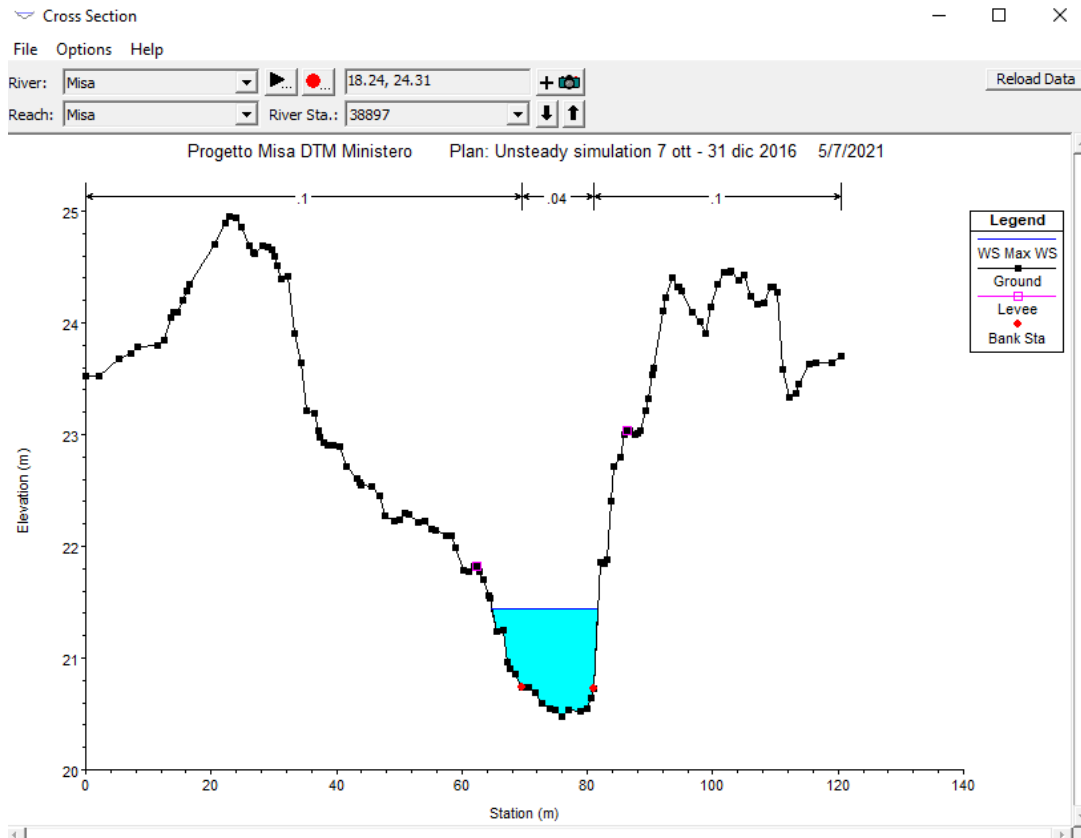


Figure 27. Water elevation at the river cross-section.

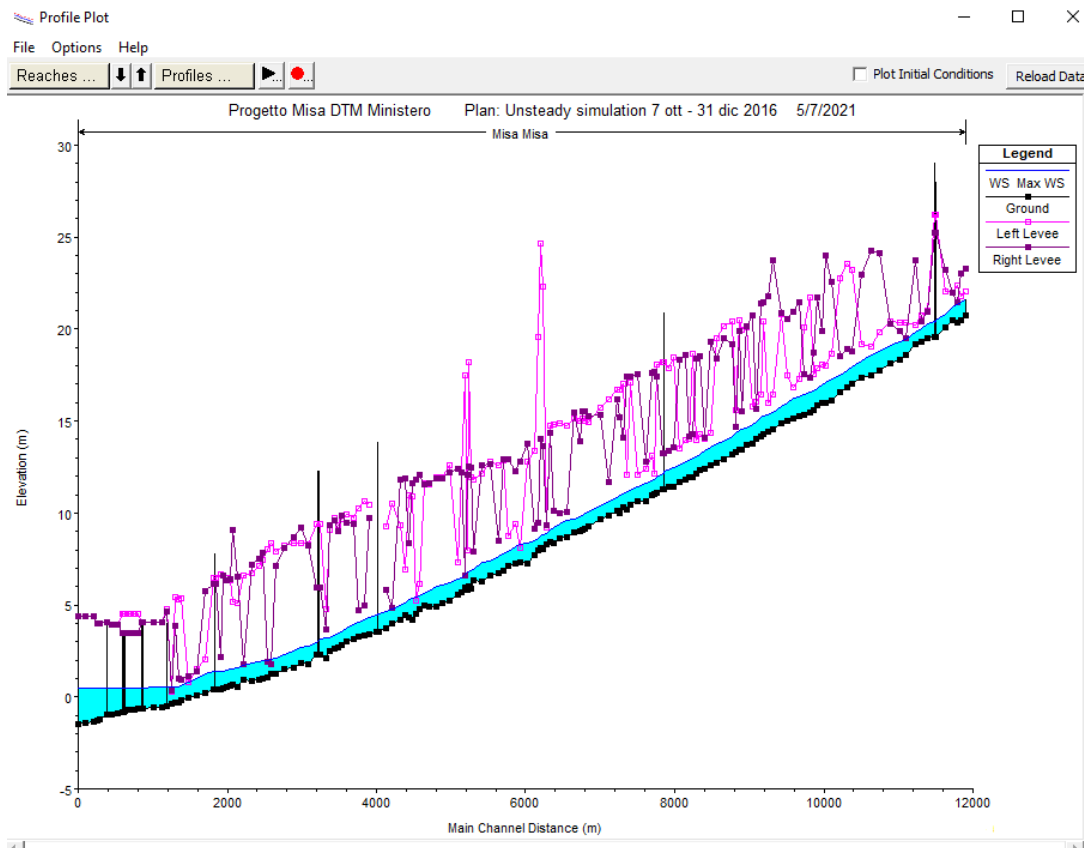


Figure 28. Water elevation at the river profile.

A further method to check the simulation outputs is by going to the “Stage and Flow Hydrograph” field where it is possible to visualize an overlap of both stage and flow values over time in a stage/flow vs time graph (Figure 29).

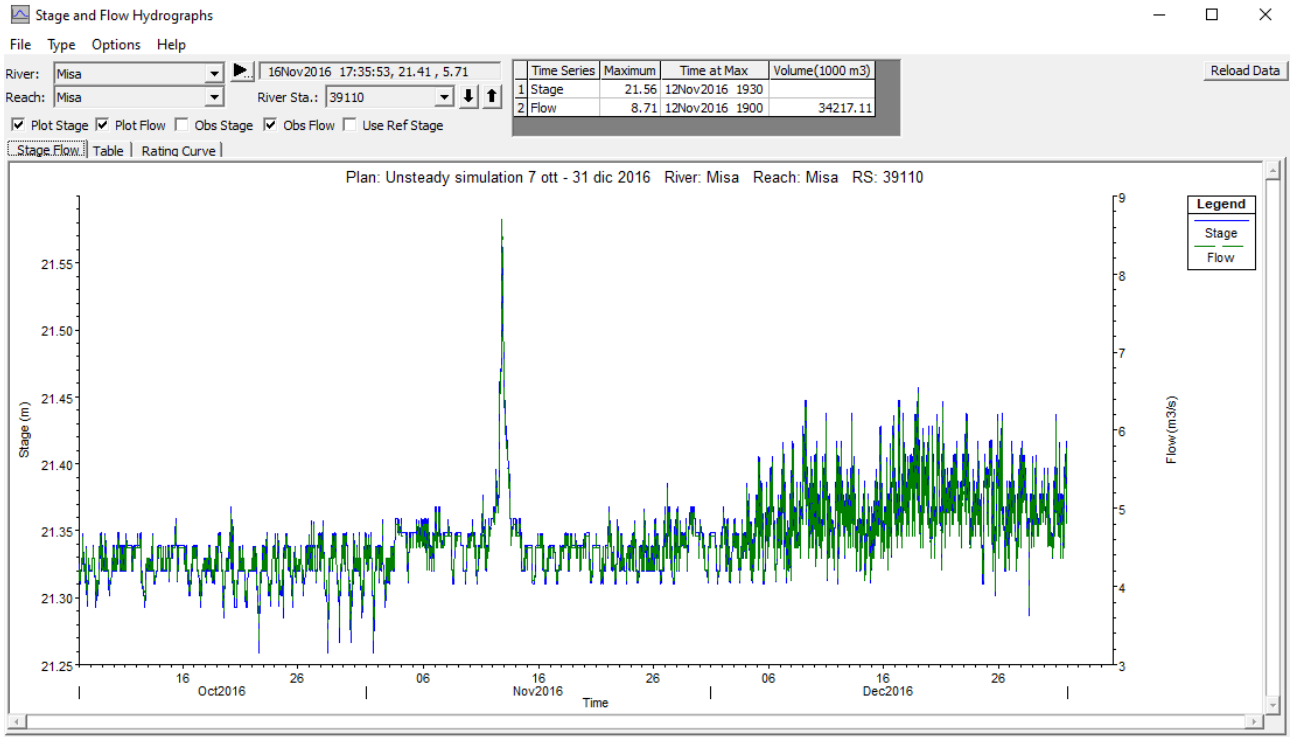


Figure 29. Stage and flow hydrograph window.

Moreover, in this field there is also the possibility to visualize the current rating curve (Figure 30).

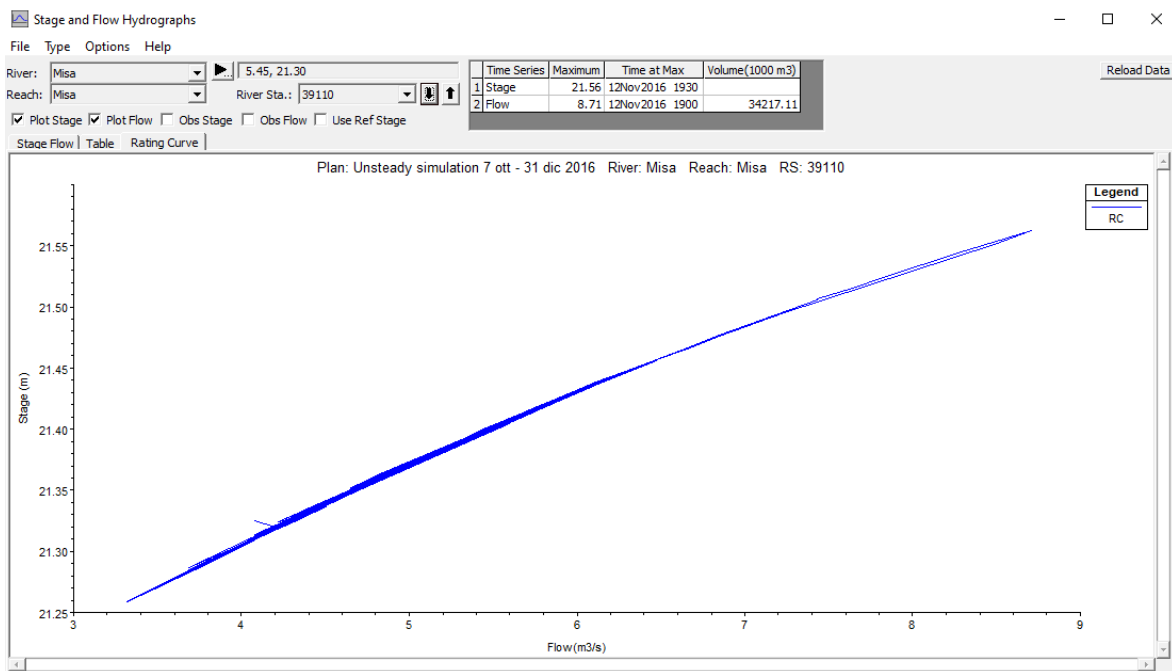


Figure 30. Rating curve representation.

3.2 Data used for the model construction

3.2.1 Data from Civil Protection of the Marche Region

SIRMIP (Sistema Informativo Regionale Meteo-Idro-Pluviometrico)

The SIRMIP is a database belonging to the Centro Funzionale Multirischi of the Civil Protection of the Marche Region, where it is possible to have access to different hydro-meteorological data, including hydrometry, pressure, precipitation, humidity, temperature, snow, solar radiation and wind data.



Figure 31. SIRMIP website main window.

These data, which were originally managed by the Servizio Idrografico e Mareografico Nazionale (SIMN) and only later by the Civil Protection (2002), are based on two distinct networks, a mechanical and a telemetric one.

The former was developed by the SIMN in the 1916 and owned thermometers, pluviometers and hydrometers as sensors. Further, when these tasks were addressed to the Civil Protection, 21 thermometers and 83 pluviometers were in operation.

For what concerns the latter, following the strengthening program for the weather, hydro, pluviometric monitoring stations, the Marche Region were equipped with a telemetric monitoring system, consisting of 53 thermometers, 77 pluviometers, 13 anemometers, 15 barometers, 30 hygrometers, 7 snow-meters and 70 hydrometers along with a hydrometric rod for the calibration measures. In January 2019 the telemetric network fully replaced the mechanical one and both the number and the types of the sensor increased. Since the 2005, on some hydrometric stations, the discharges are estimated in continuous.

Thanks to this database, it has been possible to download the data needed for the hydraulic analysis of the Misa River.

The first step has been the selection of the desired category of data, that, for the aim of this work, has been represented by both the hydrometric and the rainfall data.

Considering the hydrometric data, there is the possibility of choosing either the basin and/or the province and/or the municipality where the data acquisition is required.

Subsequently, it is possible to select the needed sensors (the place of the stations) together with the type of data to download. In particular, the data that have been downloaded are those regarding the stage, the rating curves, the coordinates of the stations and the hydrological characteristics. These kinds of data can be directly downloaded in both text and excel format, depending on their availability.

For what regards the rainfall data, the steps to be followed are the same of those of the hydrometric data. In both cases, it is possible to choose the time period over which to extract the data, and considering that the maximum time interval is of 180 days, the download of different years data requires the use of different sheets.

From the website, different data regarding both the Bettollelle and the Ponte Garibaldi river stations have been extracted. For what concerns the former, the downloaded data regarded both the stage levels and the rating curves, whereas, the data downloaded from the Ponte Garibaldi river station were only referred to the stage values, since no rating curve is currently available. Considering the stage values, the extracted data range from 2016 to 2021 and are displayed in excel format as in Figure 32:

Codice sensore	Data: Anno	Mese	Giorno	Ora	Minuto	Livello idrometrico [m]	Livello idrometrico in secca [0/1]	Codice stazione
1112	2020	1	1	0	0	1.02	0	26
1112	2020	1	1	0	30	1.02	0	26
1112	2020	1	1	1	0	1.02	0	26
1112	2020	1	1	1	30	1.02	0	26
1112	2020	1	1	2	0	1.01	0	26
1112	2020	1	1	2	30	1.01	0	26
1112	2020	1	1	3	0	1.02	0	26
1112	2020	1	1	3	30	1.01	0	26
1112	2020	1	1	4	0	1.02	0	26
1112	2020	1	1	4	30	1.03	0	26
1112	2020	1	1	5	0	1.02	0	26
1112	2020	1	1	5	30	1.02	0	26
1112	2020	1	1	6	0	1.01	0	26
1112	2020	1	1	6	30	1.02	0	26
1112	2020	1	1	7	0	1.02	0	26
1112	2020	1	1	7	30	1.02	0	26
1112	2020	1	1	8	0	1.02	0	26
1112	2020	1	1	8	30	1.02	0	26
1112	2020	1	1	9	0	1	0	26
1112	2020	1	1	9	30	1	0	26
1112	2020	1	1	10	0	1.01	0	26
1112	2020	1	1	10	30	1.02	0	26
1112	2020	1	1	11	0	1.03	0	26
1112	2020	1	1	11	30	1.03	0	26
1112	2020	1	1	12	0	1.03	0	26

Figure 32. Example of SIRMIP downloaded data.

The first column identifies the sensor (1112 stays for Bettolle sensor), the subsequent five columns identify the date and the time of data acquisition, the seventh column the stage and the last two columns the water level in dry conditions and the station, respectively. In order to better managing the data, both the date (year, month, and day) and the time have been concatenated. This operation allows the creation of serial numbers which have turned out to be useful for the graphical representation of the simulation results (Figure 33).

2020/1/1	0:0	43831	0	43831
2020/1/1	0:30	43831	0.020833	43831.021
2020/1/1	1:0	43831	0.041667	43831.042
2020/1/1	1:30	43831	0.0625	43831.063
2020/1/1	2:0	43831	0.083333	43831.083
2020/1/1	2:30	43831	0.104167	43831.104
2020/1/1	3:0	43831	0.125	43831.125
2020/1/1	3:30	43831	0.145833	43831.146
2020/1/1	4:0	43831	0.166667	43831.167
2020/1/1	4:30	43831	0.1875	43831.188
2020/1/1	5:0	43831	0.208333	43831.208
2020/1/1	5:30	43831	0.229167	43831.229
2020/1/1	6:0	43831	0.25	43831.25

Figure 33. Transformation of date in serial numbers.

The same process has been done also for the Ponte Garibaldi, by considering the same interval of years.

At this point, the discharge values referred to each stage value have been computed by means of the rating curves (Figures 34 (a) and 34 (b)).

2005	1	1	0	1	2006	1	1	0	0
2006	1	1	0	1	2007	1	1	0	0
2007	1	1	0	1	2008	12	13	7	0
2008	12	13	7	1	2011	1	1	0	0
2011	1	1	0	1	2011	3	1	10	30
2011	3	5	0	1	2015	5	23	6	30
2011	3	5	0	1	2015	5	23	6	30
2015	5	23	6	31	2017	3	7	16	0
2015	5	23	6	31	2017	3	7	16	0
2015	5	23	6	31	2017	3	7	16	0
2017	3	7	16	1	2018	3	5	0	0
2017	3	7	16	1	2018	3	5	0	0
2019	12	15	0	0	2030	1	1	0	0
2019	12	15	0	0	2030	1	1	0	0
2019	12	15	0	0	2030	1	1	0	0
2019	12	15	0	0	2030	1	1	0	0

Figure 34 (a). Bettolle rating curves. The first five columns indicate the year, the month, the day, the hour and the minute of the beginning of validity period of the rating curves, whereas the last five columns indicate the year, the month, the day, the hour and the minute of the end of validity period of the rating curves.

0.56 <= H <= 4.34	$Q = 8.39 * [H - (0.55)]^{2.323} + 0$
1.02 <= H <= 5.01	$Q = 23.351 * [H - (1.011)]^{1.659} + 0$
0.77 <= H <= 4.33	$Q = 9.4265 * [H - (0.76)]^{2.137} + 0$
0.77 <= H <= 4.01	$Q = 11.4929 * [H - (0.76)]^{1.8516} + 0$
0.77 <= H <= 9999	$Q = 11.4929 * [H - (0.76)]^{1.8516} + 0$
0.55 <= H <= 4.39	$Q = 6.195 * [H - (0.517)]^{2.576} + 0$
4.4 <= H <= 6.35	$Q = 185.568 * [H - (4.39)]^{1.138} + 202.776$
0.2 <= H <= 1.51	$Q = 5.9 * [H - (0.148)]^{2.934} + 0$
1.52 <= H <= 3.01	$Q = 27.549 * [H - (1.51)]^{1.188} + 14.609$
3.02 <= H <= 6.5	$Q = 101.284 * [H - (3.01)]^{1.061} + 59.209$
0.95 <= H <= 3.02	$Q = 14.388 * [H - (0.942)]^{1.974} + 0$
3.03 <= H <= 6.5	$Q = 100.396 * [H - (3.02)]^{1.068} + 60.954$
0.85 <= H <= 1.03	$Q = 2.33 * [H - (0.84)]^{0.79} + 0$
1.04 <= H <= 2.1	$Q = 19.68 * [H - (1.03)]^{1.24} + 0.6$
2.11 <= H <= 3.8	$Q = 64.05 * [H - (2.1)]^{1.26} + 22.01$
3.81 <= H <= 5.5	$Q = 155.87 * [H - (3.8)]^{1.16} + 146.7$

Figure 34 (b). Bettolle rating curves. The first column indicates the stage interval, the second column indicates the equations of the rating curves.

For what concerns the precipitation data, the downloading procedure is the same as that of the hydrometric data, but in this case the data have a time interval of 15 minutes rather than 30 minutes.

3.2.2 Data from surveys

In 2001, the Civil Protection of the Marche Region undertook a survey campaign devoted to the acquisition of the Marche Region rivers cross-sections, among which also the Misa River appears. In particular, 53 cross-sections have been used to represent the river stretch from Bettollelle to the estuary of the Misa River. Being these cross-sections not recent and composed of a low amount of points, they have been employed in the model mainly to check its correctness.

In order to have a better representation of the actual conditions at Bettollelle cross-section, which is the place where both discharge and stage values are available, a more recent cross-section has been requested to the Civil Protection of the Marche Region (Figure 35).

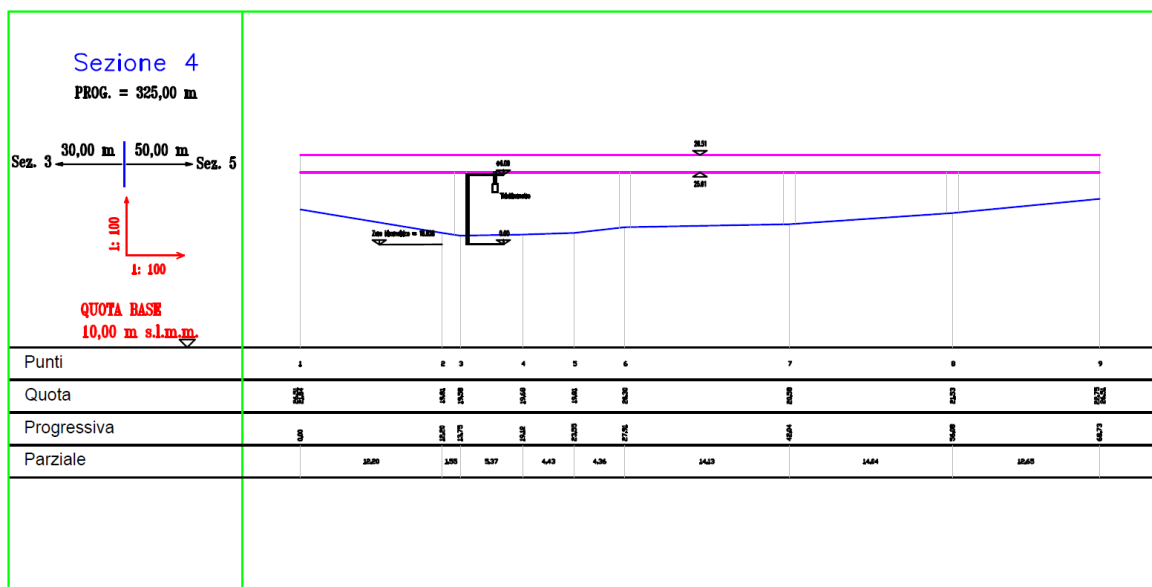


Figure 35. Civil Protection Bettollelle cross-section 2019.

This cross-section dates back to 2019, thus it can be considered more representative for the present numerical simulations.

Further cross-sections relative to the Ponte Garibaldi and to the location in which the H-ADCP (described in the following section) is installed coming from a 9th September 2019 survey, have been used into the model to enhance the reliability of the river geometry.

From the Ministero dell’Ambiente e della Tutela del Territorio e del Mare, different data regarding the river stretch from Bettollelle to the river estuary have been requested to overcome the problem linked to the use of old cross-section provided with a low number of points. In particular, digital terrain model (DTM), digital surface model first return (DSM first), digital surface model last return

(DSM last) and the point cloud in *.xyz format, representing the area of interest, have been employed into the model with the goal of building up a more detailed river geometry, considering that with this type of data, an infinite number of cross-sections can be directly extracted from the DTMs. These data are part of a surveying campaign promoted by the Ministero dell’Ambiente e della Tutela del Territorio e del Mare in the period between 2008-2009, and have been acquired through the use of the Lidar (Light Detection and Ranging) technology. They are georeferenced in the WGS84 (EPSG4326) reference system, and are available with a resolution of 1 m or 2 m depending on the selected area. In order to provide a preliminary organization of these data, the QGIS software has been employed. QGIS (Geographic Information System) is an open-source software, born in 2002 and allowing the analysis and the organization of spatial data. It supports both vector and raster data and it is the most common GIS software worldwide (Figure 36).

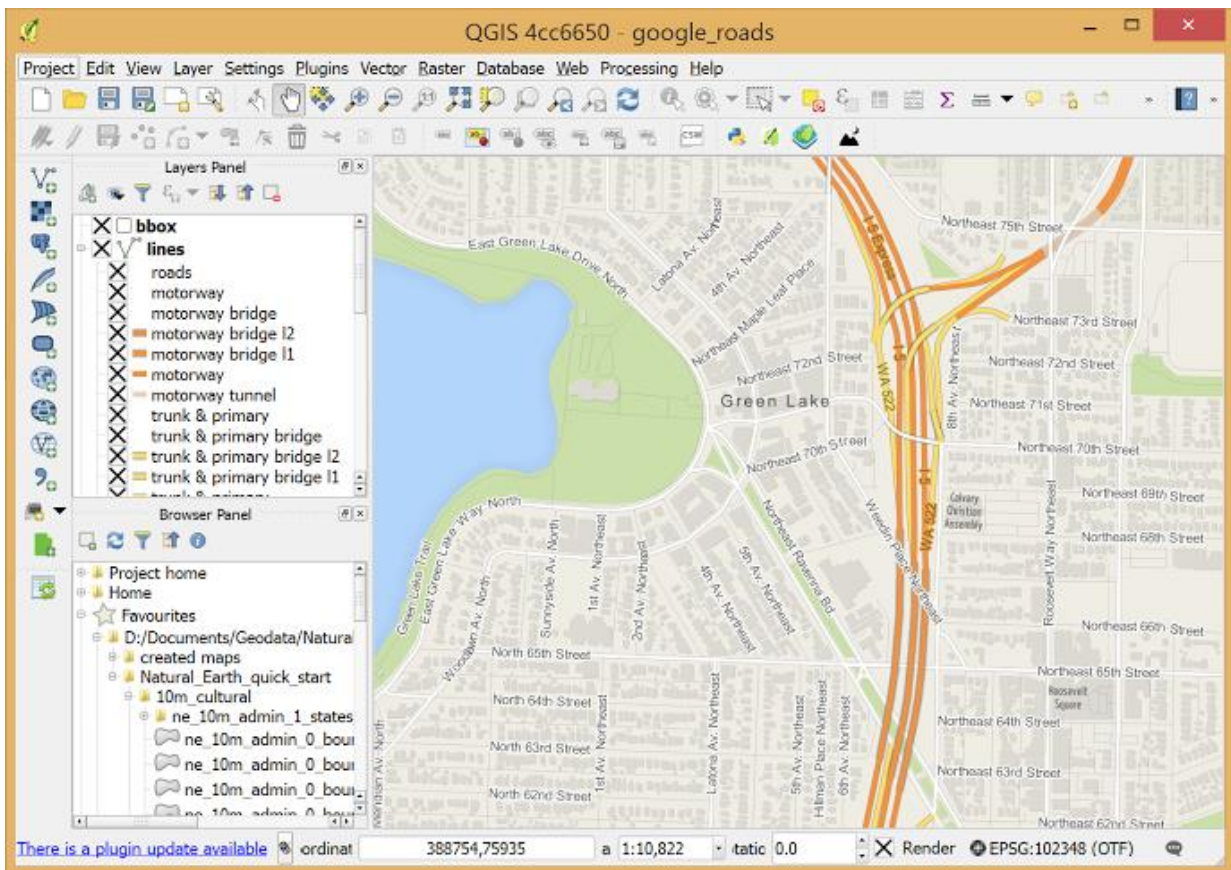


Figure 36. QGIS main window.

The QGIS offers different functions, which can be gathered in the following categories:

- Data visualization: different data formats of both raster and vector data and projections, can be visualized and overlapped inside the software without the need of conversion into a default internal format;
- Data exploration and map creation;
- Data creation, modification, management and exports: vector files can be created, modified managed and exported in different formats. For what regards raster data, they must be previously imported in GRASS (Geographic Resources Analysis Support System) in order to be edited and exported in other formats. QGIS offers the possibility of the creation and modification of shapefiles along with images georeferencing through the specific plugin;
- Data analysis: possibility of exploiting different tools for the data analysis among which there is the sampling, the georeferencing and the geometry management of the vector data database.

Considering that the river estuary is deeper if compared to more upstream cross-sections, the above-described Lidar data are not able to reach the deepest points of the estuarine cross-sections. For this reason, available bathymetric surveys of the nearby coastal and estuarine area, provided by the Socotec Italia Srl and referred to the 2015, 2018, 2020 years, have been used to reconstruct the missing bathymetry (Figure 37).

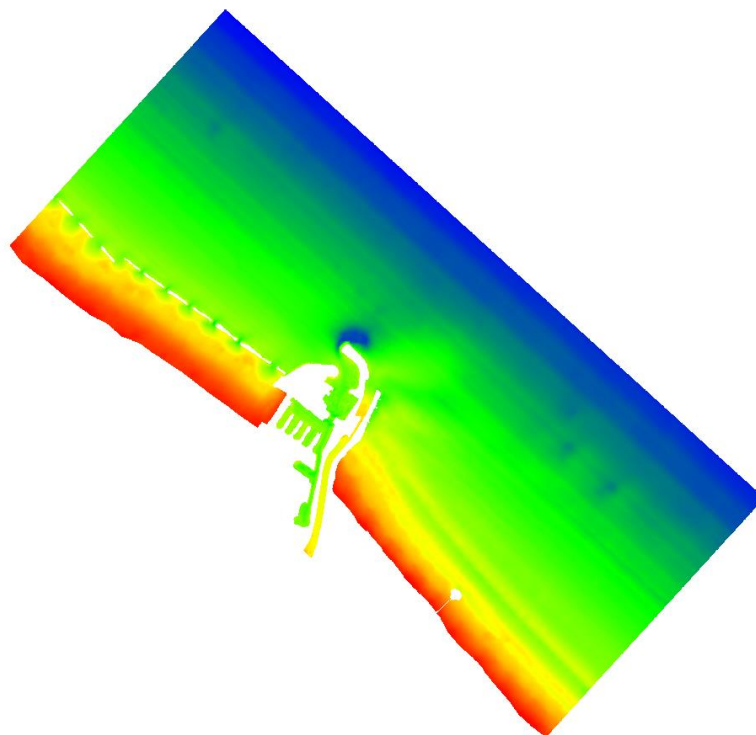


Figure 37. Example of Misa river estuary bathymetric survey.

3.2.3 Hydrodynamic data

The data deriving from the Modeling and Observation of River-Sea Exchanges at a microtidal estuary (MORSE) project, have been taken into account for the model calibration. The MORSE project was mainly carried out with the aim at understanding the interaction processes between the river and sea actions, which lead to the modification of the beach morphology and to the sediment transport (with the consequent transport of potential pollutants and nutrients). The equipment used in the MORSE project is composed of a Horizontal Acoustic Doppler Current Profiler (H-ADCP) (Figure 38), located about 21 meters upstream of the Ponte Garibaldi. This is an instrument devoted to collection of both river velocity and water surface elevation.



Figure 38. H-ADCP frontal view.

Its principle is that of sending acoustic pulses from the transducers faces through the water column, measuring the time required by the pulses to come back to the transducer faces when reflected by the hit particles. However, the time required by the returning signal to reach the transducers is affected by the Doppler effect, which is generated due to particle motion. Thanks to this phenomenon, the instrument is able to calculate the time differences measured in the returned signal, which are used to assign a velocity value to the flow.

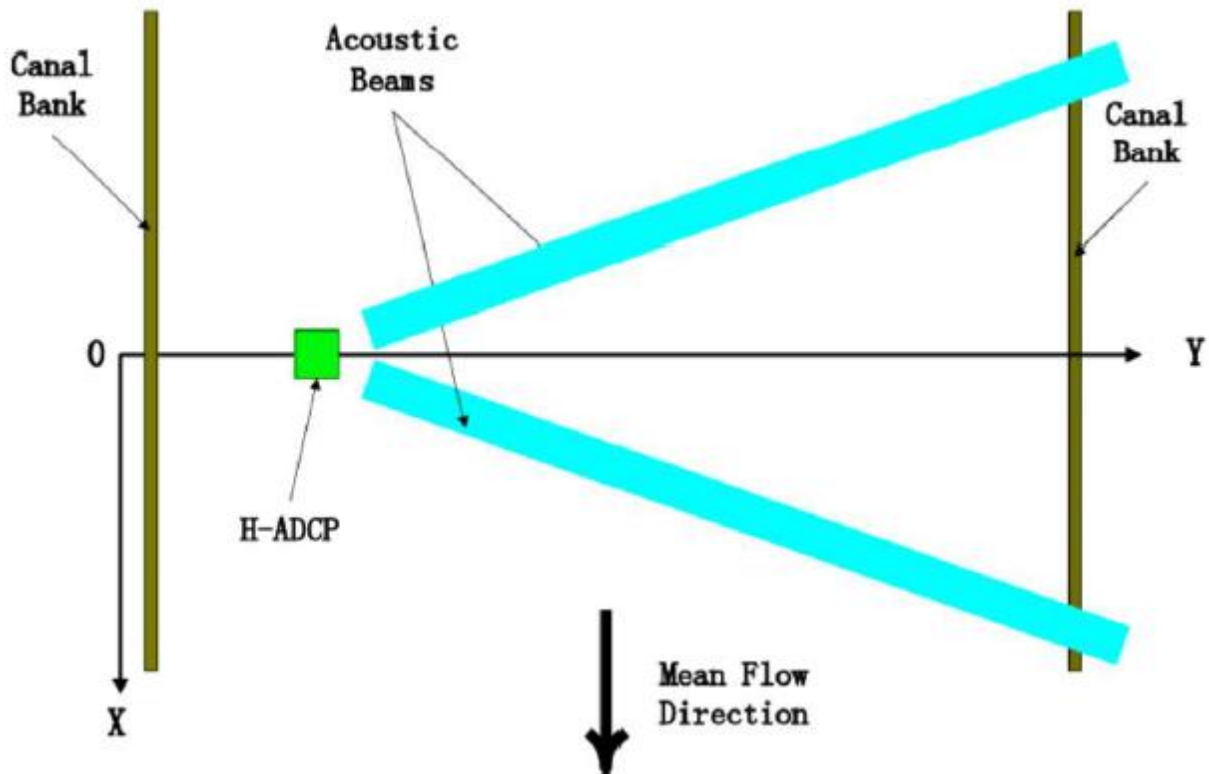


Figure 39. H-ADCP beams influence.

The stage and flow data coming from the H-ADCP used in this work, are related only to a limited period of time, since the instrument requires a significant water elevation (it has to be completely covered by water) to start acquiring data.

For what concerns the implementation of the tidal stages, the data recorded by the tide gauge located at Ancona harbor have been considered. The Servizio Mareografico Nazionale (SMN) of the Istituto Superiore per la Protezione e la Ricerca Ambientale (ISPRA), is aimed at taking care of all the aspects related to the marine climate, the coast status and the marine levels, providing the publication of the observed and elaborated data, accompanied by cartography, standards and collection methods. In the marine environment, the SMN has assumed the management of the Rete Ondametrica Nazionale (RON), which has led to the empowerment and development of the Rete Mareografica Nazionale (RMN).

The RMN utterly replaces the preexisting oceanographic detection system, and is composed of 36 measuring stations, which are evenly distributed on the national territory, and mainly located within the port facilities.

Actually, for almost all stations of the RMN, the hydrometric level is monitored by using a microwave sensor (radar) that owns a millimetric accuracy, and it is coupled with a second floating gauge. Moreover, also the historical ultrasound hydrometric sensor is in operation. By comparing the outputs coming from these three sensors, where the ultrasound one is used as verification, the ISPRA is able to efficiently calibrate the radar sensor, in order to achieve an excellent accuracy in stage data.

Each stage sensor computes the reading with respect to an oceanographic rod whose height has been set in relation to the Istituto Geografico Militare (I.G.M.) altimetric network, by connecting to the closest I.G.M. cornerstone. The stations are also equipped with an anemometric sensor which gathers wind direction and velocity data at 10 meters above ground level, a barometric sensor, an air temperature sensor and a water temperature sensor along with a relative moisture sensor. Furthermore, 10 stations come with a multiparametric probe aimed at evaluating the water quality. The measured parameters are the water temperature, pH, conductivity and redox.

All stations are provided with local system for the management and the storage of data, and with a transmission apparatus (UMTS) linked directly to the SMN headquarter in Rome. In addition, for 9 strategic stations addressed to particular phenomena measurements (rogue waves), is present a second satellite transmission data system, which ensures the connection even in the case of UMTS system black-out events.

All the data collected by the SMN are available and can be easily download from the ISPRA website. For what regards the aim of this work, tidal excursion data relative to different time periods coming from the Ancona station have been used. The choice of the Ancona station has been dictated by two aspects: the first one is that actually there is not an available tidal station at Senigallia; secondly, because large differences in tidal excursions between Senigallia and Ancona municipalities do not exist, so that the error is negligible.

The Ancona station is located at a latitude of $43^{\circ}37'29.16''$ and at a longitude of $13^{\circ}30'23.46''$ and it is placed right on the S.Primiano harbor. The station is equipped with altimetric cornerstones, where each of them is set with the average sea level measured at Genova municipality by the ancient Thomson tidal gauge.

In order to download the desired data from the website, after the selection of the station, it is possible to enter one of the submenus that will open up, as shown in Figure 40.



▼ Informazioni generali	<h3>ANCONA</h3> <p>LATITUDINE 43° 37' 29.16"  LONGITUDINE 13° 30' 23.46"</p> <p> descrizione della stazione</p> <p>Visualizzazione dati, periodo disponibile 01.01.2010 - 13.04.2021</p> <ul style="list-style-type: none">▶ livello idrometrico▶ temperatura acqua▶ temperatura aria▶ umidità relativa▶ pressione atmosferica▶ velocità e direzione vento▶ confronto tra parametri <p>Livello idrometrico Periodo disponibile 00:00 01.01.2010 - 08:40 13.04.2021 GMT Seleziona l'intervallo temporale</p> <p>inizio <input type="text" value="00"/> : <input type="text" value="00"/> <input type="text" value=""/> <input type="text" value=""/> <input type="text" value=""/></p> <p>fine <input type="text" value="00"/> : <input type="text" value="00"/> <input type="text" value=""/> <input type="text" value=""/> <input type="text" value=""/> <input type="button" value="PROCEDI"/></p>
▼ Reti di misura	
Mareografica	
Onde anomale	
▼ Livellazione	
▼ Stazioni	
Ancona	
Anzio	
Bari	
Cagliari	
Carloforte	
Catania	
Civitavecchia	
Crotone	
Gaeta	
Genova	
Ginostra	
Imperia	
La Spezia	
Lampedusa	
Livorno	
Marina di Campo	
Messina	
Napoli	
Ortona	
Otranto	

Figure 40. National Tidegauge Network main window.

From here, it is possible to input the initial and final time interval over which to extract the data. The available time interval starts on 1st January 2010.

Even though the first simulation attempts have been performed by using the normal depth (considered as the mean slope of the river stretch) as downstream condition, thus without requiring any further datum in addition to the stage and the flow data, they cannot be used for the model calibration because the considered river stretch is characterized by the presence of the estuary, thus a contribution deriving from the tidal motion has to be considered into the model.

Although the employed tidal data derive from the Ancona station, they can be taken as suitable for the Senigallia coastal area, since no relevant discrepancies are observed between the measurements recorded at Ancona harbor and those recorded at Senigallia harbor by a recently installed tide gauge (Figure 41).

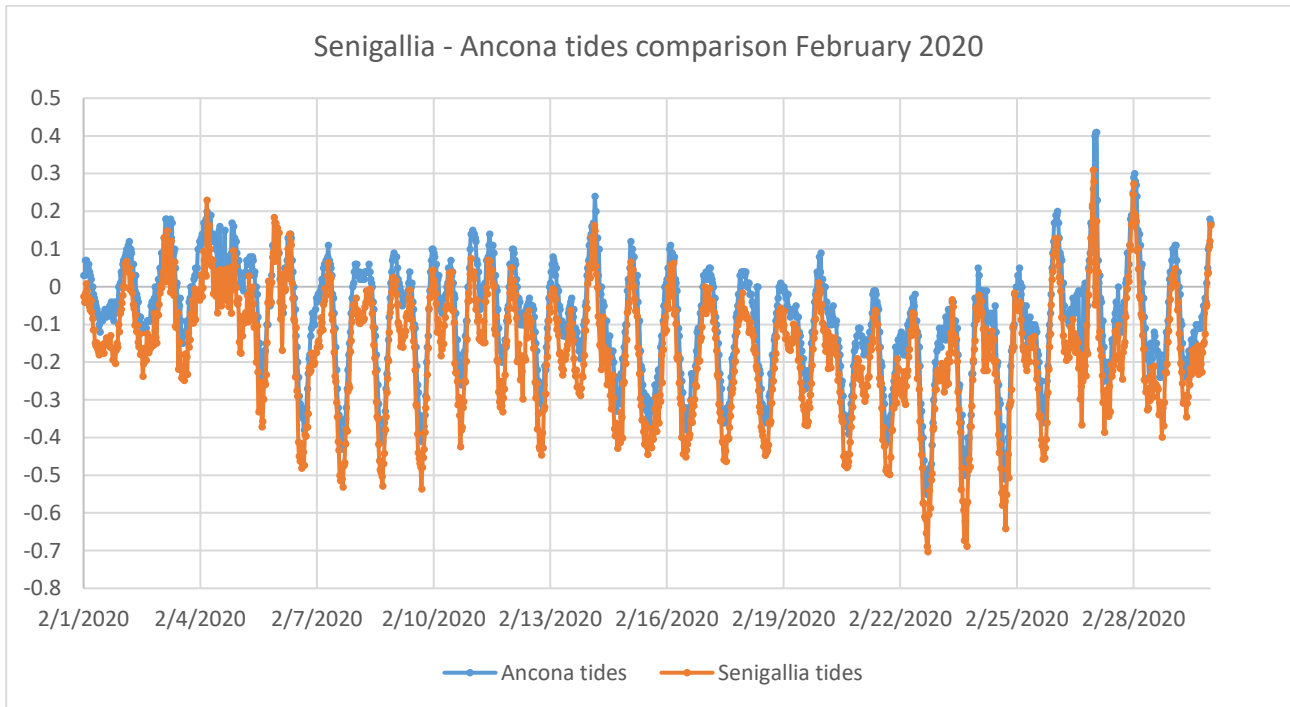


Figure 41. Comparison between Ancona and Senigallia tidal motion.

Once the needed data from the Rete Mareografica Nazionale have been downloaded, the next step has been the interpolation of these data. This operation has been necessary since the data extracted from the SIRMIP website have an interval time of 30 minutes, whereas the data extracted by the Rete Mareografica Nazionale have an interval time of 10 minutes, thus, in order to have a match between the stage/flow data and the tidal data, the latter have been worked out to be reconducted to an interval time of thirty minutes (Table 1).

Tides 4 feb - 18 feb 2017		
Date	Time	Marea
2017/2/4	0:0	0.01
2017/2/4	0:30	0.04
2017/2/4	1:0	0.03
2017/2/4	1:30	0.07
2017/2/4	2:0	0.03
2017/2/4	2:30	0.07
2017/2/4	3:0	0.1
2017/2/4	3:30	0.04
2017/2/4	4:0	0.06
2017/2/4	4:30	0.14
2017/2/4	5:0	0.04
2017/2/4	5:30	0.04
2017/2/4	6:0	0.03
2017/2/4	6:30	0.01
2017/2/4	7:0	0
2017/2/4	7:30	-0.05
2017/2/4	8:0	-0.05

Table 1. Tidal data elaboration.

Considering the presence of a wastewater treatment plant located between Bettolle and Ponte Garibaldi, the discharges coming from the plant have been analyzed. Specifically, the data which have been requested to the Viva Servizi S.p.A. cover the periods between the 4th February 2017 - 18th February 2017 and the 3rd March 2017 – 24th April 2017, and are composed of both the ordinary flows and the by-pass flows which are present when the treatment capacity of the plant is not able to treat all the incoming water (Table 2).

Date	Time	Outflow (m ³ /h)	By-pass (m ³ /h)
6/2/2017	12:00:15 AM	595.4861	0
6/2/2017	12:00:30 AM	547.4537	1.157407
6/2/2017	12:00:45 AM	544.5602	0.5787037
6/2/2017	12:01:00 AM	511.5741	0
6/2/2017	12:01:15 AM	510.4167	2.314815
6/2/2017	12:01:30 AM	489.0046	0.5787037
6/2/2017	12:01:45 AM	488.4259	0
6/2/2017	12:02:00 AM	469.3287	1.157407
6/2/2017	12:02:15 AM	468.1713	0.5787037
6/2/2017	12:02:30 AM	456.5972	0
6/2/2017	12:02:45 AM	455.4398	0
6/2/2017	12:03:00 AM	457.1759	0.5787037
6/2/2017	12:03:15 AM	456.5972	0
6/2/2017	12:03:30 AM	451.9676	2.314815
6/2/2017	12:03:45 AM	452.5463	0.5787037
6/2/2017	12:04:00 AM	458.3333	0
6/2/2017	12:04:15 AM	454.8611	0
6/2/2017	12:04:30 AM	450.8102	0.5787037
6/2/2017	12:04:45 AM	451.9676	0
6/2/2017	12:05:00 AM	448.4954	0
6/2/2017	12:05:15 AM	451.3889	0.5787037
6/2/2017	12:05:30 AM	445.6018	0
6/2/2017	12:05:45 AM	448.4954	0
6/2/2017	12:06:00 AM	458.3333	0.5787037

Table 2. Wastewater treatment plant data from Viva Servizi S.P.A.

4 MODEL CONSTRUCTION

In order to perform a steady state analysis of the Misa River, a project created by exploiting the cross-section of the Civil Protection of the Marche Region has been used. This project dates back to 2001 and it is characterized by 53 cross-sections covering essentially the river stretch from Bettollelle to the estuary (Figure 42).

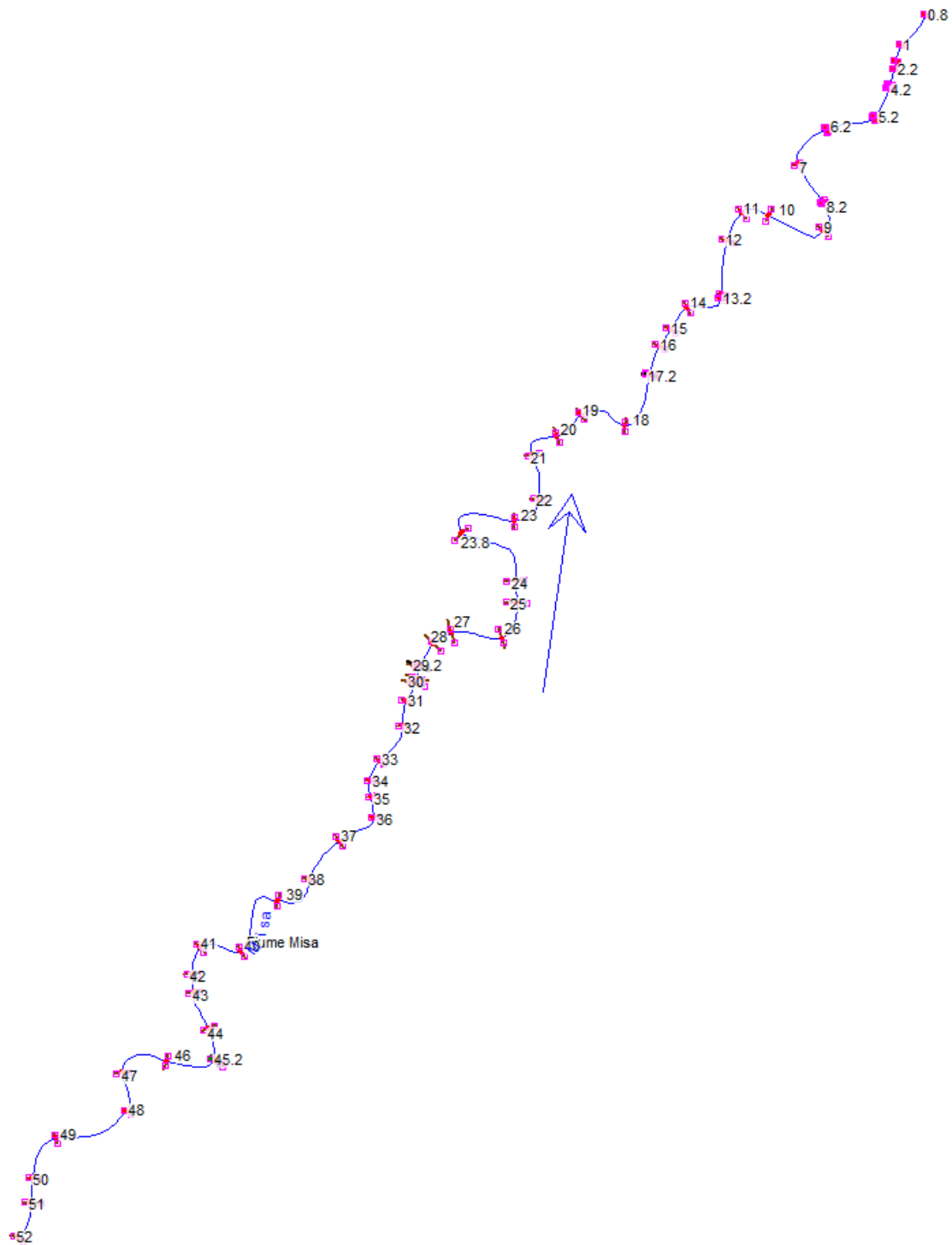


Figure 42. Overview of the 2001 Misa River project.

The steady state analysis has been conducted mainly to verify the correctness of the model, being this kind of analysis the simplest one.

4.1 Cross-section removal

Before performing the simulation, an adjustment relative to the most upstream portion of the river have been conducted in order to work with a geometry as representative as possible. For this reason, the first step has been the removal of the sections which were located upstream the section 45 (Figure 43). This operation has been made because the available HEC-RAS boundary conditions allow to enter the flow values directly at the most upstream section and, being the most upstream cross-section too far with respect to the section 44.2, i.e., in the location where both stage and flow values are measured, this would slightly affect the simulation results. It was not possible to directly consider the cross-section 44.2 as upstream boundary condition because, in presence of bridges, the HEC-RAS software needs at least two free cross-sections upstream of the bridge in order to avoid simulation instability phenomena.

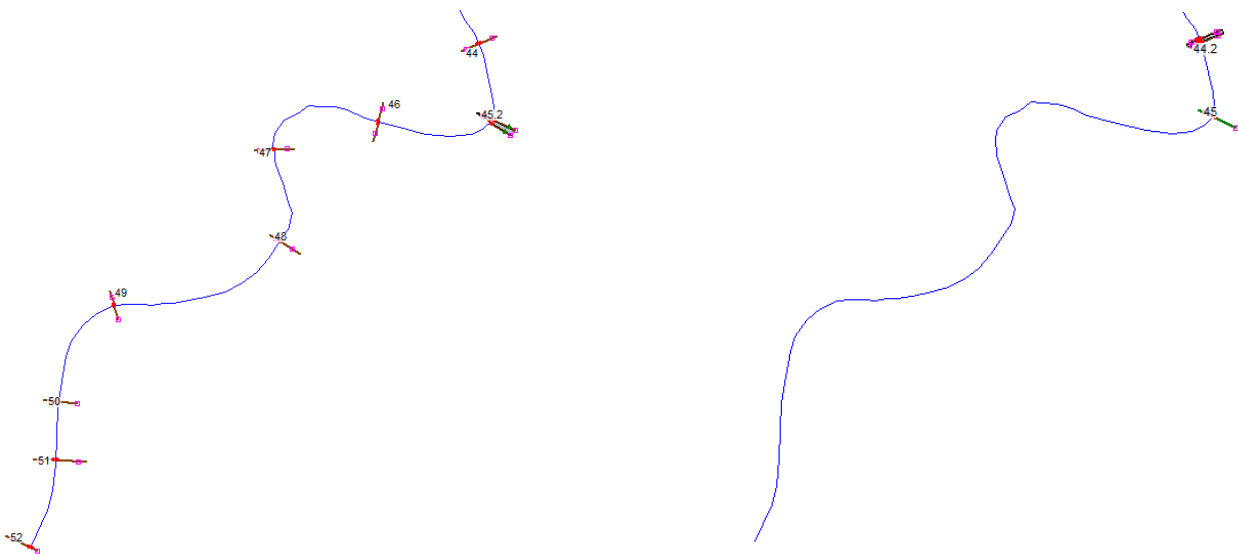


Figure 43. Upstream cross-sections removal.

The removal of these sections has been carried out by acting on the GIS Tools menu of the Geometric Data window. Since all the cross-sections are georeferenced, the simple removal of the undesired ones from the HEC-RAS software, would have provoked an instantaneous readjustment of all the remaining cross-sections, rearranging them in order to cover all the initial length of the river, with a subsequent offset of the distances between the cross-sections. To overcome this issue, the

georeferencing has been removed only to the desired cross-sections, and only after this operation, the unnecessary cross-sections have been removed.

4.2 Bettollelle bridge positioning

From a comparison between the cross-sections of the model, the AutoCAD file representing the cross-sections of the river derived from the Marche Region survey, and the Google Earth images, it has been possible to identify an inconsistency relative to the Bettollelle bridge positioning. In particular, the bridge inside HEC-RAS was assigned to a wrong section.

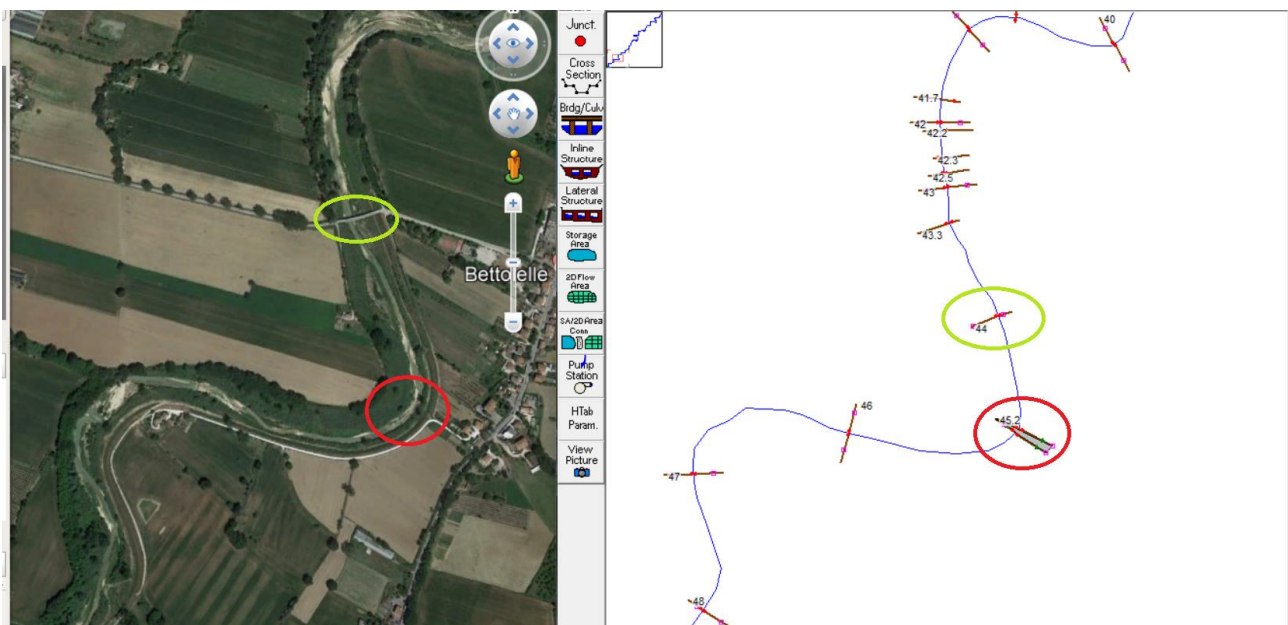


Figure 44. Bettollelle bridge positioning. The left image shows the Google Earth top view of the Bettollelle bridge while the right image shows the assignation of the bridge in HEC-RAS. The green circles indicate the correct positioning of the bridge while the red circles indicate the wrong bridge assignation.

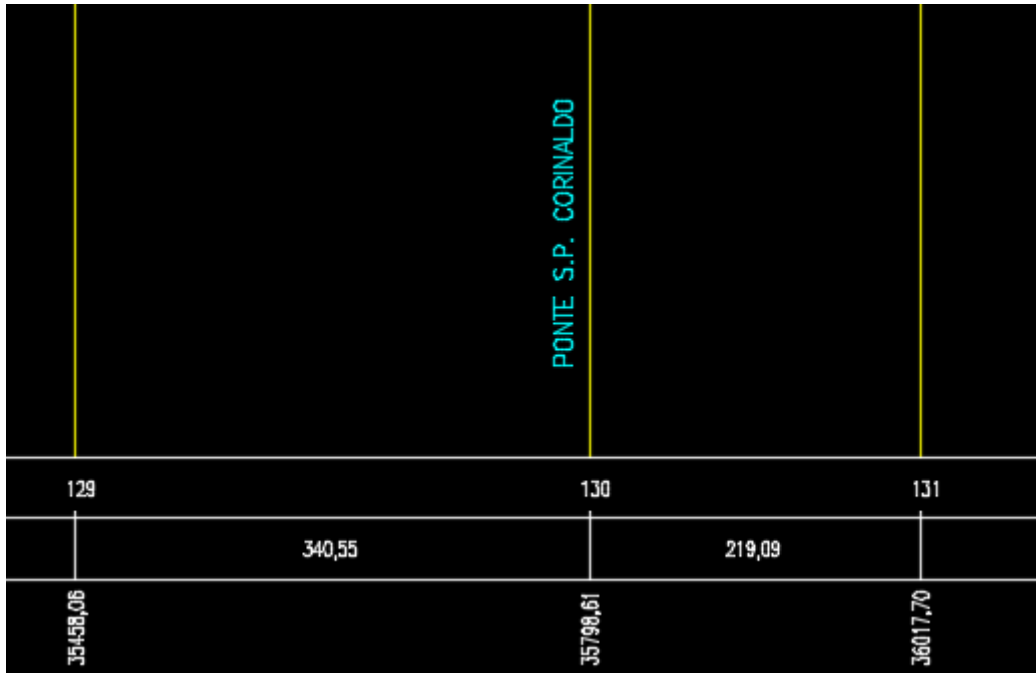


Figure 45. Bettolle bridge wrong positioning in AutoCAD.

As noticeable from the (Figures 44 and 45), the bridge was assigned to the cross-section 130 (identified with the number 45) rather than to the cross-section 131 (identified with the number 44). Therefore, before starting the simulation, the bridge has been moved back to the correct position (Figures 46 and 47).

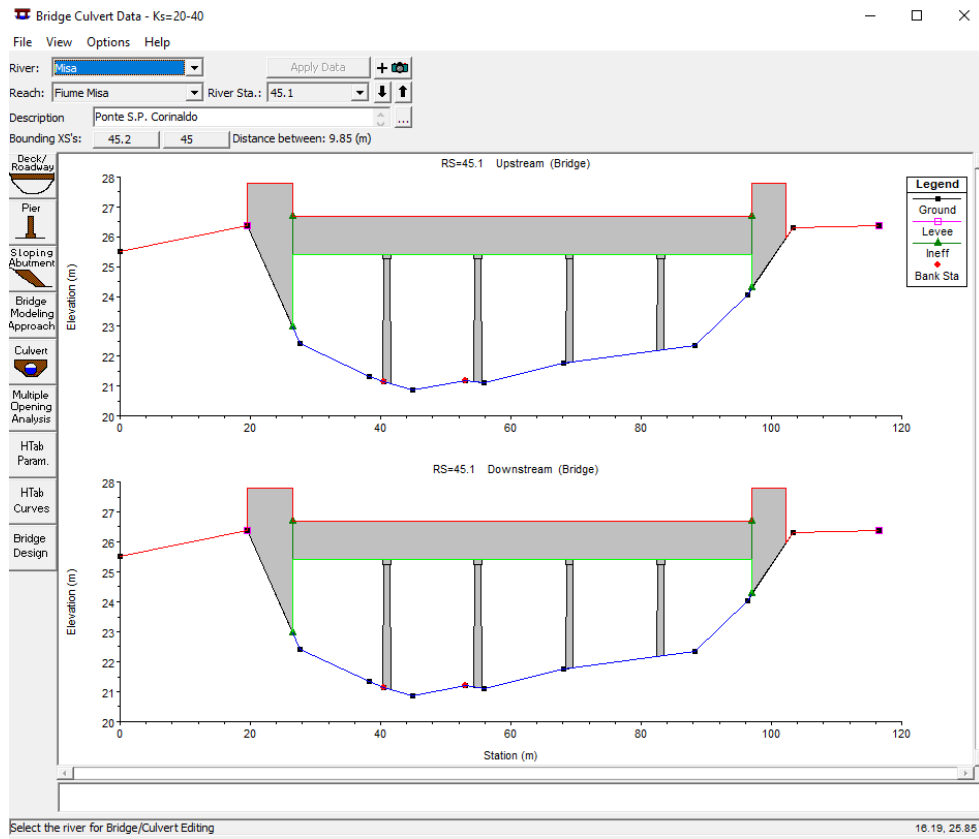


Figure 46. Bettolle bridge before modification.

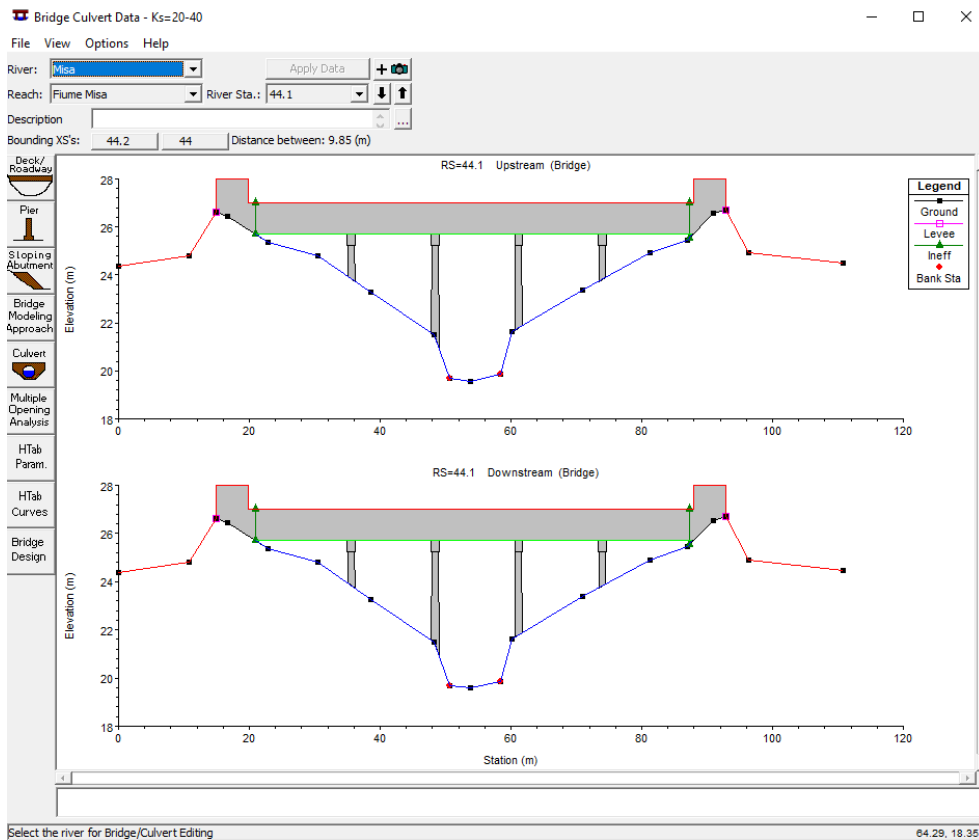


Figure 47. Bettolle bridge after modification.

Once the bridge was in the correct position a steady state simulation has been carried out showing a lack of errors, meaning that all the required parameters were correctly set (Figure 48).

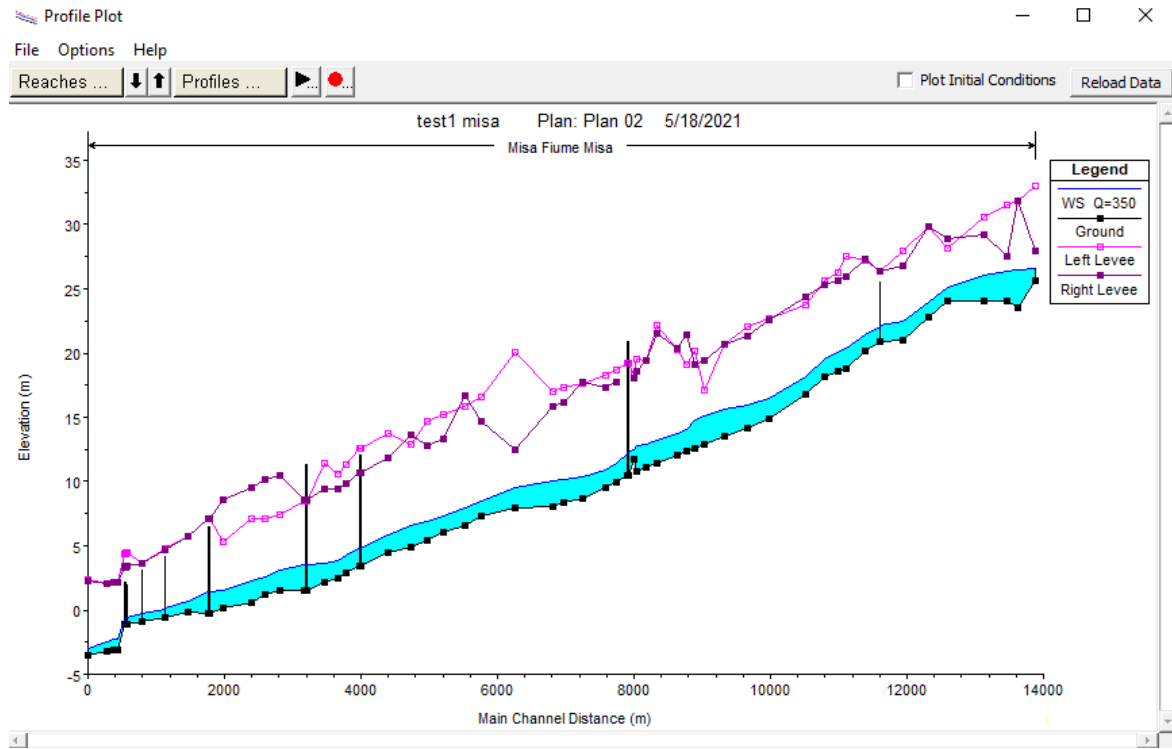


Figure 48. Steady state simulation result.

4.3 Bettollelle and Ponte Garibaldi 2019 cross-section implementation

For a better representation of the real conditions, since the cross-sections of this project date back to 2001, updated cross-sections of both Bettollelle and Ponte Garibaldi dating back to 2019 have been requested to the Civil Protection of the Marche Region and then implemented into the model.

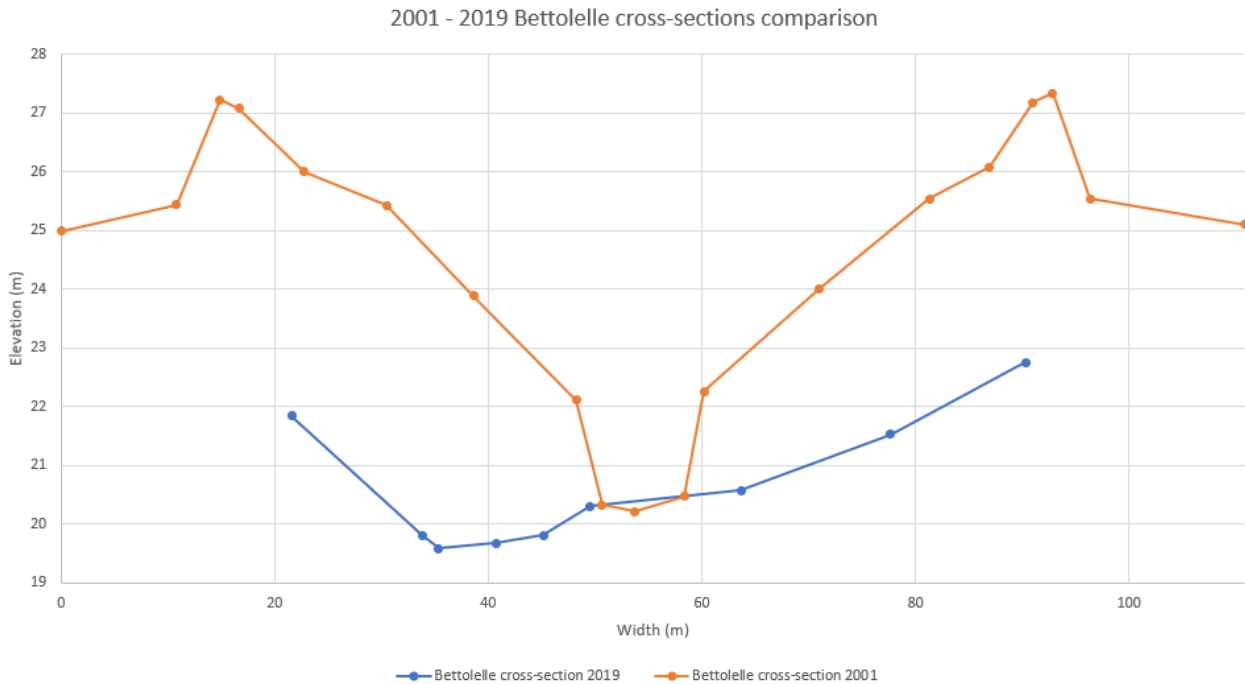


Figure 49. Comparison between Bettollelle 2001 and Bettollelle 2019 cross-sections.

As shown in Figure 49, the main channel of the 2019 Bettollelle cross-section considerably differs from that of the 2001 one, in particular, over the years, the main channel changed significantly, probably due to erosion phenomena. Unfortunately, the updated cross-section was not fully surveyed and the levees are missing. Since the absence of the levees would not have allowed simulations characterized by high flows, due to unrealistic flooding phenomena, the 2019 cross-section levees have been reconstructed, taking into account the fact that the levees are only slightly subjected to geometry variation over time. In order to do so, the two cross-sections have been previously aligned by looking at the bridge piers as reference, and successively the levees of the 2019 cross-section have been extended up to the 2001 cross-section ones, as shown in Figure 50.

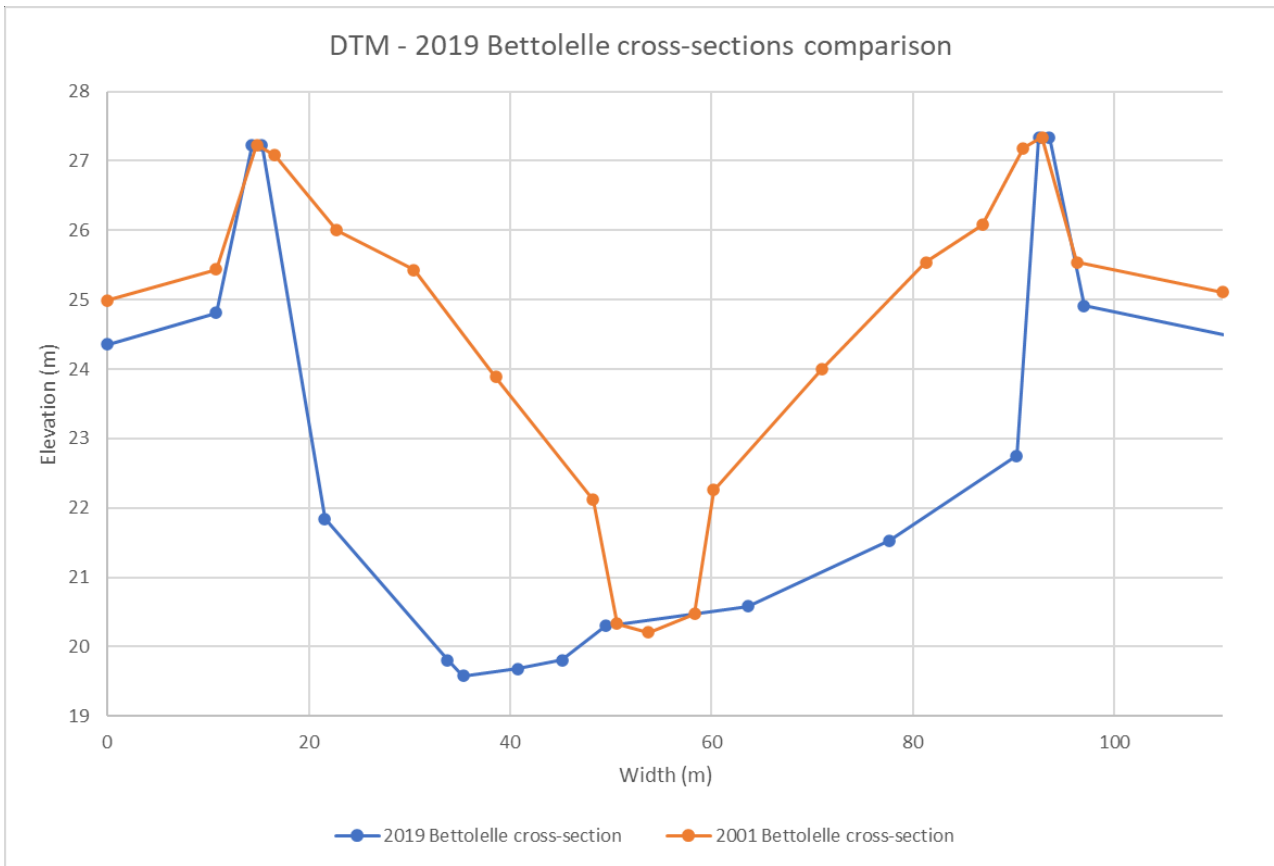


Figure 50. Bettollelle 2019 cross-section levees reconstruction.

For what concerns the Ponte Garibaldi cross-section, even though it is characterized by the presence of lateral walls, thus, not subjected to geometry variation over time, it is still affected to bathymetric modifications which impact on the simulation results. For this reason, the updated cross-section has been added into the model by following the survey of the 9th September 2019 (Figure 51).

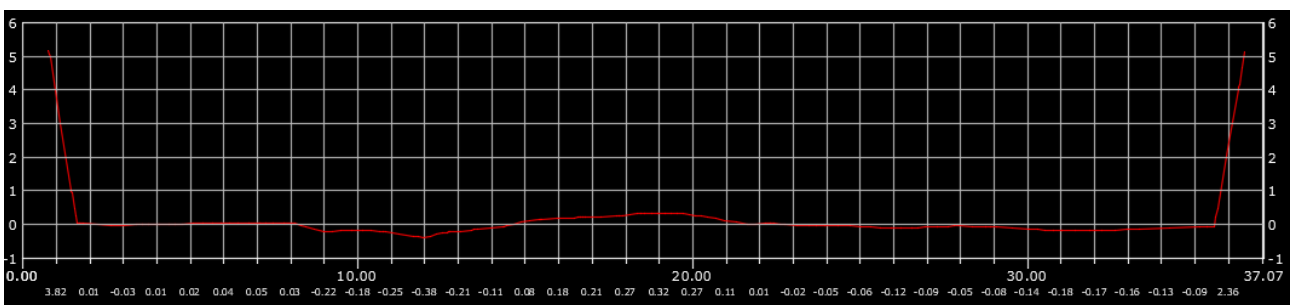


Figure 51. Ponte Garibaldi cross-section.

4.4 Boundary conditions

Once the river geometry has been correctly set, different simulations have been performed in order to evaluate how far the model outputs were if compared to the measured (real) data. In practice, for each simulation, a flow hydrograph characterized by an interval time of 30 minutes has been considered as upstream boundary condition (Figure 52). Regarding the downstream boundary condition, a stage hydrograph has been applied corresponding to the tidal motion measured at Ancona harbor (Figure 53), which well represents the tidal motion occurring at Senigallia as verified using data recently collected at Senigallia harbor.

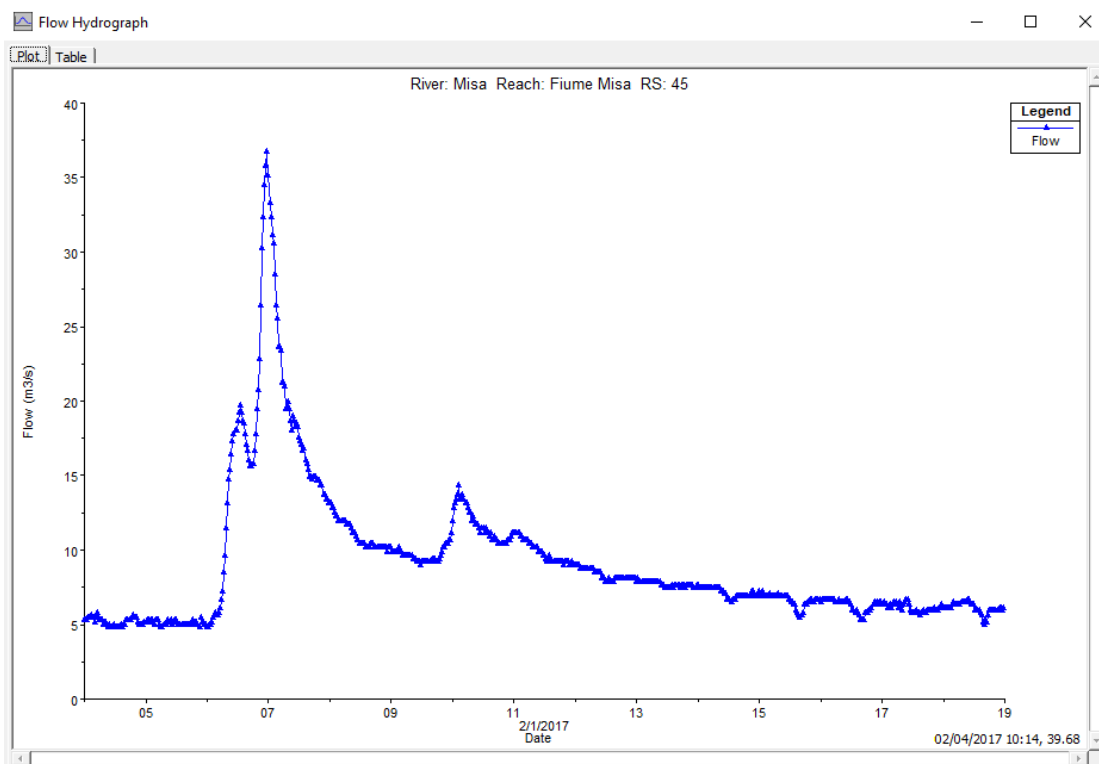


Figure 52. Flow hydrograph.

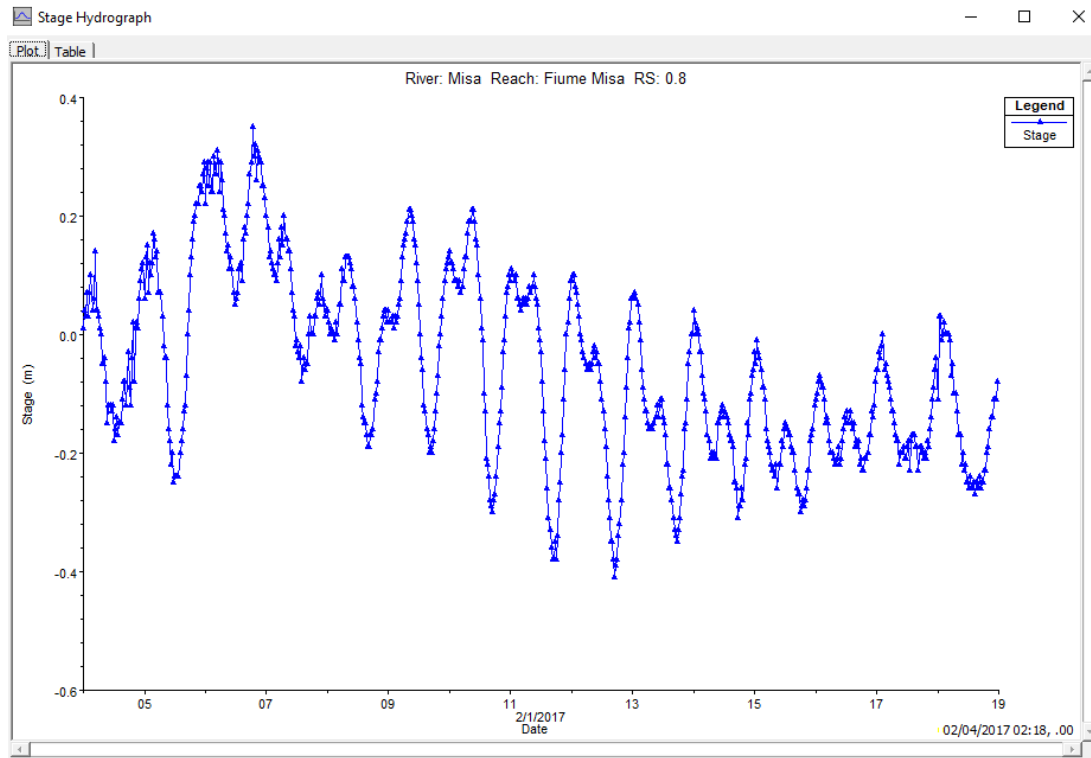


Figure 53. Stage hydrograph.

With the boundary conditions set, in the “Unsteady Flow Analysis” field, different trials concerning the simulation settings have been performed with the aim to optimize the software outputs. For the vast majority of the simulations, a computational interval of 5 minutes has been deemed the best one, balancing on one hand, the level of accuracy of the simulations and on the other hand, the time required to perform the analysis. Moreover, the time interval related to the simulation results has been set equal to 30 minutes in order to be compared with the data extracted from the SIRMIP website which represent the real stage values of the river.

Once all the previously mentioned operations have been performed, several simulations have been run with the aim of verifying the accuracy of the model with respect to the measured data (SIRMIP). In particular, among all simulations, the most relevant refer to the following periods:

- November 1st – November 30th 2016;
- January 26th – February 3rd 2017;
- February 4th – February 18th 2017;
- March 3rd – April 24th 2017;
- February 18th – March 5th 2018;
- December 27th – December 31st 2020.

4.5 Ponte Garibaldi runoff estimation

Since no rating curve is available at the Ponte Garibaldi to calculate the discharge values and, in turn, to have an indication of the surface runoff, an analysis in this regard has been carried out. To verify how much the surface runoff present between Bettolle and Ponte Garibaldi impacts on the river discharge, a graph “specific discharge vs area of the basin” has been realized considering both the annual average discharges and the maximum discharges of three river stations belonging to the same basin of the Misa River. Precisely, the stations that have been taken into account have been Serra de’Conti, Corinaldo, Bettolle and Ponte Garibaldi. In order to build up the graphs, the years 2017 – 2018 – 2020 of the Serra de’Conti, Corinaldo and Bettolle stations have been worked out to get the respective annual average discharges and the maximum discharges for each of the considered years. Afterwards, the discharge values have been divided for the respective area of the basin in order to obtain the specific discharge. The following calculation is only referred to the yearly maximum discharge.

	Yearly maximum discharge		
	Serra de Conti	Corinaldo	Bettolle
2017	135.59955	67.93603	88.44215
2018	30.81258	72.14205	77.99226
2020	16.66189	29.13030	22.59771

Table 3. Yearly maximum discharges.

$$\begin{aligned}
 \text{2017 Serra de Conti yearly maximum specific discharge} &= \frac{135.59955}{72900000} \\
 &= 1.86008 \cdot 10^{-6} \left(\frac{m}{s}\right)
 \end{aligned}$$

$$\begin{aligned}
 \text{2018 Serra de Conti yearly maximum specific discharge} &= \frac{30.81258}{72900000} \\
 &= 4.22669 \cdot 10^{-7} \left(\frac{m}{s}\right)
 \end{aligned}$$

$$\begin{aligned}
 \text{2020 Serra de Conti yearly maximum specific discharge} &= \frac{16.66189}{72900000} \\
 &= 2.28558 \cdot 10^{-7} \left(\frac{m}{s}\right)
 \end{aligned}$$

$$2017 \text{ Corinaldo yearly maximum specific discharge} = \frac{67.93603}{119500000} = 5.68502 \cdot 10^{-7} \left(\frac{m}{s}\right)$$

$$2018 \text{ Corinaldo yearly maximum specific discharge} = \frac{72.14205}{119500000} = 6.03699 \cdot 10^{-7} \left(\frac{m}{s}\right)$$

$$2020 \text{ Corinaldo yearly maximum specific discharge} = \frac{29.13030}{119500000} = 2.43768 \cdot 10^{-7} \left(\frac{m}{s}\right)$$

$$2017 \text{ Bettollelle yearly maximum specific discharge} = \frac{88.44215}{333590000} = 2.65122 \cdot 10^{-7} \left(\frac{m}{s}\right)$$

$$2018 \text{ Bettollelle yearly maximum specific discharge} = \frac{77.99226}{333590000} = 2.33797 \cdot 10^{-7} \left(\frac{m}{s}\right)$$

$$2020 \text{ Bettollelle yearly maximum specific discharge} = \frac{22.59771}{333590000} = 6.77410 \cdot 10^{-8} \left(\frac{m}{s}\right)$$

	Yearly maximum specific discharge (m/s)		
	Serra de Conti	Corinaldo	Bettollelle
2017	1.86008E-06	5.68502E-07	2.65122E-07
2018	4.22669E-07	6.03699E-07	2.33797E-07
2020	2.28558E-07	2.43768E-07	6.77410E-08

Table 4. Yearly maximum specific discharges.

Average Serra de Conti specific discharge

$$= \frac{1.86008 \cdot 10^{-6} + 4.22669 \cdot 10^{-7} + 2.28558 \cdot 10^{-7}}{3} = 8.37101 \cdot 10^{-7} \left(\frac{m}{s}\right)$$

Average Corinaldo specific discharge

$$= \frac{5.68502 \cdot 10^{-7} + 6.03699 \cdot 10^{-7} + 2.43768 \cdot 10^{-7}}{3} = 4.71990 \cdot 10^{-7} \left(\frac{m}{s}\right)$$

Average Bettollelle specific discharge

$$= \frac{2.65122 \cdot 10^{-7} + 2.33797 \cdot 10^{-7} + 6.77410 \cdot 10^{-8}}{3} = 1.88887 \cdot 10^{-7} \left(\frac{m}{s}\right)$$

At this point, the specific discharge values have been used in the graph together with the area of the basin relative to each station.

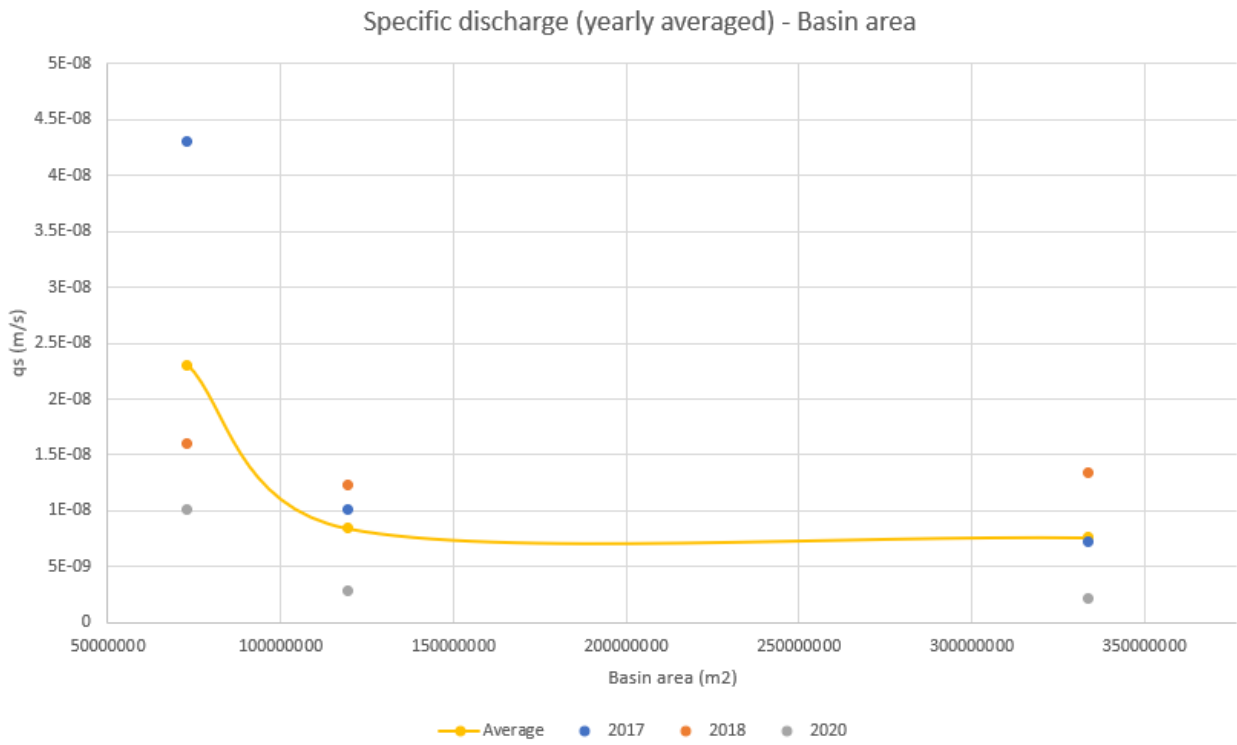


Figure 54. Yearly averaged specific discharge.

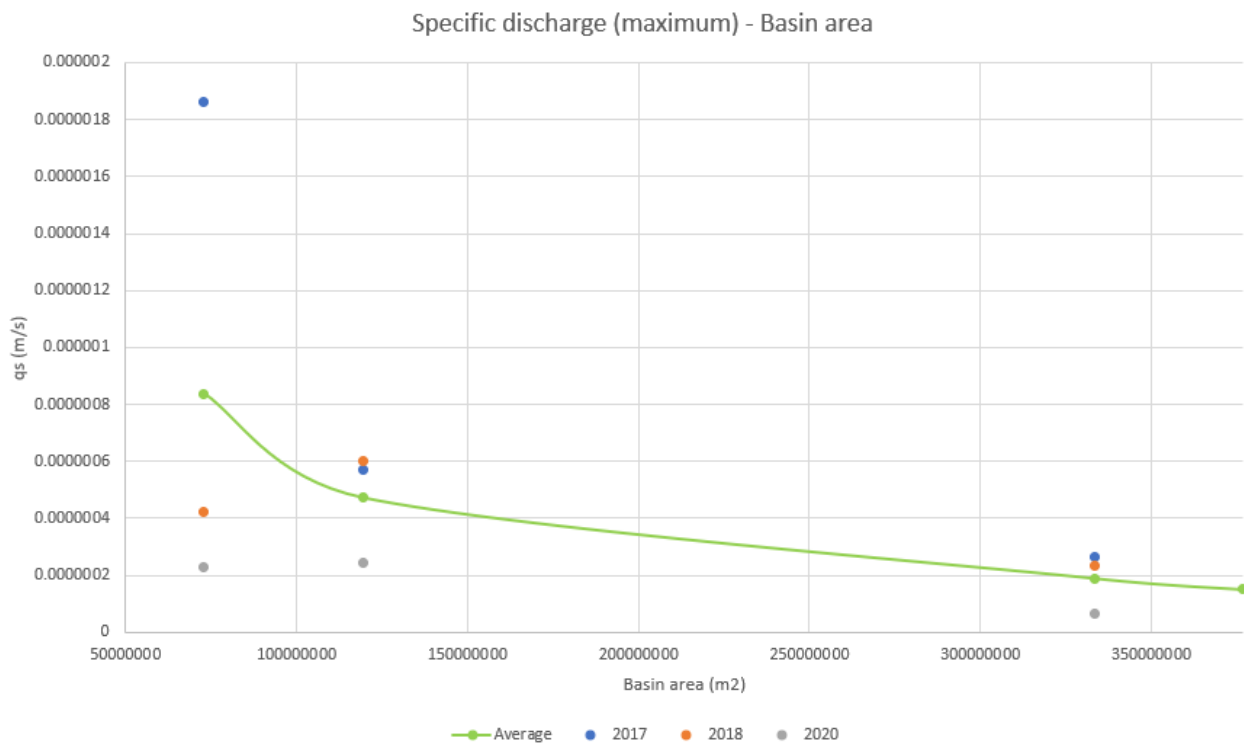


Figure 55. Yearly maximum specific discharge.

As shown in Figures 54 and 55, the colored dots represent the specific discharge of each year relative to the different considered stations. In particular, the Serra de'Conti station is the closest to the origin of the axis, considering that it accounts for a basin area of 72.9 km², while, the stations of Corinaldo (119.5 km²) and Bettolle (333.59 km²) follow. The two graphs present in Figure 54 and 55, display a similar shape, even though the one which considers the maximum discharges owns a more pronounced decreasing trend if compared to the other one, as highlighted by the average solid green line, meaning that a lower specific discharge occurred moving towards the coast. To have an estimate of the surface runoff present between the Bettolle and the Ponte Garibaldi stations, the solid green line, which represents the average values of the maximum discharge of the considered years, has been extended up to the area referring to the Ponte Garibaldi (383 km²). At that position, the corresponding specific discharge value has been multiplied by the area of the basin belonging to the Ponte Garibaldi station, resulting in a low discharge value that has been considered as negligible.

$$Ponte\ garibaldi\ runoff = 0.00000015 \cdot 383000000 = 57.45 \frac{m^3}{s}$$

However, this test provides just a rough estimate of the possible surface runoff, thus it cannot be considered reliable, since, due to a lack of data, it has been conducted by exploiting discharge values corresponding to only few years, while a higher number of years would have returned a more robust analysis.

4.6 Senigallia wastewater treatment plant discharge analysis

In order to account for all the possible flows contributing to the feeding of the Misa River, the discharges outgoing from the Senigallia wastewater treatment plant have been looked into. This is a plant of activated sludge type, and it is characterized by a capacity of 100,000 equivalent population treating the waters deriving from a combined sewer system (Figure 56).



Figure 56. Senigallia wastewater treatment plant top view.

Different simulations have been selected as benchmarks to verify if the contribution deriving from these discharges would have been able to bring significant variations in water elevation at the Ponte Garibaldi cross-section. To have access to the wastewater treatment plant discharges, the Viva Servizi S.p.A has been contacted, which sent the required data. The wastewater treatment plant discharge data have been filtered and brought back to an interval time of 30 minutes in order to be comparable to the recorded data, since the gauge of the wastewater treatment plant gives back a discharge value every 15 seconds. To implement this additional water contribution into the software, a Lateral Inflow Hydrograph has been added at the cross-section 14, which represents the closest available cross-section to the real position of the wastewater treatment plant (Figures 57 and 58).

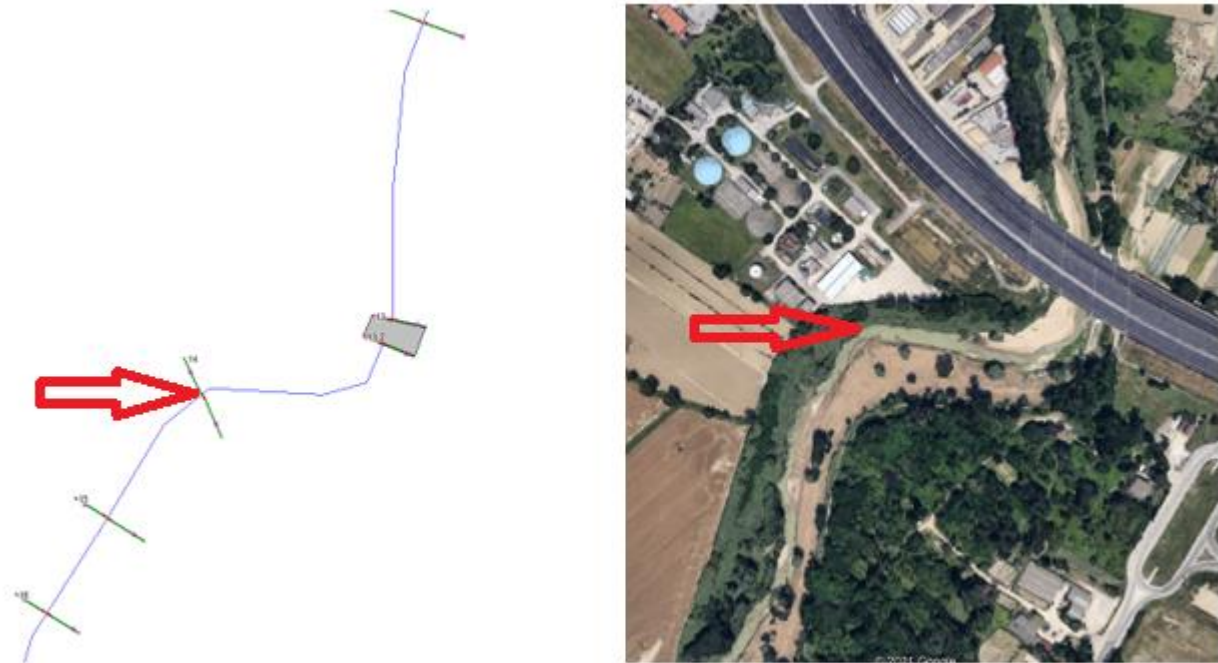


Figure 57. Cross-section selection for the wastewater treatment plant discharge implementation.

Lateral Inflow Hydrograph

River: Misa Reach: Fiume Misa RS: 14 to 13.2

Read from DSS before simulation Select DSS file and Path

File:

Path:

Enter Table Data time interval: 30 Minute

Select/Enter the Data's Starting Time Reference

Use Simulation Time: Date: 04FEB2017 Time: 0000

Fixed Start Time: Date: 04FEB2017 Time: 0000

No. Ordinates

Hydrograph Data			
	Date	Simulation Time (hours)	Lateral Inflow (m3/s)
1	03Feb2017 2400	00:00	0.08
2	04Feb2017 0030	00:30	0.133
3	04Feb2017 0100	01:00	0.063
4	04Feb2017 0130	01:30	0.12
5	04Feb2017 0200	02:00	0.069
6	04Feb2017 0230	02:30	0.117
7	04Feb2017 0300	03:00	0.126
8	04Feb2017 0330	03:30	0.134
9	04Feb2017 0400	04:00	0.136
10	04Feb2017 0430	04:30	0.146
11	04Feb2017 0500	05:00	0.139
12	04Feb2017 0530	05:30	0.128
13	04Feb2017 0600	06:00	0.064
14	04Feb2017 0630	06:30	0.11
15	04Feb2017 0700	07:00	0.043

Time Step Adjustment Options ("Critical" boundary conditions)

Monitor this hydrograph for adjustments to computational time step

Max Change in Flow (without changing time step):

Min Flow: Multiplier:

Figure 58. Lateral inflow hydrograph implementation.

The simulation results have shown a minimal influence of the wastewater treatment plant discharges on the Ponte Garibaldi station stages, increasing the water level of 1 cm at most. For this reason, the wastewater treatment plant contribution has been considered as negligible and has not been taken into account for the following simulations.

4.7 Digital terrain models implementation

Considering that the cross-sections belonging to the previous model date back to 2001, except for the Bettolle and Garibaldi ones, and that those cross-sections feature only a limited number of points, another way to get more updated cross-sections were needed. Since for the considered river stretch updated surveying campaigns were not available, the use of digital terrain models, which allows to both have more updated cross-sections and a higher number of points, have been considered. The Istituto Nazionale di Geofisica e Vulcanologia (INGV) offers the possibility of downloading for free either the digital elevation model of the whole Italy with a resolution of 100 meters, or smaller tablets with higher resolution (10 meters) always covering the whole Italian territory, both of them georeferenced and dated back to 2007. Considering that the DEM of the entire Italy would have had a too low resolution, only the tablet identifying the region of interest have been downloaded from the INGV site (Figures 59 and 60).

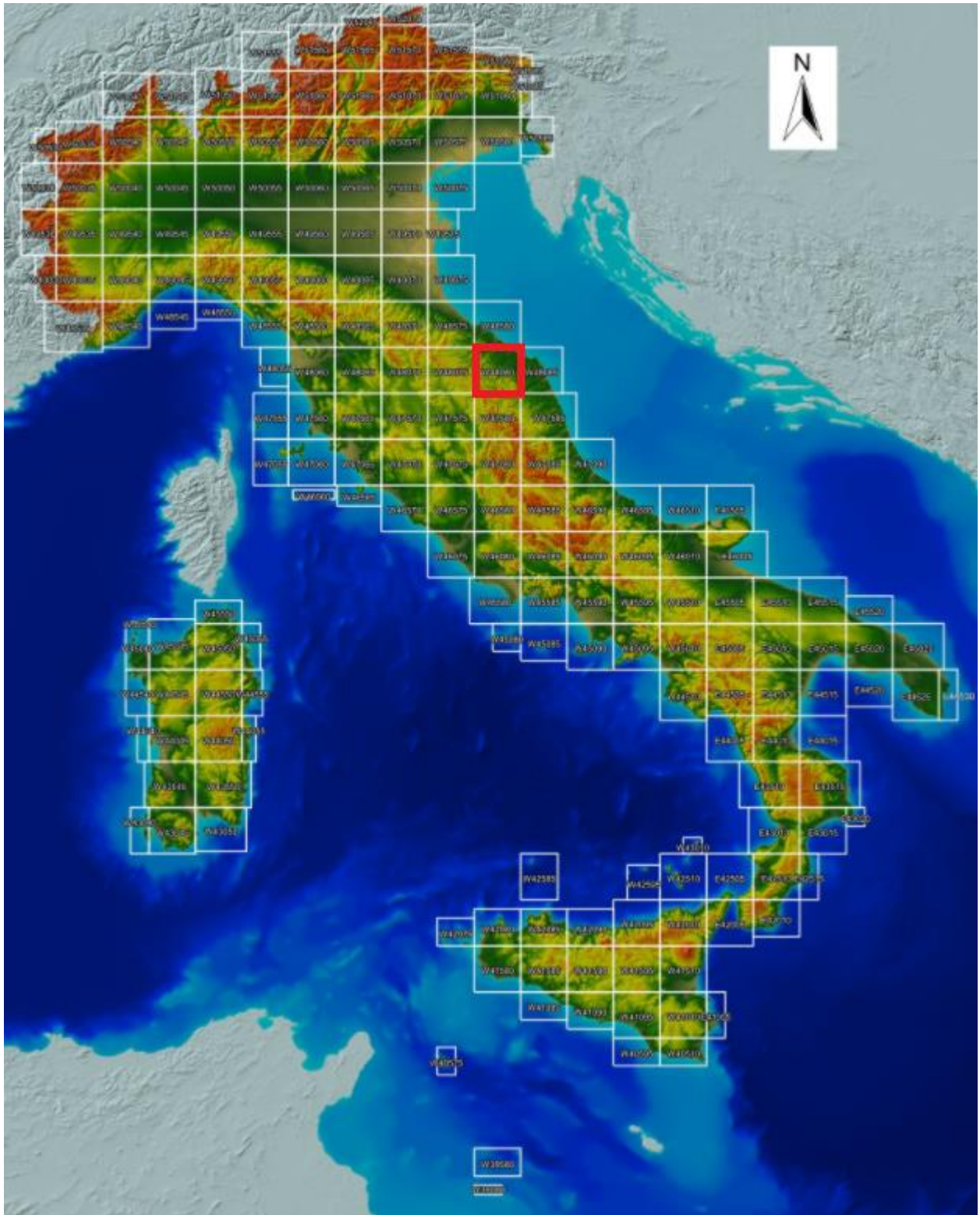


Figure 59. INGV DTM selection.

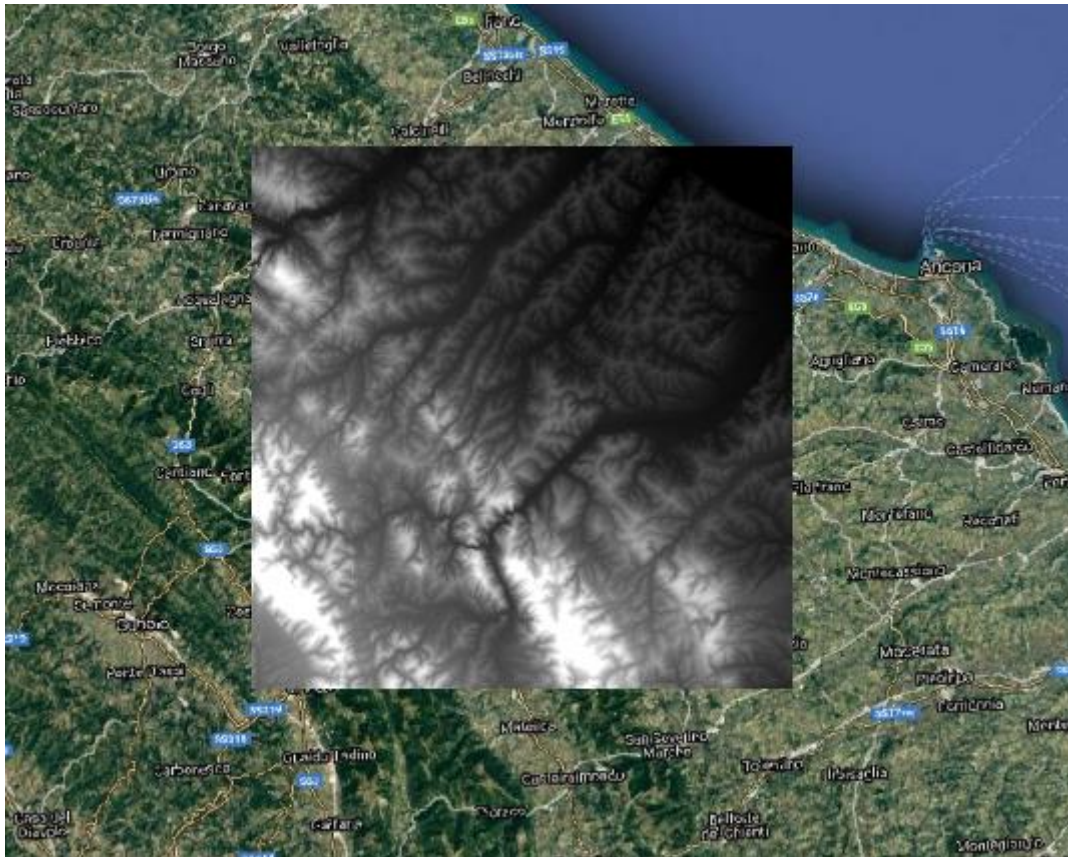


Figure 60. INGV DEM tablet for the area of interest.

Once the DEM has been downloaded, being it georeferenced, it has been opened with the QGIS software with the goal of extracting the projections which are needed to orient the raster when a new HEC-RAS project in RAS Mapper has to be created. However, the resolution of the latter has turned out to be still too low, denying the possibility of correctly identifying the river and subsequently to work with (Figure 61).

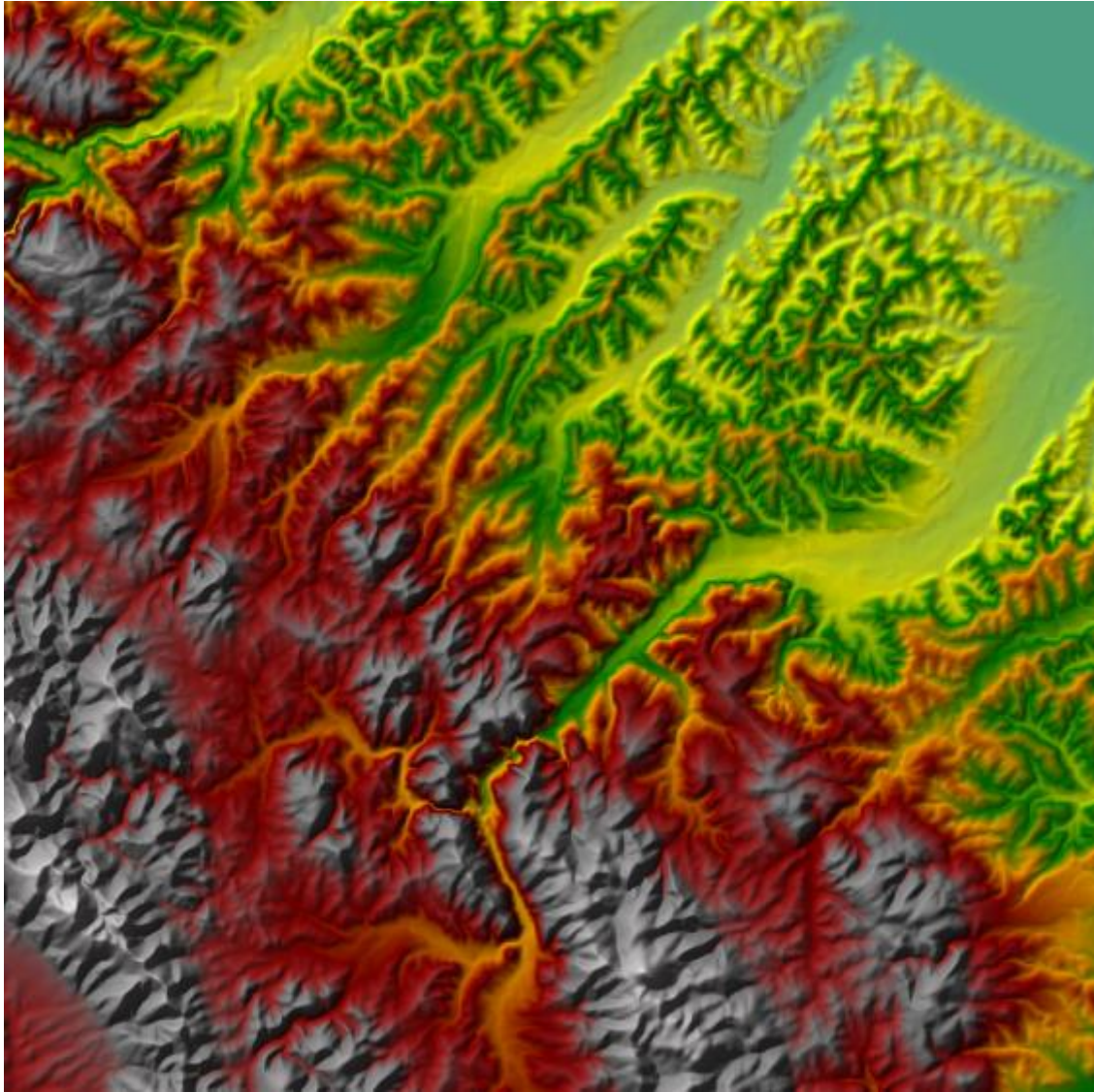


Figure 61. INGV DEM in HEC-RAS.

Even forcing the identification of the river by means of an imaginary layer, the number of the cross-sections points which would have been obtained from such a DEM, would not have been sufficient for a detailed characterization of the cross-sections of the river. In order to overcome this problem, a formal data request to the Ministero dell'Ambiente e della Tutela del Territorio e del Mare has been submitted with the aim at getting different Lidar data of the region of interest.

The requested data have been the digital terrain model (DTM), the digital surface model first return (DSM first), the digital surface model last return (DSM last) and the point cloud in *.xyz format, all referred to the 2008 survey. The DTM defines a generic statistic surface on which at a defined couple of points (X, Y), is attributed an elevation value (Z). The main difference between a DTM and a DSM lies on the fact that the former accounts only for the natural trend on the soil, whereas the latter

considers also the objects that are present on the ground surface, such as anthropic elements (buildings) or natural ones (trees). The DSM first and DSM last indicate the impulses derived from the Lidar laser rays which are reflected in relation to the met objects. In particular the DSM first returns the characteristics of all the points that are hit by the laser rays, while, considering the DSM last, if the laser scanner is capable of performing more scans, a less detailed model devoid of redundant points is obtained. The cloud point in *.xyz format, is the raw result of the laser acquisition, and it is composed of all the points collected by the Lidar provided with spatial coordinates.

Firstly, each single DTM table has been opened with the QGIS program, in order to remove the unnecessary tables, maintaining only the desired ones (Figure 62).

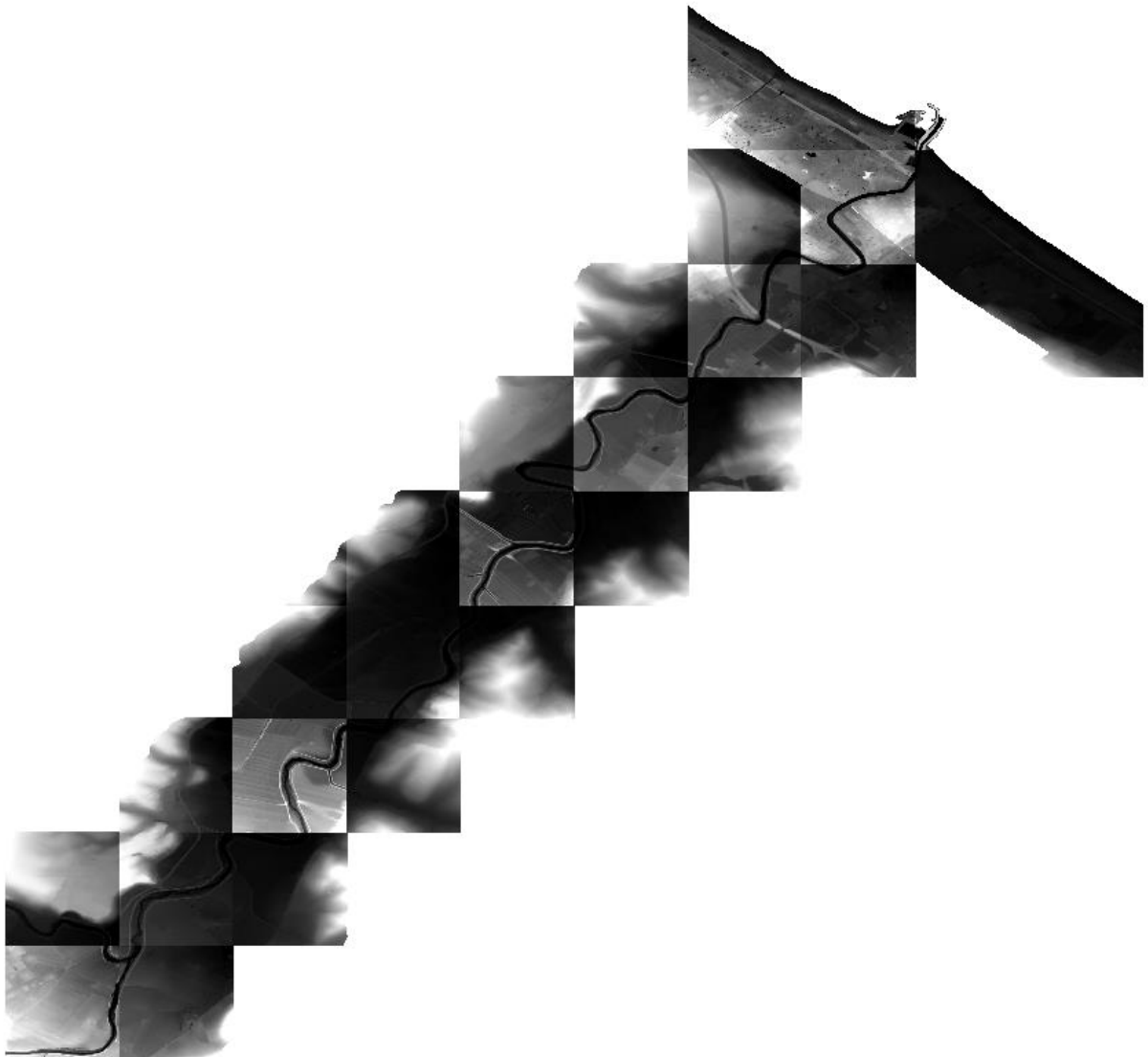


Figure 62. Selected DTM tables.

Before being opened with the HEC-RAS software, the single DTM tables have been reprojected, passing from the EPSG: 4326 coordinate reference system to EPSG: 32633 system, i.e., from geographic to cartographic coordinates referred to the WGS84, since the latter does not create positioning problems in the software. Subsequently, the projections relative to the merged DTM have been extracted from the QGIS software.

In HEC-RAS, the next step has been the selection of the projections which are needed for the representation of the digital terrain models. As the projections have been set up, the different DTMs have been implemented into the software through the window shown in Figure 63 in order to create a new terrain model:

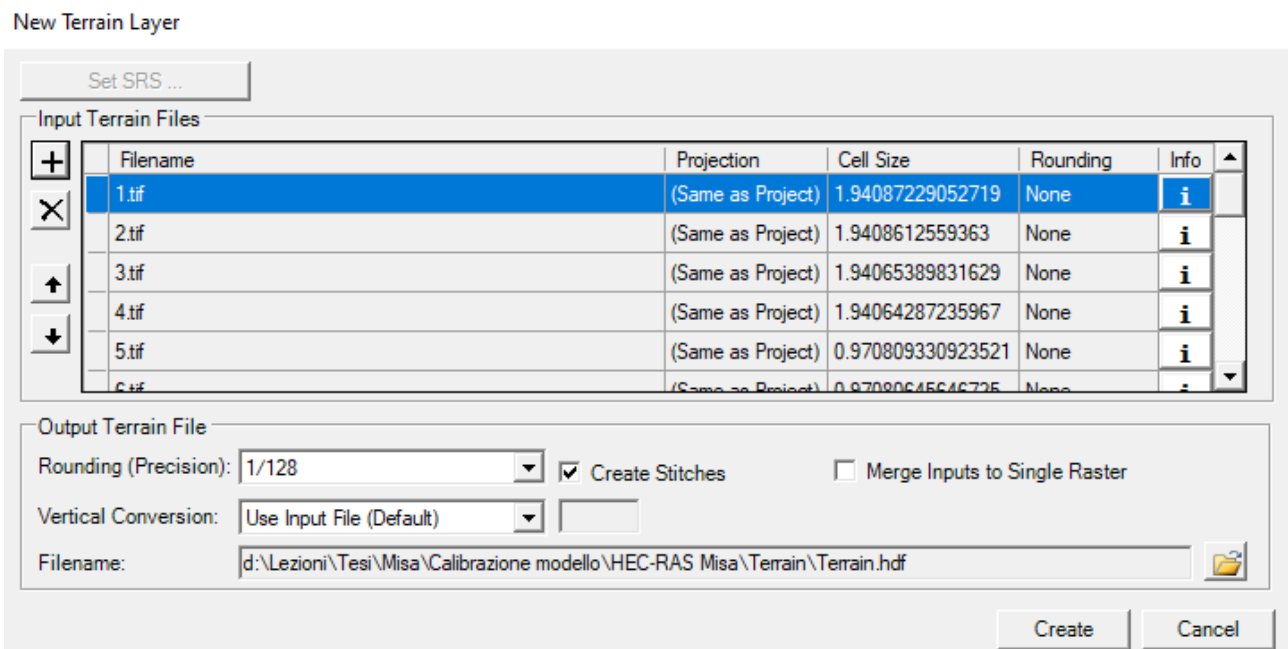


Figure 63. DTMs implementation.

Here, there is the possibility to either add just a single digital terrain model or different ones. In this work the DTM tables have been added into the software singularly. The different characteristics of the DTM such as the cell size (resolution of the DTM) and the Rounding, which indicates the elevation precision of the new terrain data layer, have been left as default.

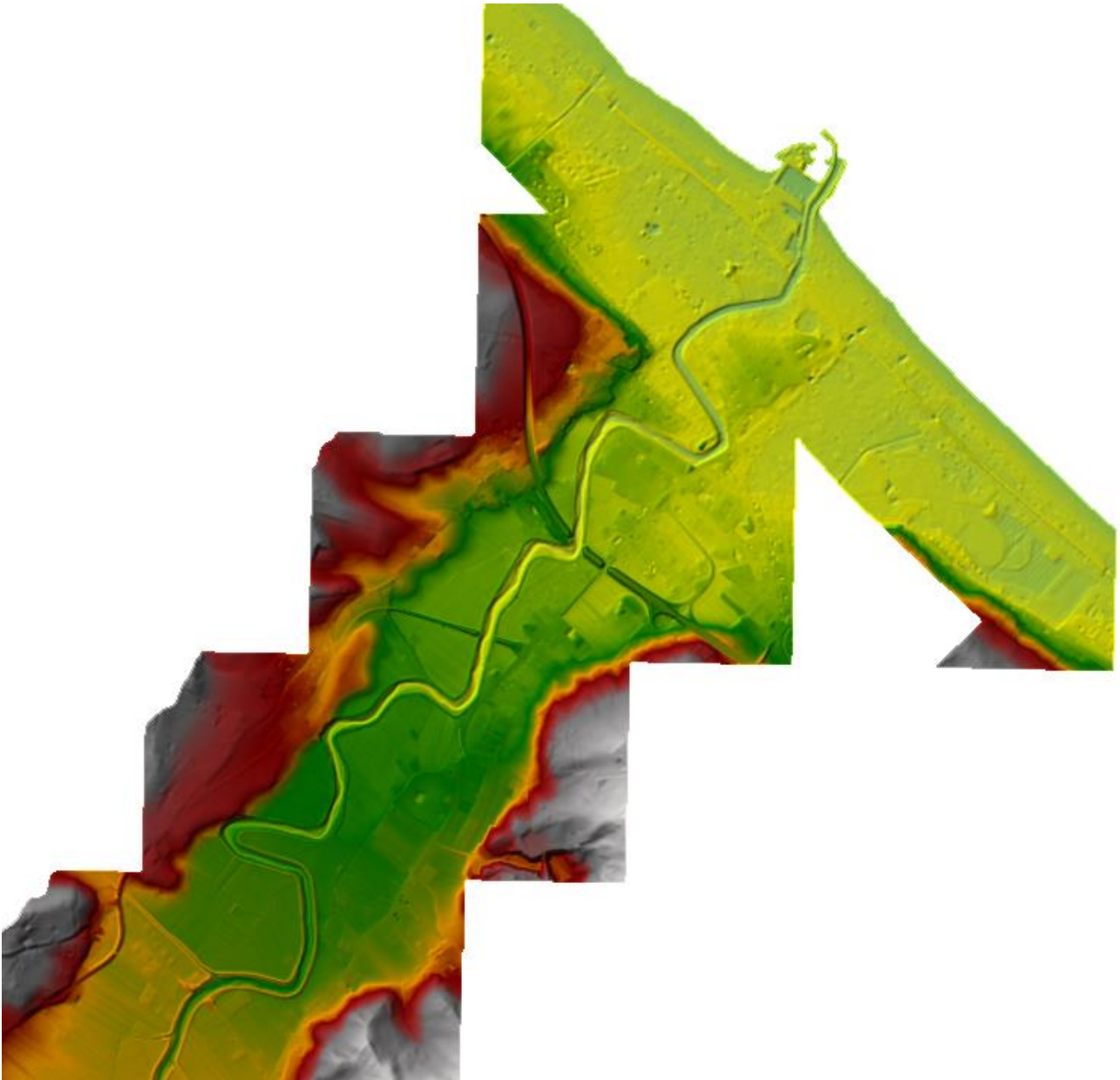


Figure 64. Misa River DTM in HEC-RAS.

Once the tables have been implemented into RAS Mapper (Figure 64), the addition of an imaginary layer, which represents a satellite image (for this work Google Satellite has been used), has been used as a method to check if the current terrain had been correctly created, in particular in terms of projections. Considering that the imaginary layer overlapped the terrain, the selected projections have been considered as correct (Figure 65).



Figure 65. DTM implementation check.

At this point, the next operation has been the creation of a new geometry. In order to build up the new geometry, the river flow direction, the bank lines, the flow path (which stands for the extension of the floodplain) and the desired cross-sections (which have been increased in number in correspondence of curves and cross-section variations), have been directly drawn on the terrain by means of the dedicated tools (Figure 66).

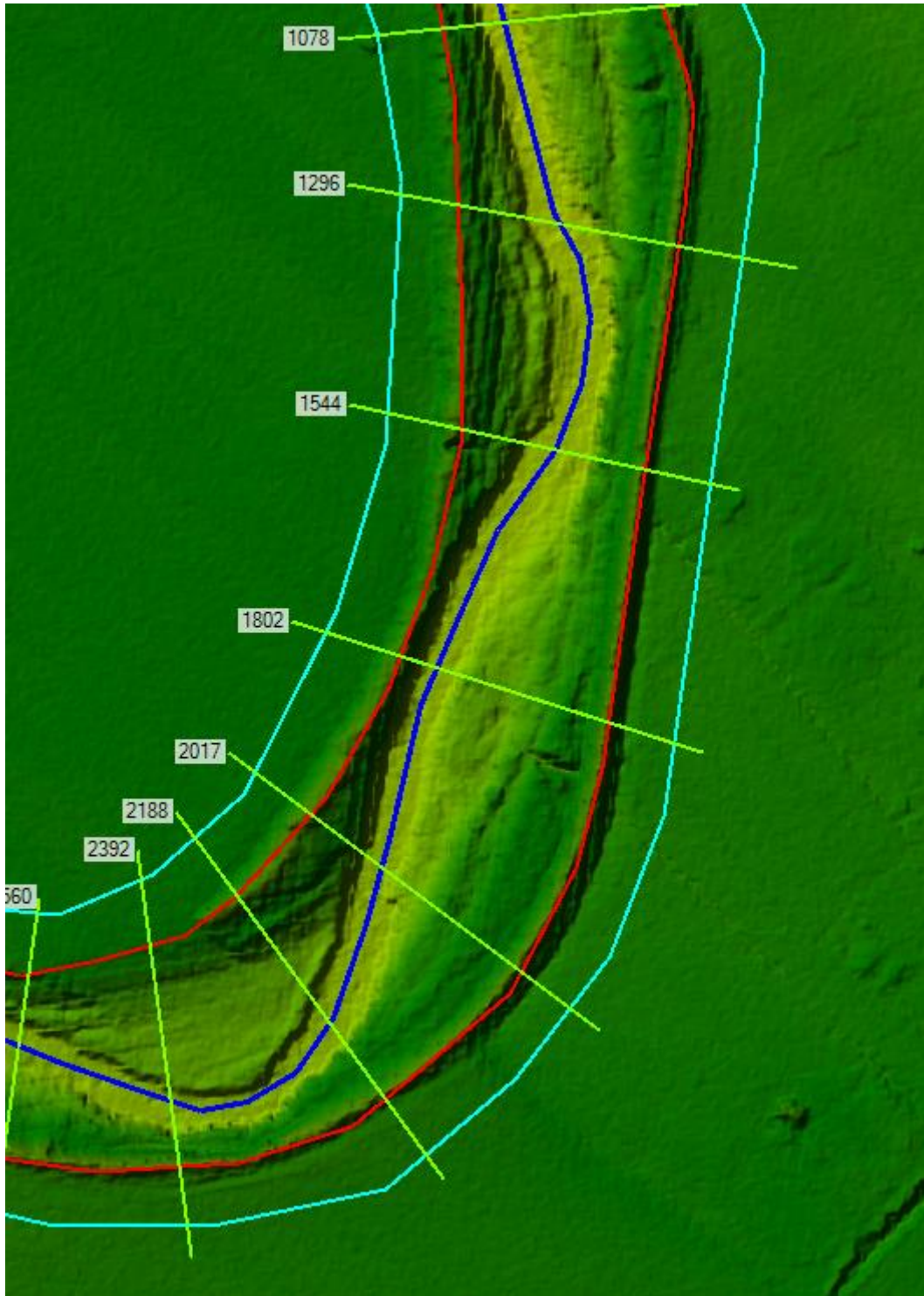


Figure 66. Misa River geometry in RAS Mapper. In blue the river flow direction, in red the bank lines and in cyan the flow path.

In particular the first step of the geometry construction has been the drawing of the river center line which has to be drawn starting from upstream and moving towards downstream in order to identify the river flow direction. Later, the bank lines have been drawn, positioning them in correspondence

of the levees. The same procedure has been applied for the implementation of the flow path. For what concerns the cross-sections, they have been added on the digital terrain model starting from the most upstream one, trying to implement a sufficient number to avoid instability of the software.

Once the geometry has been correctly set, the different drawn cross-sections have been interpolated.

The interpolation is a useful operation which allows to link different points within consecutive cross-sections of the DTMs in order to have a continuity of the terrain (Figure 67 and 68).

To perform the interpolation of the selected cross-sections, which has been directly done in RAS Mapper, different steps have been performed:

- Selection of the extraction method. There are essentially two ways to execute the extraction: the first one is devoted to the creation of a GeoTiff file which considers only the main channel for the interpolation, and in this case only the portion of DTM bounded by the bank lines will be extracted; the second way accounts for both the main channel and the overbanks and has been the one used to model the Misa River;
- Selection of the size with which the terrain will be extracted, considering that to a lower size corresponds a higher definition but also a higher computation time and vice versa. For this reason, a size of 0.5 m has been selected;
- Implementation of the extracted geometry with the current terrain in the “New Terrain Layer” window, paying attention to let the extracted file as first file in order to maintain its characteristic.



Figure 67. River geometry before interpolation.

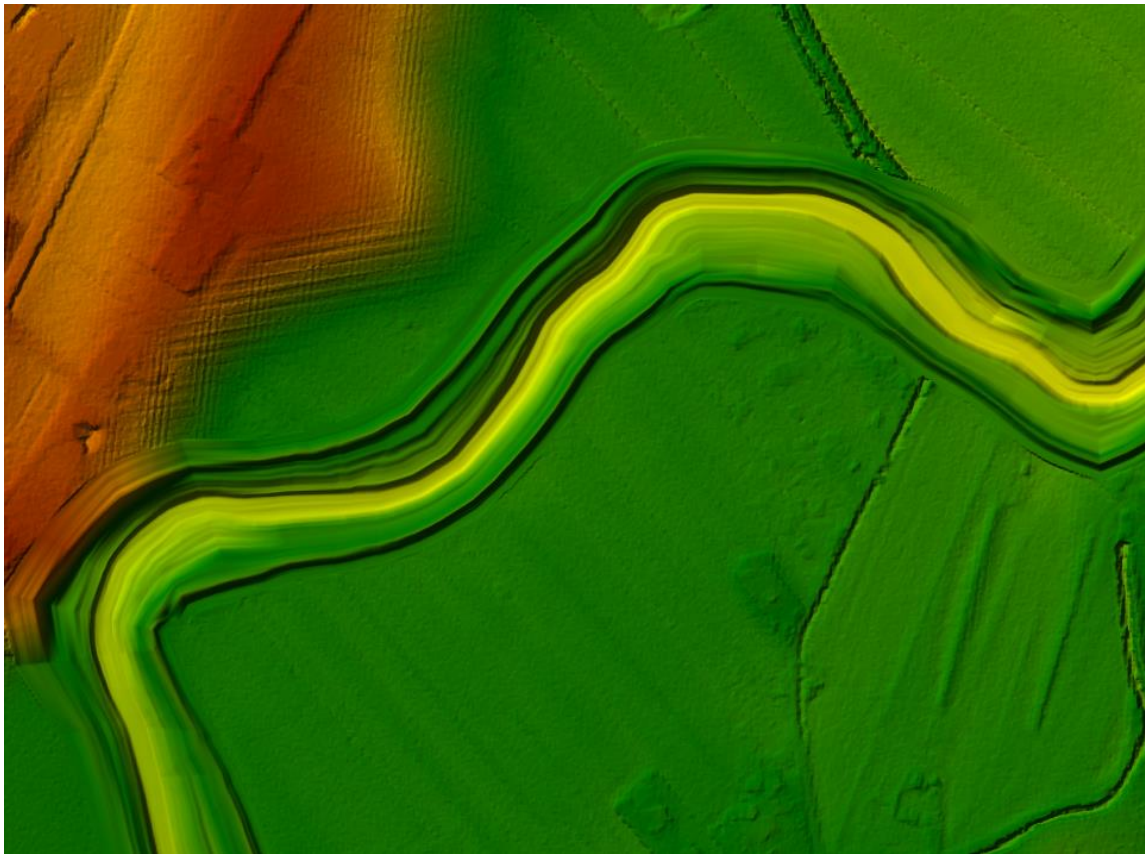


Figure 68. River geometry after interpolation.

The interpolation operation has been performed every time a new modification was implemented into the model, always following the previously mentioned procedure.

4.8 Walls implementation

Due to the fact that the walls present in the last stretch of the river (about 1.3 km upstream of the river mouth) were not well represented by the Lidar survey of the Ministry, the cross-sections belonging to that area have been manually modified, reconstructing the walls relying on the cross-sections of the Civil Protection of 2001 (Figures 69 and 70).

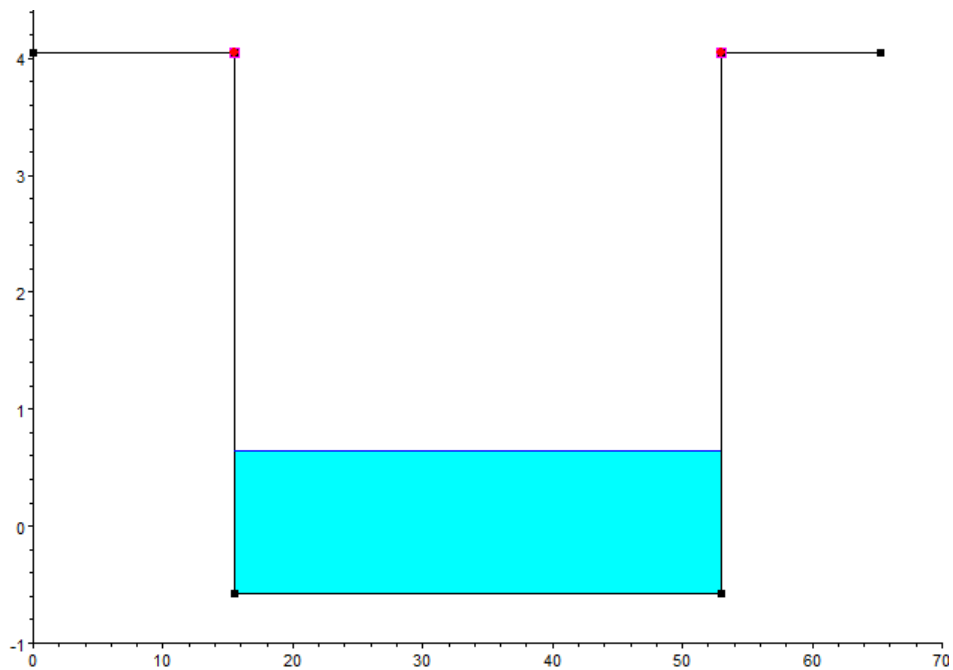


Figure 69. Walls reconstruction.

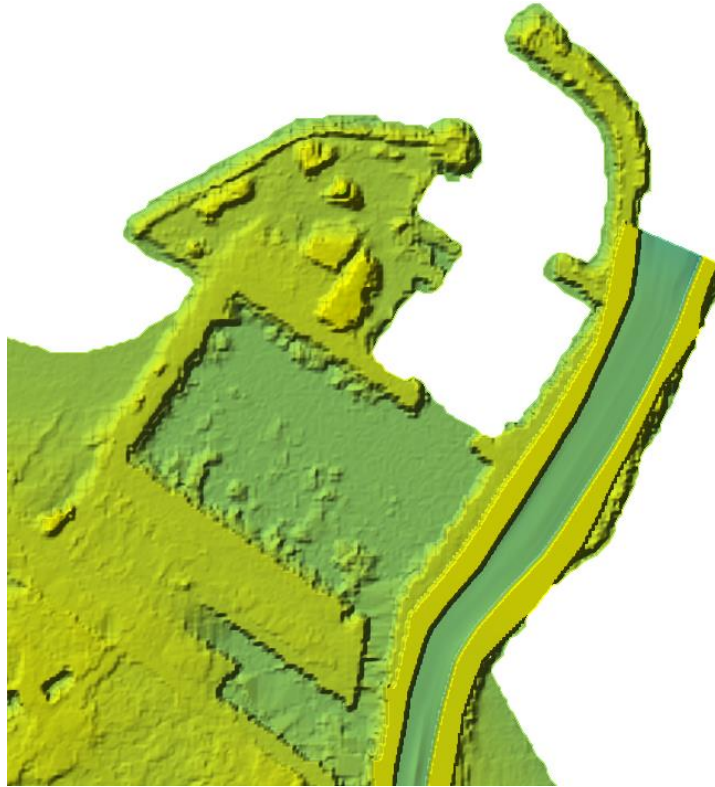


Figure 70. River geometry after the walls implementation.

4.9 DTM Bettollelle cross-section – Civil Protection 2019 Bettollelle cross-section comparison

At this point, a comparison between the DTM Bettollelle cross-section and the Civil Protection 2019 Bettollelle cross-section has been done to evaluate how much the two cross-sections differed one from the other (Figure 71).

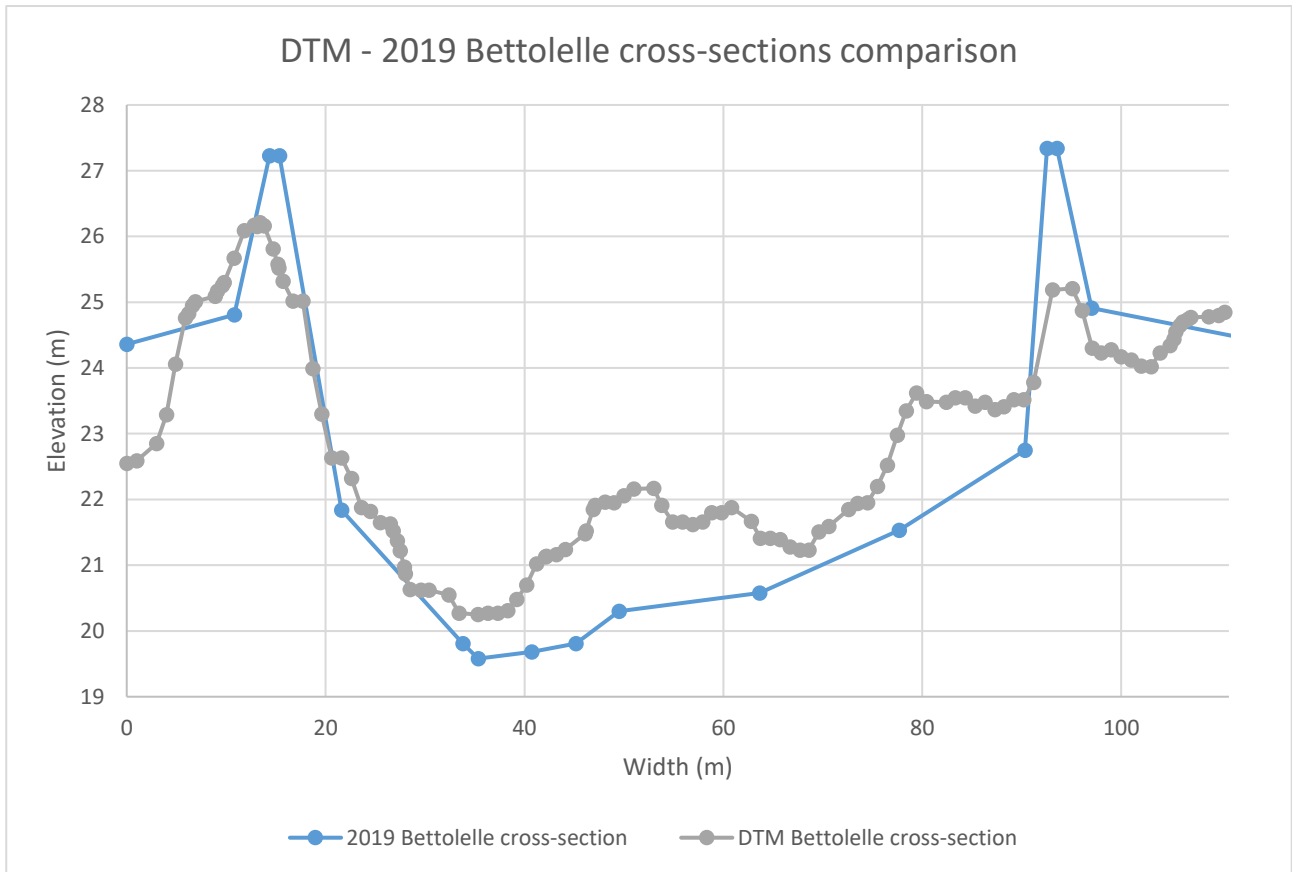


Figure 71. Comparison between the Civil protection 2019 and the DTM Bettollelle cross-sections.

Since from the comparison a significant difference in terms of levees height has emerged, the levees of 2019 Bettollelle cross-section have been reduced in order to be in line with those deriving from the DTM cross-section (Figure 72), being the latter more updated, hence more reliable if compared to the cross-section dated back to 2001.

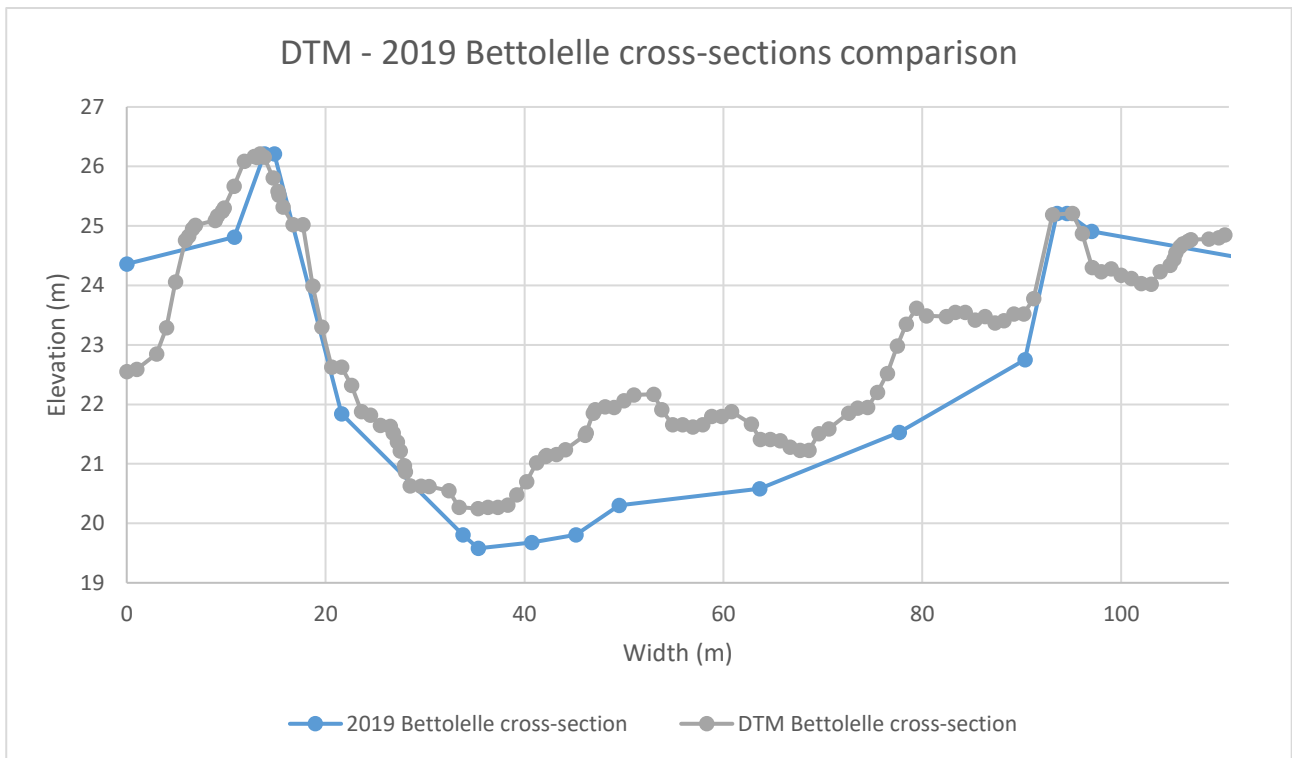


Figure 72. Comparison between the Civil protection 2019 and the DTM Bettollelle after levees adjustments cross-sections.

The differences between the DTM Bettollelle cross-section and the Civil Protection 2019 Bettollelle cross-section are lower if compared to the differences between the Civil Protection 2001 Bettollelle cross-section and the Civil Protection 2019 Bettollelle cross-section. Nonetheless, being the Civil Protection 2019 Bettollelle cross-section more recent than the DTM one, it has been added into the model. Similarly, also the Civil Protection 2019 Ponte Garibaldi cross-section has been implemented into the software.

4.10 Bridges implementation

The next step has been the addition of bridges. In this case, the bridges have been added into the model by taking into consideration the dimensions found in the project developed by the Civil Protection in 2001. However, since the cross-sections deriving from the use of digital terrain models significantly change if compared to those of the 2001, the bridge piers have been readapted to fit the new geometry (Figures 73 and 74).

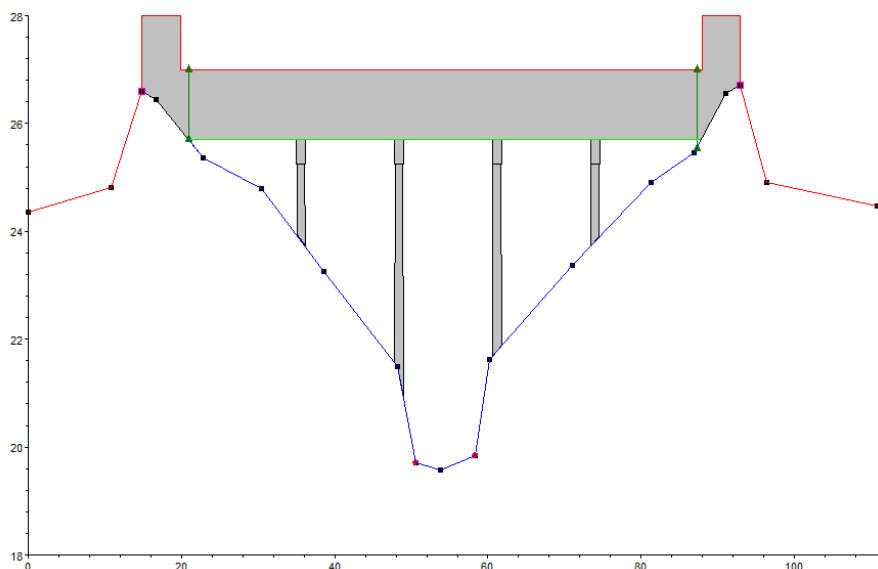


Figure 73. Bridge section in the 2001 Bettolle cross-section.

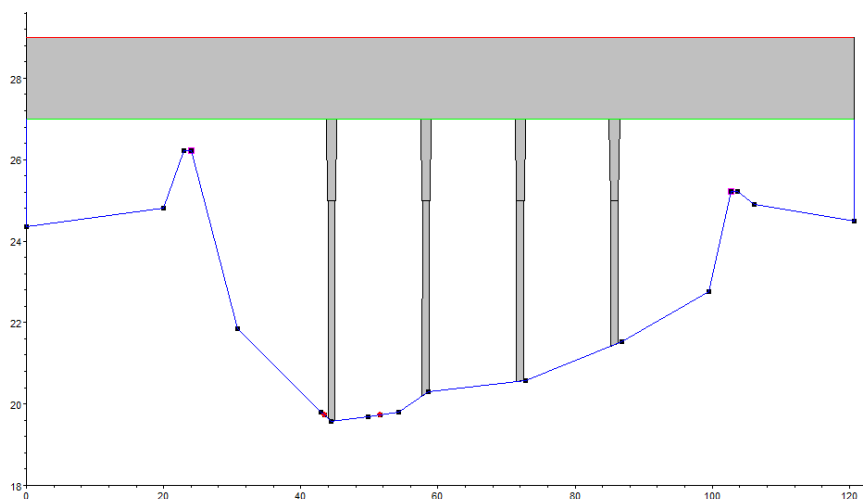


Figure 74. Bridge section in the 2019 Bettolle cross-section.

4.11 Bathymetry implementation

In the presence of deep waters, the laser rays of the Lidar technology with which the DTM tables have been acquired, are not able to penetrate the water. For this reason, in the most downstream part of the river, where the water stages are significant, the bathymetry was not available. In order to overcome this problem, different bathymetric surveys provided by the Socotec Italia Srl and belonging to the years 2015, 2018 and 2020 have been employed. Considering that these bathymetric data have been provided as a cloud point (*.xyz format), before being opened through the QGIS software, the cloud point has been transformed into a raster file and exported by means of the CloudCompare software (Figure 75).

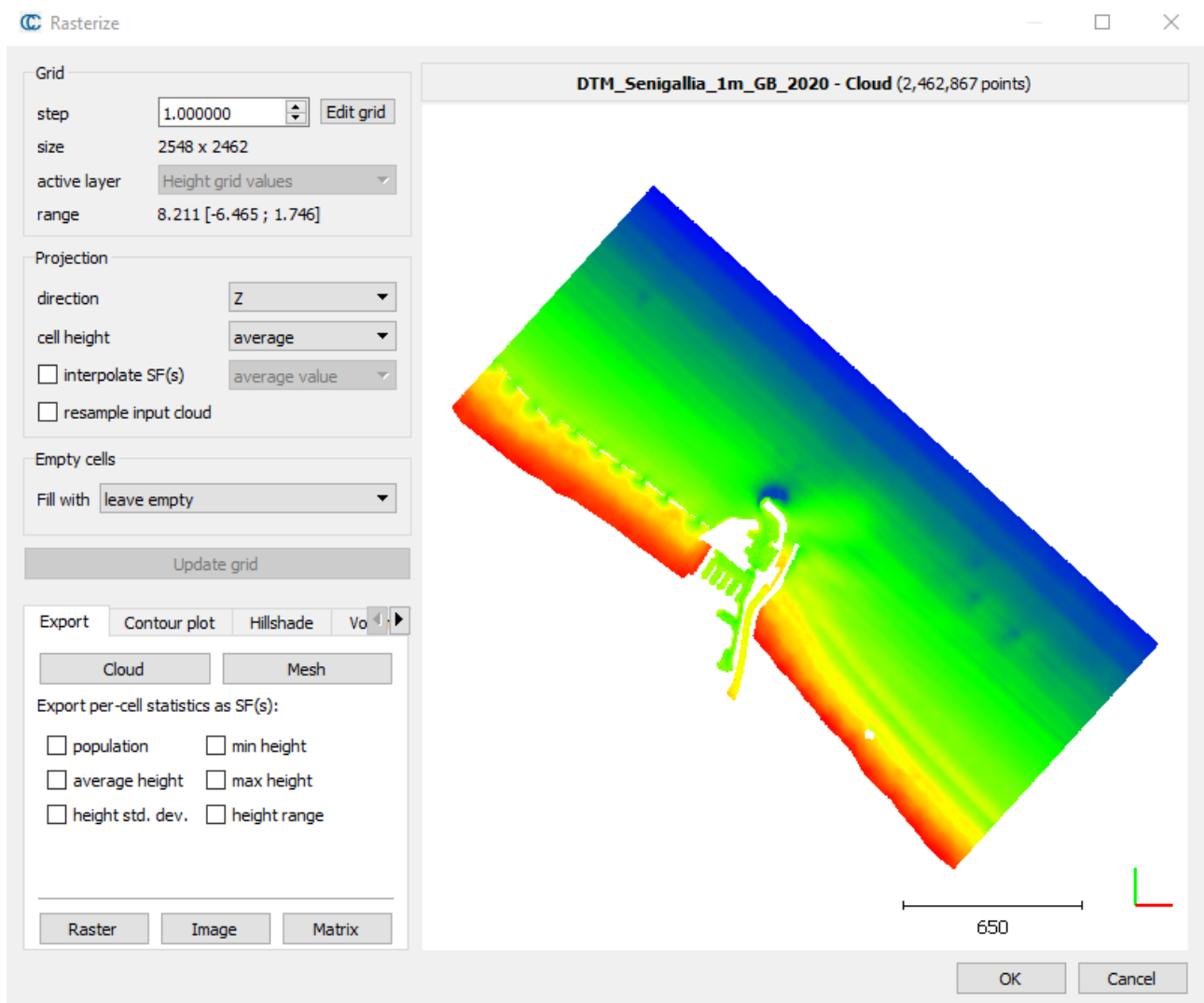


Figure 75. CloudCompare rasterization operation.

Subsequently, the raster file has been opened in QGIS and via the Terrain Profile plugin (Figure 76), the bathymetric data relative to the desired cross-sections have been extracted from the file and implemented into the HEC-RAS software (Figure 77).

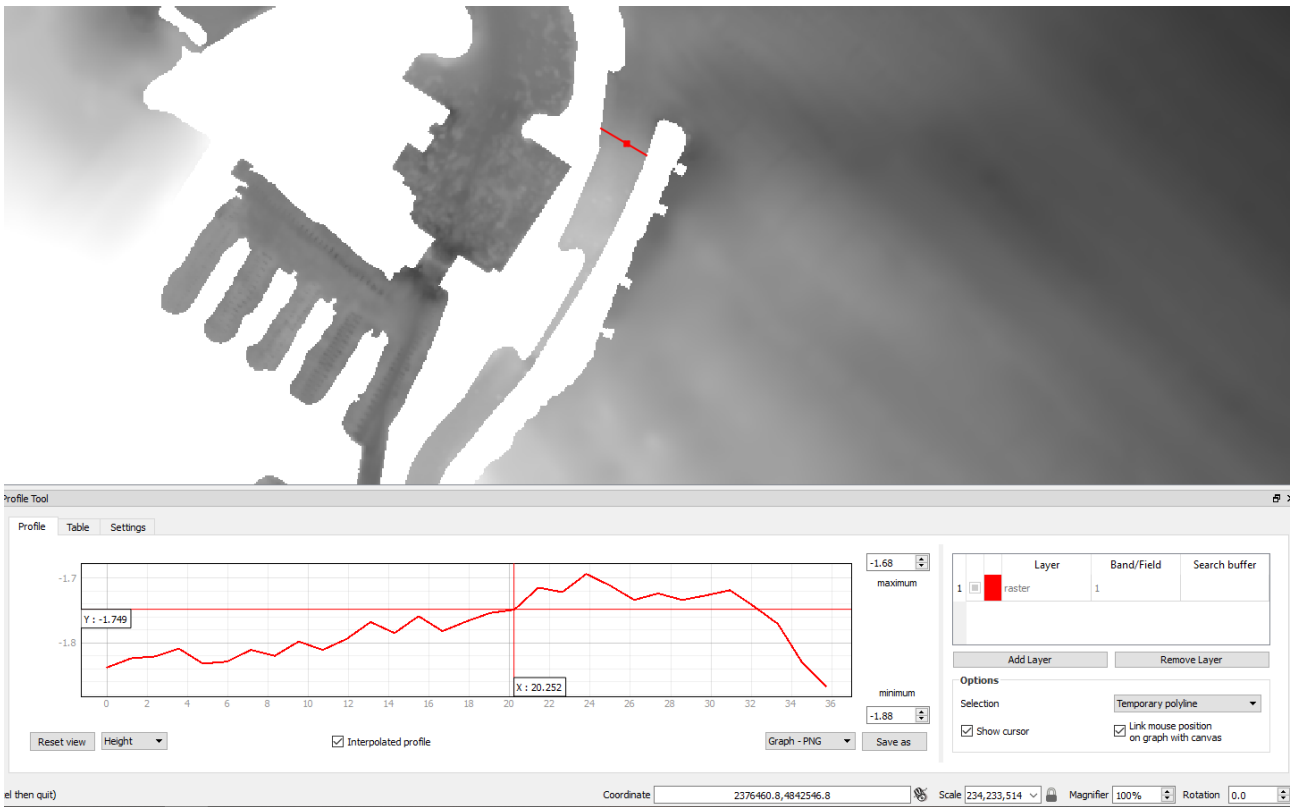


Figure 76. QGIS bathymetry extraction.

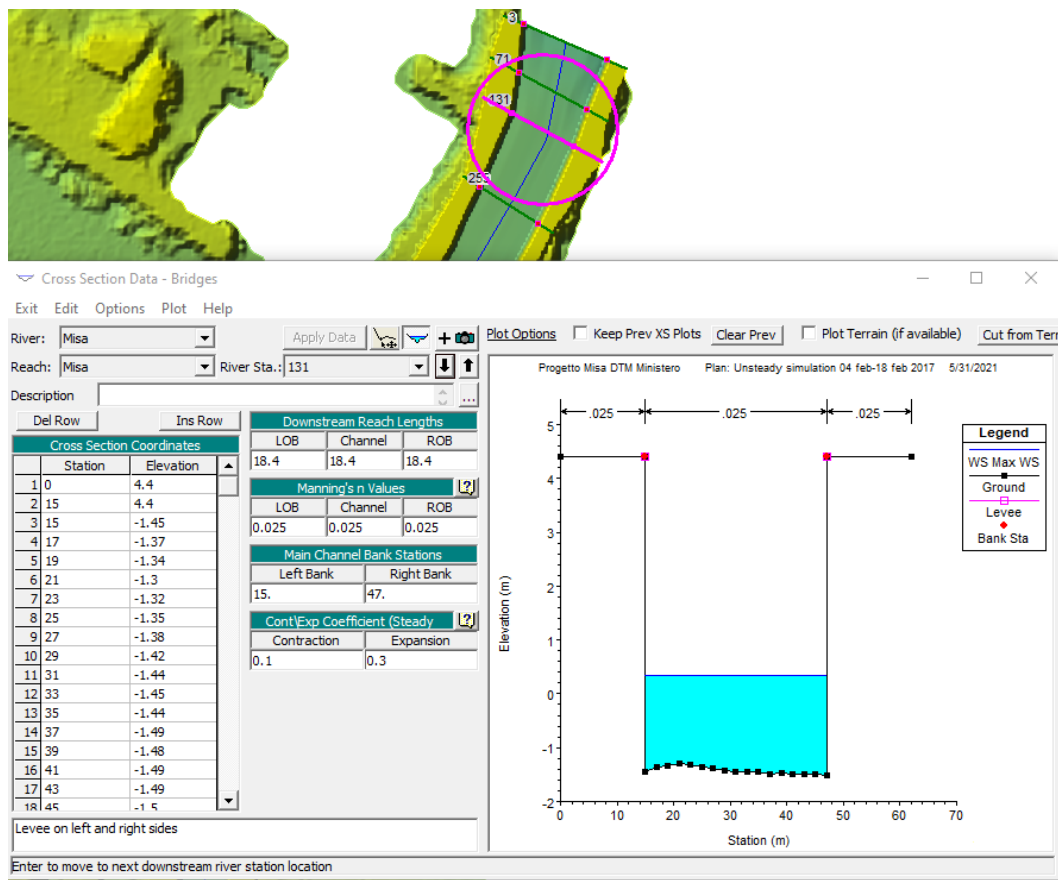


Figure 77. Bathymetry implementation in HEC-RAS.

The last step regarding the model construction, has been represented by the implementation of a further cross-section, which stands for the location where the H-ADCP is installed. The H-ADCP is located 21.1 m upstream of the SIRMIP hydrometer and its cross-section has been built up by following the 9th September 2019 survey (Figure 78).

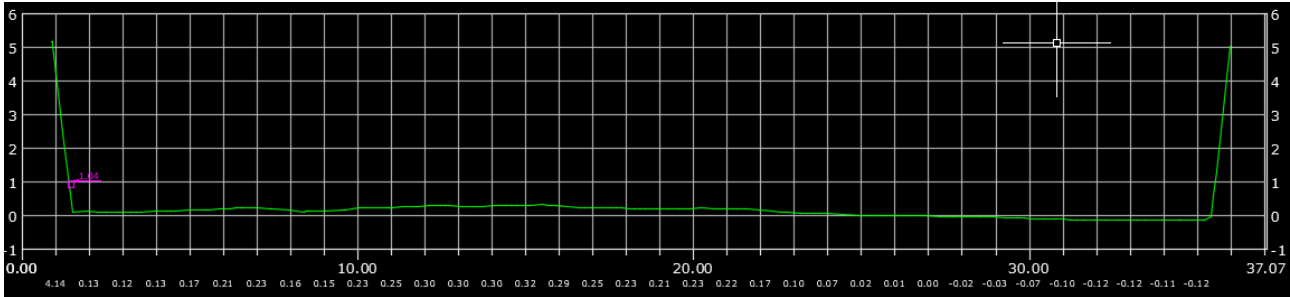


Figure 78. H-ADCP cross-section.

5 MODEL CALIBRATION

The calibration of the model has been carried out by only considering the river geometry obtained through the use of the digital terrain models, since it has turned out to be the most reliable among the others.

In order to reach the model calibration, the Bettollelle and Ponte Garibaldi cross-sections have been selected as benchmarks, due to the fact that they are the only two cross-sections belonging to the considered river stretch in which stage data from the SIRMIP website are available. Moreover, a further cross-section referred to the H-ADCP has been taken into account in order to have also a comparison between the data acquired by the river gauge and the simulation results. The model calibration has been carried out by applying different hydrographs at the Bettollelle cross-section (obtained through the use of rating curves and stage values) along with the corresponding tidal ranges at the last cross-section of the model with the goal of reaching water stages at both Bettollelle and Ponte Garibaldi cross-sections as close as possible to those measured by the SIRMIP instrumentation.

To perform the simulations, the first phase has been the selection of the period of interest, which has been chosen by following different criteria, such as:

- An interval time larger than three days;
- The presence of both precipitations and dry periods;
- Availability of stage data for the considered period in both Bettollelle and Ponte Garibaldi cross-sections;
- Discharge values possibly higher than $1 \text{ m}^3/\text{s}$ in order to avoid instability phenomena. This because HEC-RAS is a software mainly designed to deal with high discharge values, aimed at representing, for instance, flooding scenarios, thus the use of very low discharges applied to relatively large cross-sections may lead to an incorrect representation of the hydraulic characteristic of the river, giving back errors associated to a model instability.

Subsequently, the Bettollelle discharge values have been computed through the use of the rating curves knowing the stage values. As done for the unsteady simulations applied to the river geometry characterized by the absence of the DTMs implementation, the Bettollelle flow values have been used as upstream boundary condition, whereas the corresponding tidal stages have been used as downstream boundary condition. In order to compare the stage values, the same reference system has been chosen for the collected data and the simulated results at both Bettollelle and Ponte Garibaldi locations.

For what concerns the Bettollele cross-section, the thalweg has been selected as reference system. Considering that the results coming from the HEC-RAS software are always referred to the average sea level, they have been reduced by 19.58 m which represent the distance between the cross-section thalweg and the average sea level. For what regards the SIRMIP stage values, being the hydrometric zero located at 19.18 m.a.s.l. for the period prior to 2019 and 18.83 m.a.s.l. from the 2019 on, they have been reduced by a quantity of 0.4 m and 0.75 m, respectively.

The selected Ponte Garibaldi reference system has been the average sea level. For this reason, the water stages outcoming from the HEC-RAS software have been left as they were. Differently, to calculate how much the SIRMIP stage values had to be reduced, both the 2019 bathymetric survey and 2020 H-ADCP survey have been taken into account (see Table 5 and Figure 79).

Name	Identification code	Coord.Nord	Coord.Est	Height (m)
4012	sonda fluviale	4841784.770	356078.424	0.630
4002	sonda fluviale oc,sotto	4841784.688	356078.410	0.482
4003	sonda fluviale oc,sopra	4841784.687	356078.411	0.605

Table 5. H-ADCP elevations with respect to the average sea level.

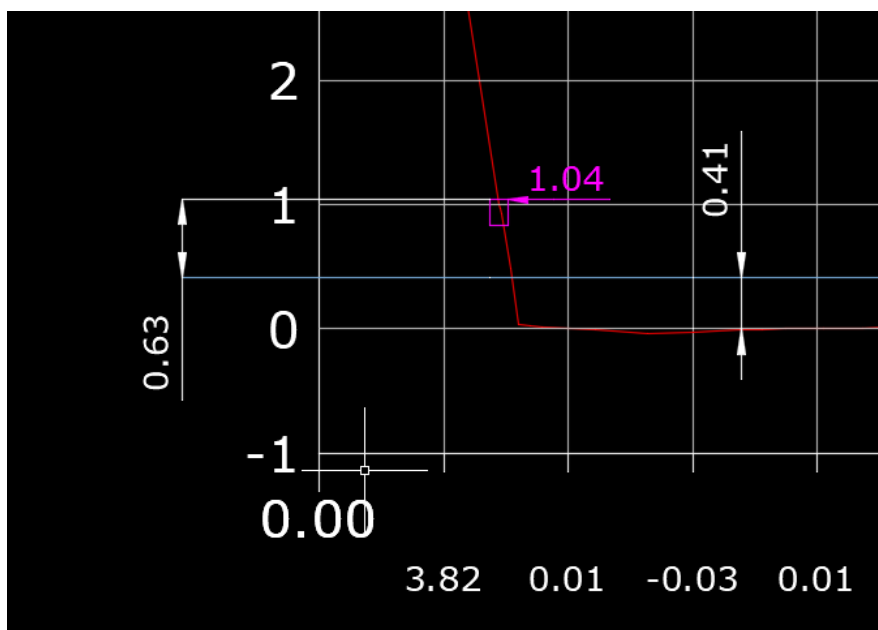


Figure 79. Selection of the Ponte Garibaldi reference system.

Considering that the distance between the topmost part of the H-ADCP and the average sea level is 0.63 m and that the SIRMIP stage values are referred to the hydrometric zero (which corresponds to the zero of the 2019 cross-section survey), the latter have been reduced by 0.41 m in order to be compared with the software results.

5.1 Roughness selection

The Manning coefficients of all the cross-sections have been set with the purpose of increasing the accuracy of the model. To do this, the Google Earth software has been employed, by relying on the possibility of moving backward in time, trying to select a time period as close as possible to that of each simulation in order to have the best estimate of the real conditions of the river in terms of roughness. This operation has been done by comparing all the cross-sections of the HEC-RAS project, which are georeferenced, with the corresponding portion of the river in Google Earth (Figures 80 and 81).

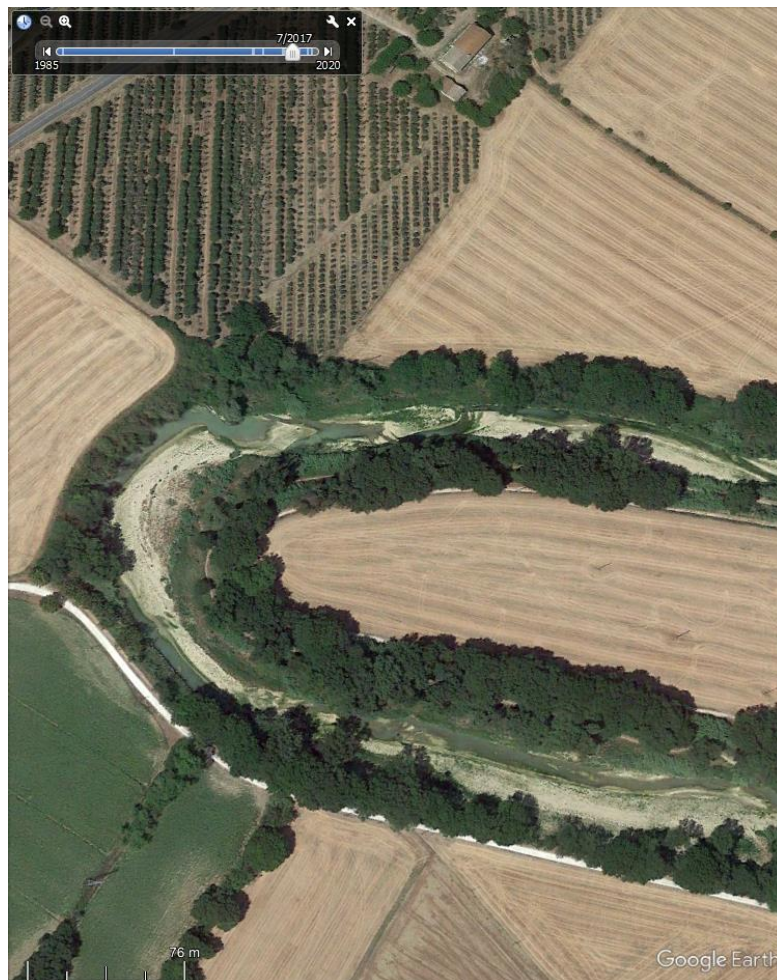


Figure 80. Example of Google Earth image for Manning coefficients estimate.

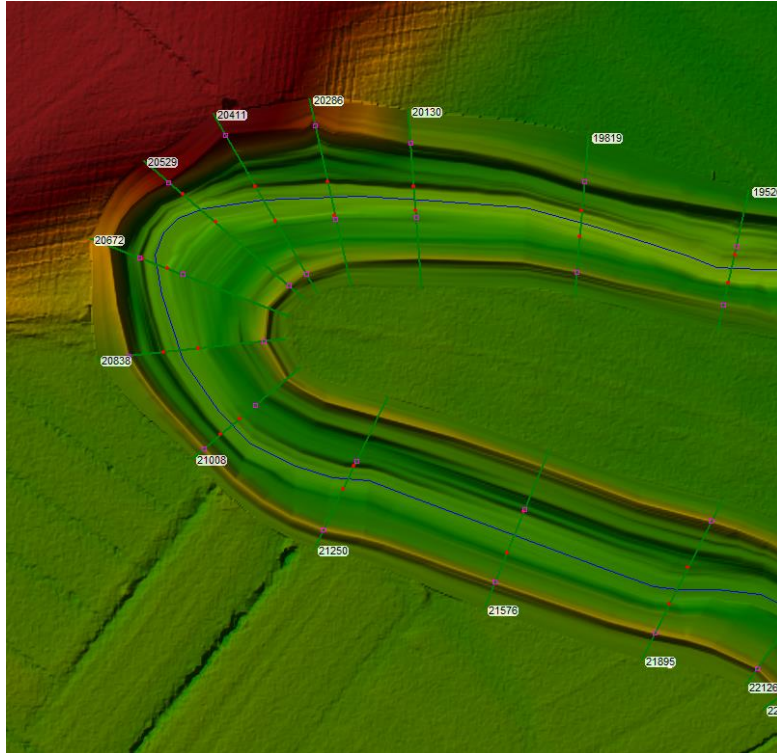


Figure 81. Example of HEC-RAS river stretch for Manning coefficients estimate.

17087	n	0.1	0.04	0.045
16946	n	0.1	0.04	0.045
16801	n	0.1	0.04	0.045
16421	n	0.045	0.04	0.1
16095	n	0.1	0.04	0.1
15842	n	0.1	0.04	0.1

Table 6. Example of HEC-RAS Manning coefficients implementation. The first column identifies the cross-section number, the second column indicates the use of the Manning coefficient as roughness coefficient, the columns three, four and five indicate the left overbank, the main channel and the right overbank, respectively.

From this comparison, it has been possible to have an indication of the vegetation along the river, which has been combined with the Manning coefficient table, to provide the suitable roughness coefficients to use. However, considering that the model is composed of cross-sections belonging to different years (2008 and 2019) and that these cross-sections cannot properly represent each simulation period due to the fact that both the river bed and the floodplains change over time, average values of the most suitable Manning coefficients relative to the period corresponding to the available cross-sections and to the performed simulations (2016-2020), have been chosen.

5.2 Other calibration parameters

A further operation aimed at optimizing the software outputs has been the correct assignation of the main channel bank stations. This phase has resulted to be decisive, since the program relies on the position of the main channel banks to assign the Manning coefficients to both the main channel and the overbanks, therefore an incorrect assignation of these parameters severely affects the river flow dynamics. To have a rough preliminary overview of the main channel bank stations for the entire considered river stretch, images from Google Earth (taking into consideration the time period) have been considered. Afterwards, the channel bank stations have been optimized through the run of several simulations, moving them spanwise in order to get results as close as possible to the measured values.

Another step in the model calibration has been the correct positioning of the levees (Figures 82 and 83). This adjustment is likewise linked to the Manning coefficients, since without a correct setting of the levees, the water that was supposed to run along the main channel would have flowed also in the floodplain region, with the subsequent alteration the river flow dynamics.

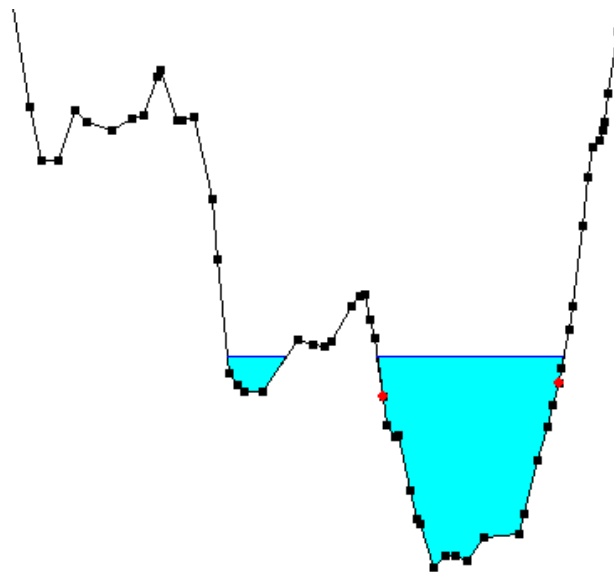


Figure 82. Cross-section without levees.

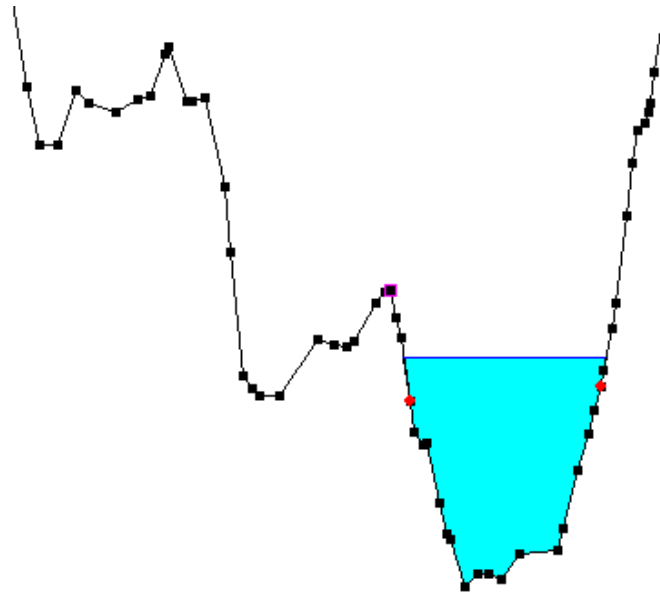


Figure 83. Cross-section after the levees addition.

Another operation aimed at enhancing the reliability of the model has been performed by the addition of the contraction/expansion coefficients. These coefficients are particularly important in presence of bridges since the bridge piles influence the flow motion at both the upstream and the downstream bridge ends. Following the HEC-RAS User Manual, the contraction/expansion coefficient have been set in both the upstream and the downstream sections of all the bridges by accounting for a value of 0.3 and 0.5, respectively.

6 DISCUSSION

The following graphs represent a comparison in terms of water elevations, between the data measured by the SIRMIP hydrometer (solid black line) and the data coming from the HEC-RAS simulations (solid green line). The precipitation depth which has been added to the graphs is that referred to Bettollelle rainfall station, which gives an idea of the precipitation falling within the watershed during the taken events.

The tidal excursion (solid red line) has been displayed only at the Ponte Garibaldi cross-section, since its contribution can be taken as negligible at Bettollelle.

In addition, scatter plots referred to the measured and simulated water stages for both Bettollelle (Figure 100) and Ponte Garibaldi (Figure 101) cross-sections, have been added with the purpose of better identifying the differences in water elevations between the two cross-sections.

For the events November 1st – November 30th 2016 (Figures 84 and 85), January 26th – February 3rd 2017 (Figures 86 and 87), February 4th – February 18th 2017 (Figures 88 and 89), the Bettollelle rating curves ((1), (2) and (3)) relative to the period ranging from May 23rd 2015 – March 7th 2017 (Tables 7 and 8) have been used.

Start of validity					End of validity				
Year	Month	Day	Hour	Minute	Year	Month	Day	Hour	Minute
2015	5	23	6	31	2017	3	7	16	0
2015	5	23	6	31	2017	3	7	16	0
2015	5	23	6	31	2017	3	7	16	0

Table 7 Rating curves validity periods

Range of validity
0.2 <= H <= 1.51
1.52 <= H <= 3.01
3.02 <= H <= 6.5

Table 8 Rating curves stage validity

$$Q = 5.9 \cdot [H - (0.148)]^{2.934} \quad (1)$$

$$Q = 27.549 \cdot [H - (1.51)]^{1.188} + 14.609 \quad (2)$$

$$Q = 101.284 \cdot [H - (3.01)]^{1.061} + 59.209 \quad (3)$$

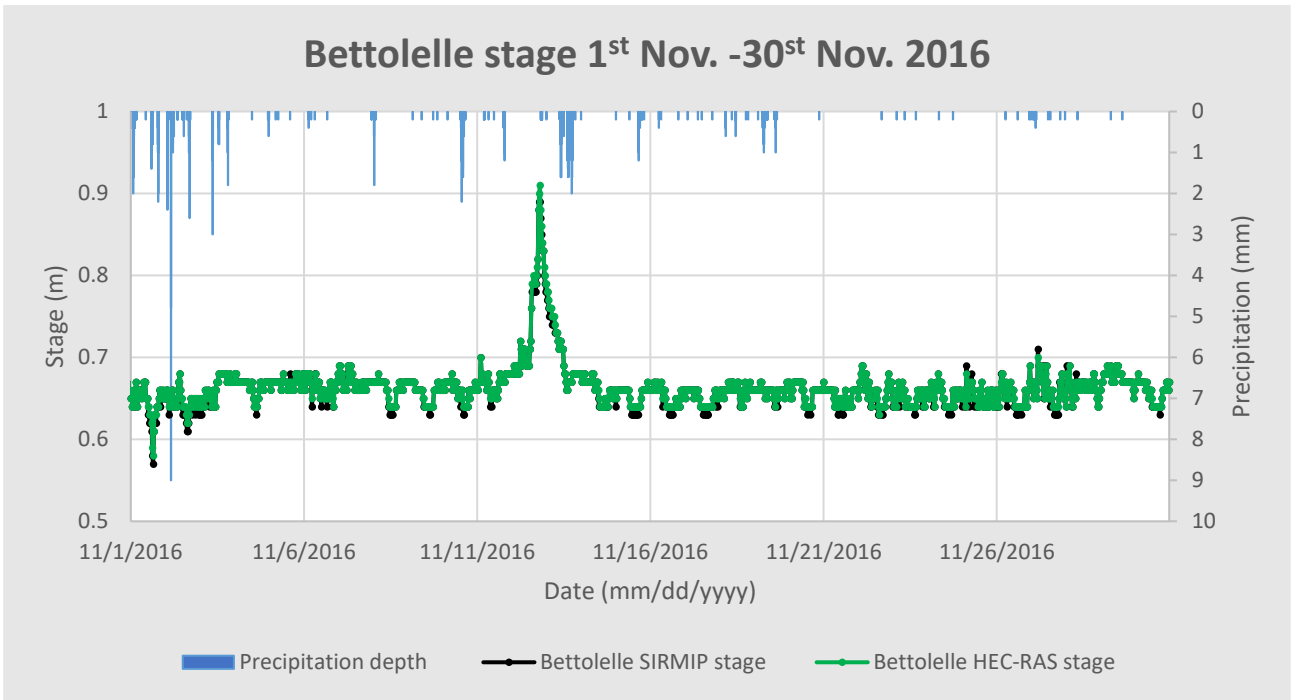


Figure 84. Simulation results at Bettollelle cross-section for the November 1st– November 30th 2016 event.

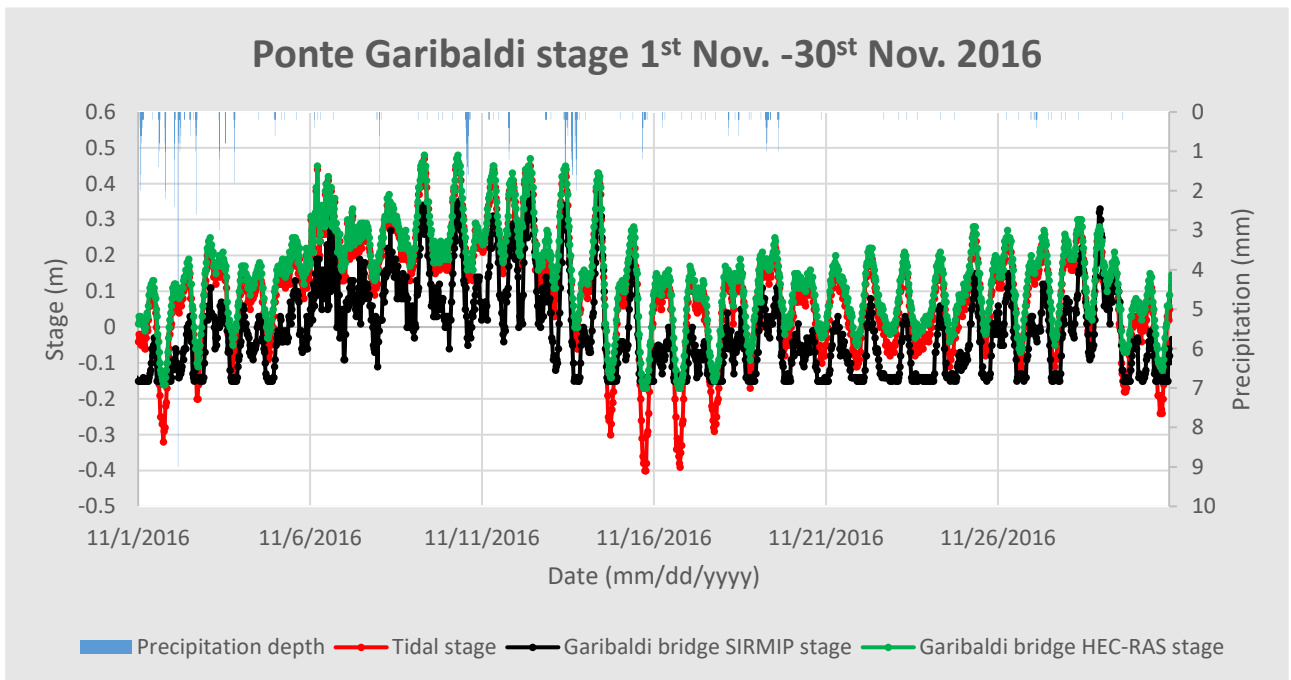


Figure 85. Simulation results at Ponte Garibaldi cross-section for the November 1st – November 30th 2016 event.

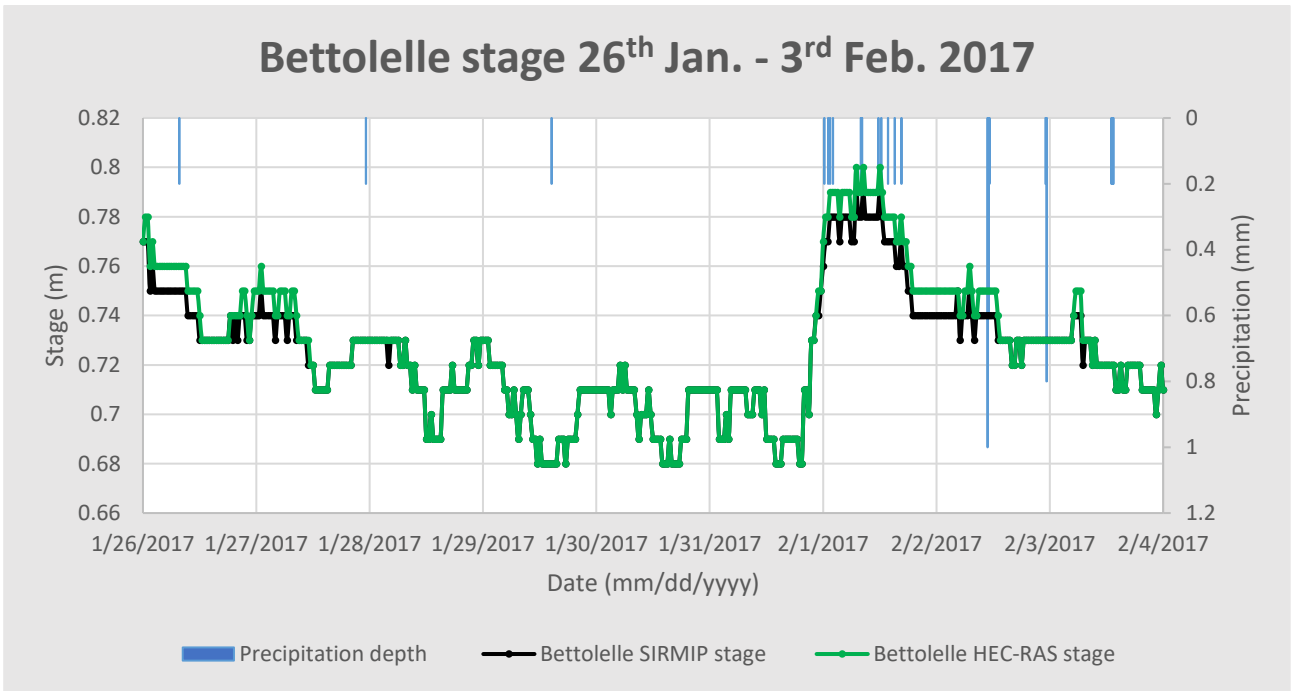


Figure 86. Simulation results at Bettolle cross-section for the January 26th – February 3rd 2017 event.

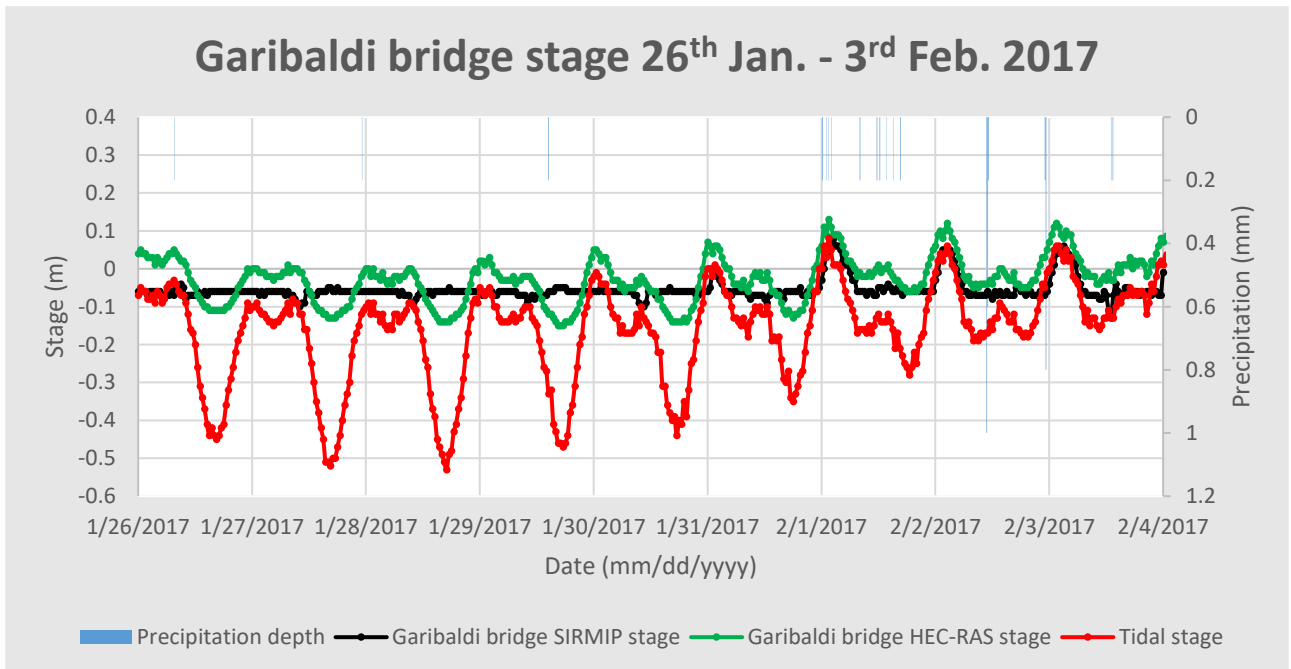


Figure 87. Simulation results at Ponte Garibaldi cross-section for the January 26th – February 3rd 2017 event.

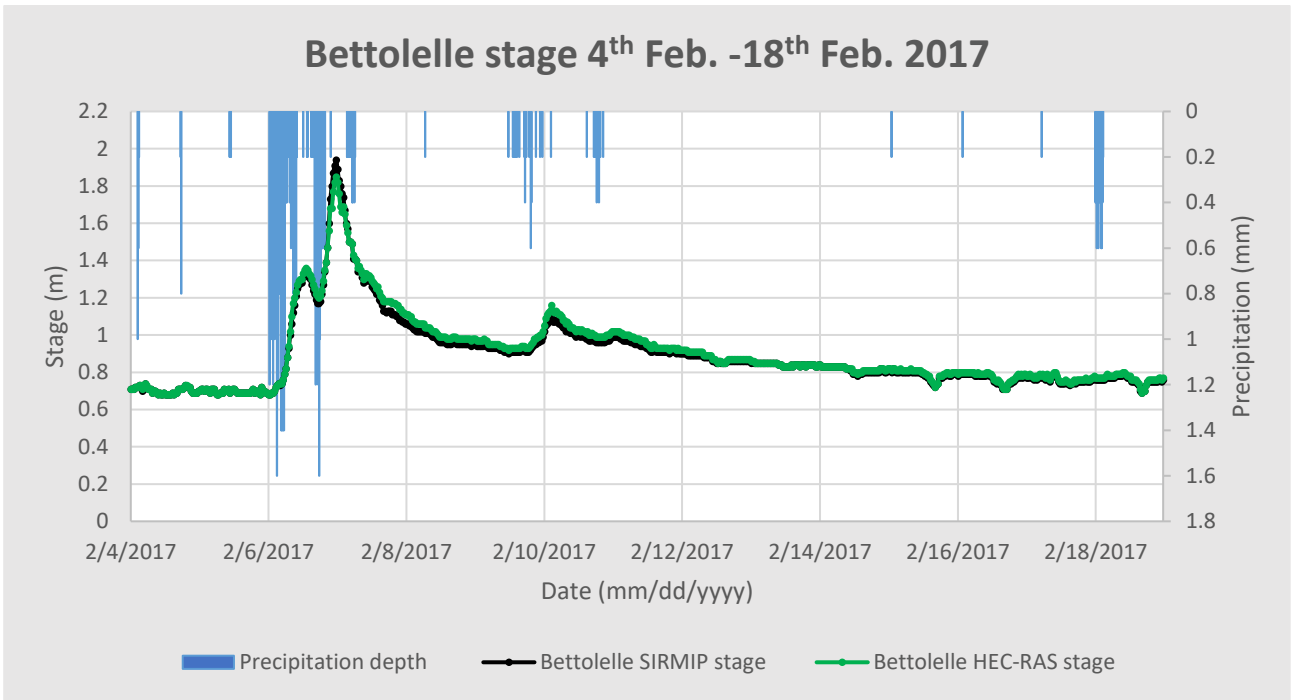


Figure 88. Simulation results at Bettolle cross-section for the February 4th – February 18th 2017 event.

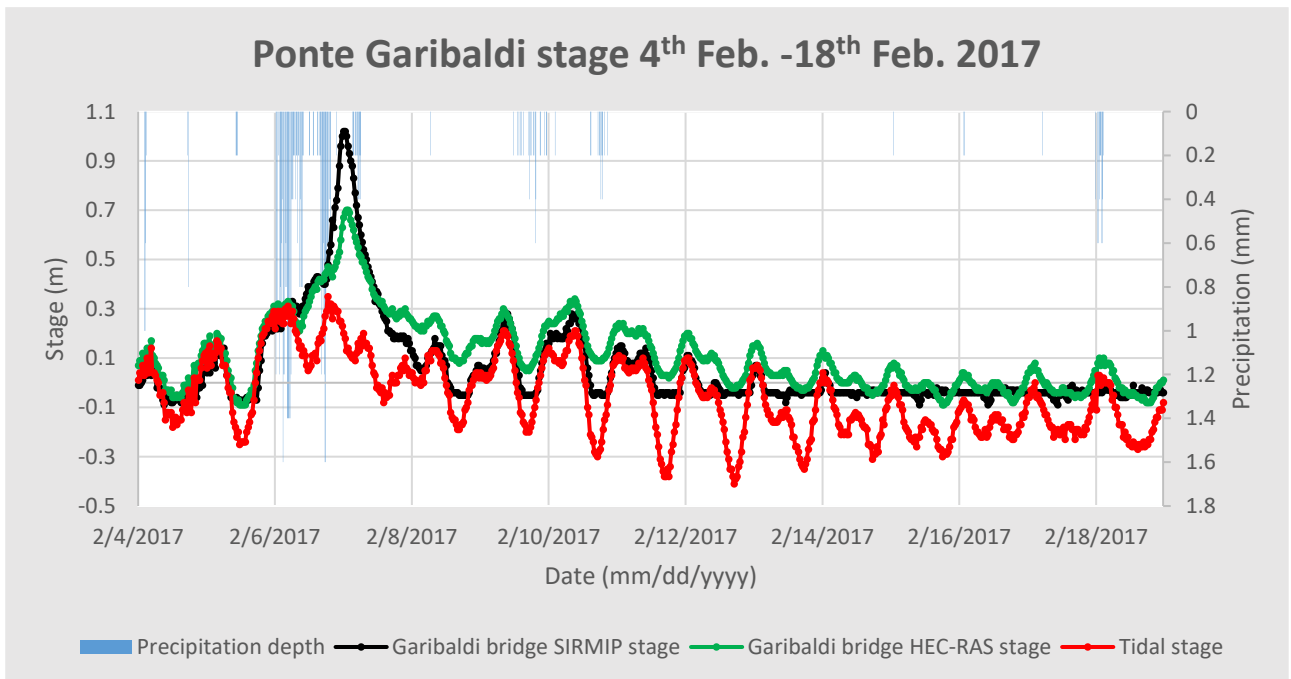


Figure 89. Simulation results at Ponte Garibaldi cross-section for the February 4th – February 18th 2017 event.

For all the three events, the employed Manning coefficients range from 0.025 to 0.2. The use of the equations (1), (2) and (3), has provided an excellent matching between the measured SIRMIP stage values and the HEC-RAS ones for what regards the Bettolelle cross-section.

For the Ponte Garibaldi cross-section, however, the simulation results are not fully in line with the SIRMIP ones.

In particular, in the November 1st – November 30th 2016 event, the SIRMIP stages are always below the HEC-RAS stages and, for the majority of the time, they are even lower than the tidal stages. This behavior might be addressed to cross-section local variations in correspondence of the hydrometer measuring point.

For the January 26th – February 3rd 2017 event, the HEC-RAS stage values have a trend similar to the tidal stage one, although with a less pronounced excursion due to the river discharge contribution, which partially compensate the reduced water elevation deriving from the negative tides. Regarding the SIRMIP stages, they present a flat shape every time a negative tidal occurs, while for tidal ranges higher than -0.05 m they follow the trend of both the HEC-RAS stages and the tidal one. Also in this case, the flat trend could be due to the presence of a low flow detection limit of the instrument.

The simulation of the February 4th – February 18th 2017 shows a good agreement between the measured and simulated water elevations, except for the SIRMIP flat trend and the peak. From these simulation results, it is possible to notice that when dealing with high discharge values, the river forcing prevails on the tidal motion, confirming what stated in Brocchini et al., (2017). The difference in stage at the peak instead, is independent of the presence of the wastewater treatment plant due to the fact that the discharges outgoing from the latter are too low to induce an increase of the water stages in the river (see section 4.6). On the other hand, this difference can be ascribed to some reasons, i.e. the runoff contribution existing between Bettolelle and Ponte Garibaldi; the uncertain validity of the rating curve used at Bettolelle for large discharges; the uncontrolled sewer outflows occurring during flood conditions, since for the dry periods this difference in water elevation does not exist.

For what regards the March 3rd – April 24th 2017 event, two different sets of Bettolelle rating curves ((1), (2), (3), (4), (5)) belonging to two different time periods (Tables 7, 8, 9 and 10) have been used. In particular, considering that during this event a change of the rating curves occurred, the simulations have been conducted in two ways: the first simulation is that referred to the use of the real rating curves of that period ((1), (2), (3), (4), (5)) (Figures 90 and 91); the other simulation has been conducted only by employing the rating curves belonging to the period May 23rd 2015 – March 7th 2017 ((1), (2), (3)) (Figures 92 and 93).

Start of validity					End of validity				
Year	Month	Day	Hour	Minute	Year	Month	Day	Hour	Minute
2017	3	7	16	1	2018	3	5	0	0
2017	3	7	16	1	2018	3	5	0	0

Table 9. Rating curves validity periods.

Range of validity
$0.95 \leq H \leq 3.02$
$3.03 \leq H \leq 6.5$

Table 10. Rating curves stage validity.

$$Q = 14.388 \cdot [H - (0.942)]^{1.974} \quad (4)$$

$$Q = 100.396 \cdot [H - (3.02)]^{1.068} + 60.954 \quad (5)$$

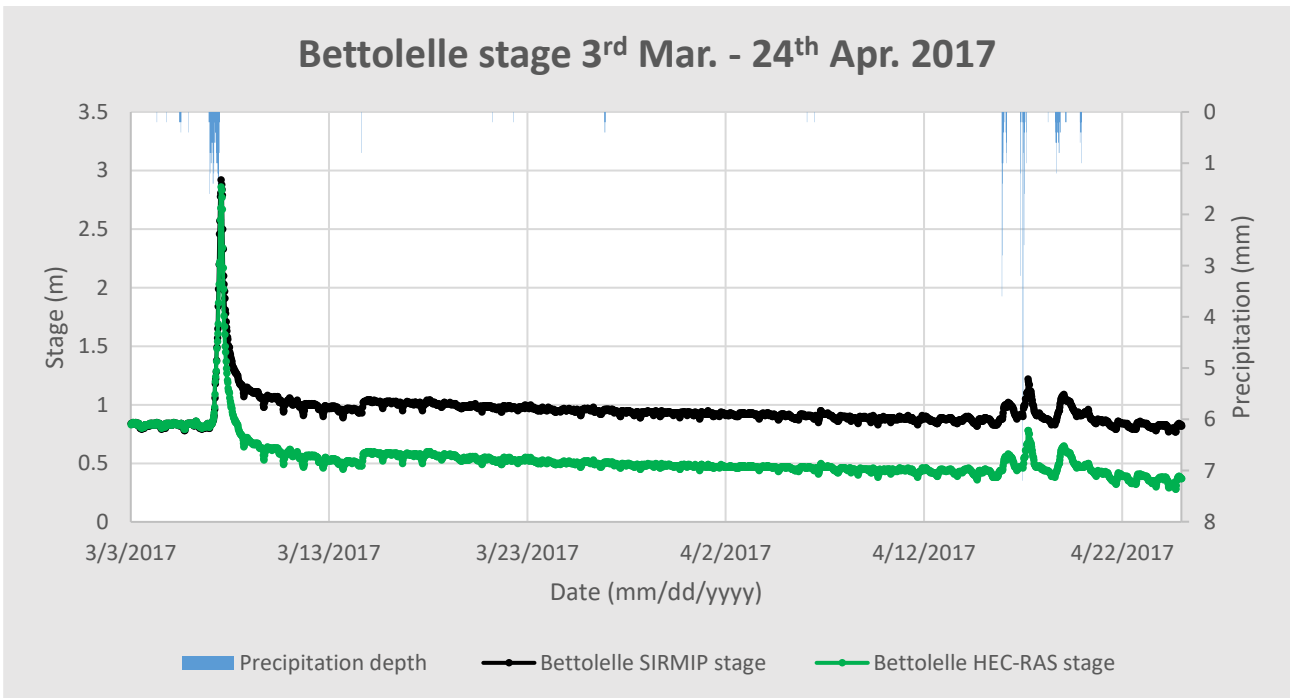


Figure 90. Simulation results at Bettollelle cross-section for the March 3rd – April 24th 2017 event performed using the (1), (2), (3), (4), (5) rating curves equations.

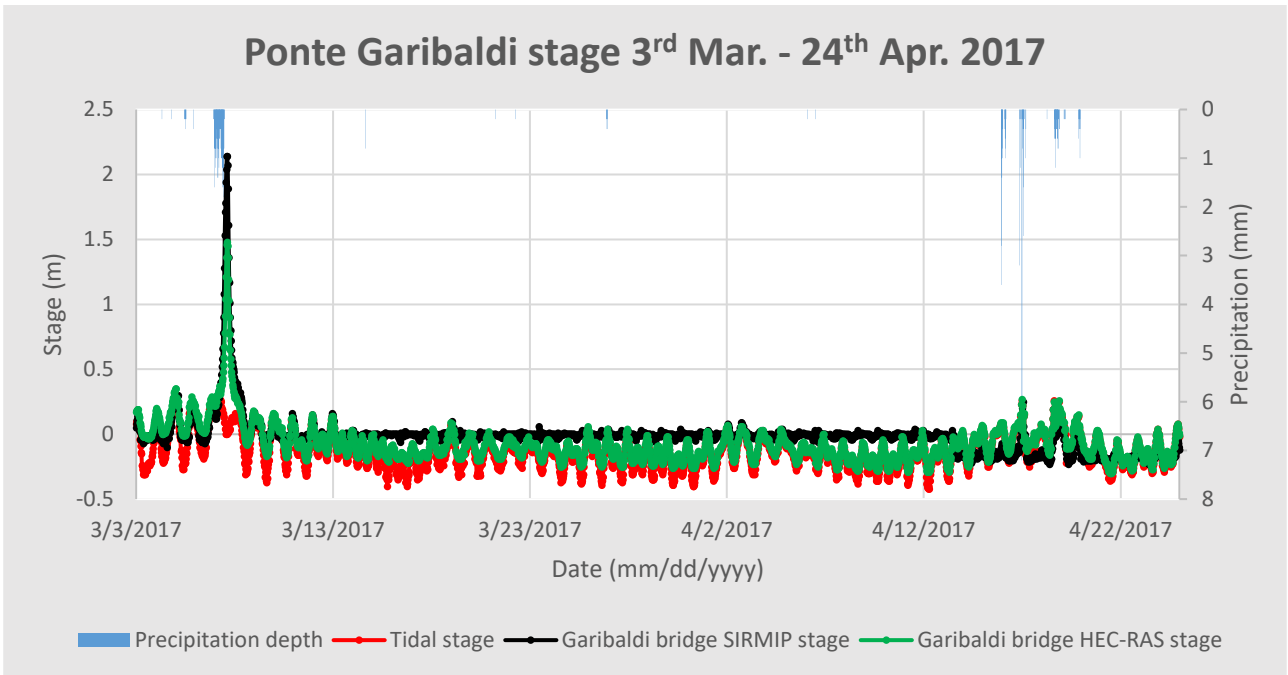


Figure 91. Simulation results at Ponte Garibaldi cross-section for the March 3rd – April 24th 2017 event performed using the (1), (2), (3), (4), (5) rating curves equations.

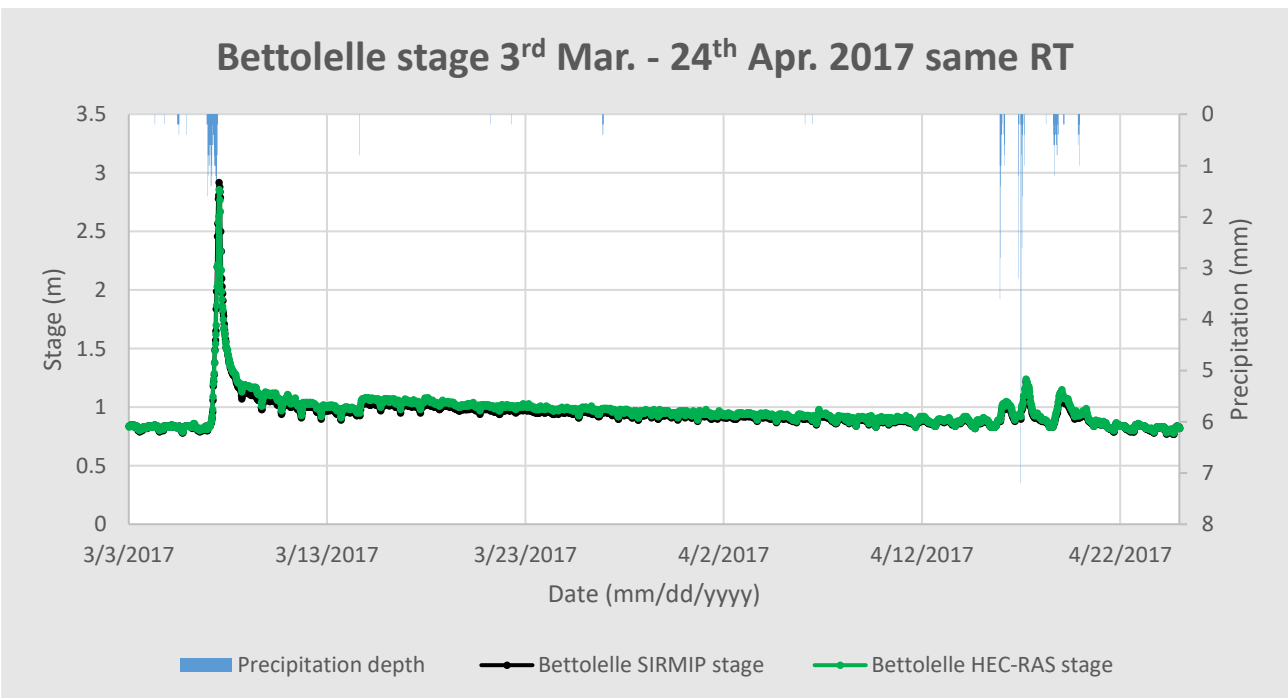


Figure 92. Simulation results at Bettolle cross-section for the March 3rd – April 24th 2017 event performed using the (1), (2), (3) rating curves equations.

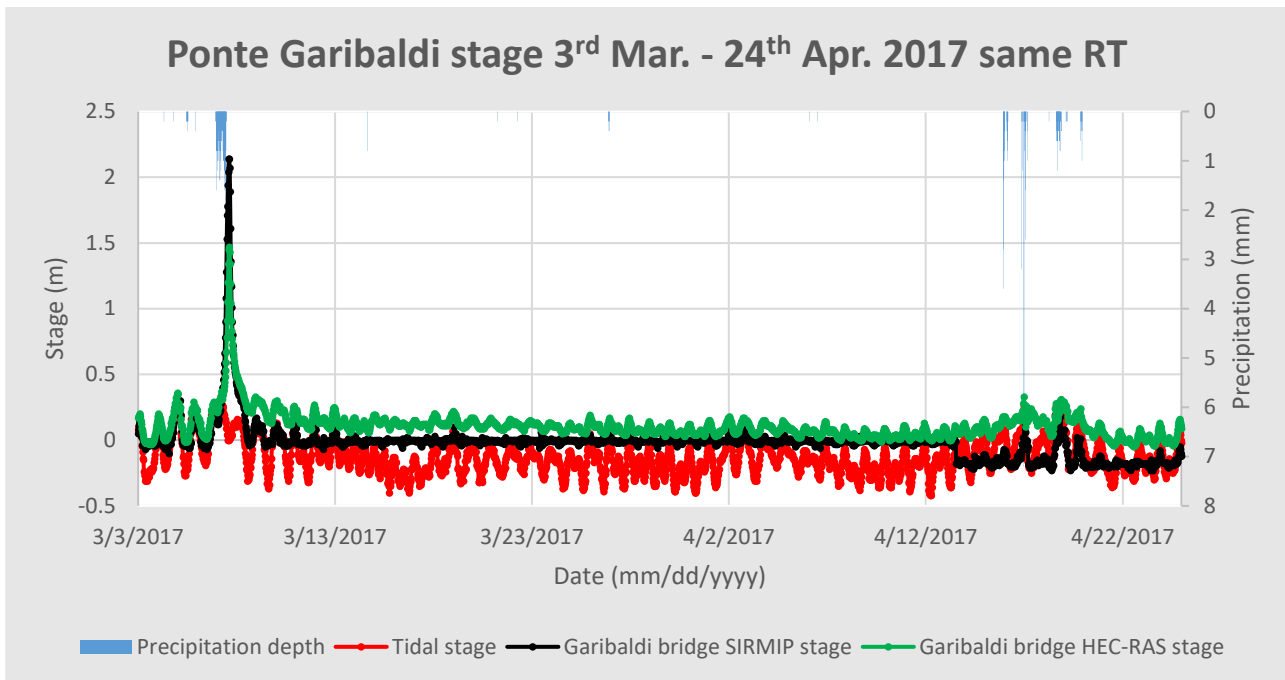


Figure 93. Simulation results at Ponte Garibaldi cross-section for the March 3rd – April 24th 2017 event performed using the (1), (2), (3) rating curves equations.

Analyzing the Bettollelle cross-section results, there is an almost perfect matching between the simulated and the measured water elevations until the end of the period of validity of the May 23rd 2015 – March 7th 2017 rating curves. After March 7th, a different set of rating curves has been used in accordance to the Civil Protection. However, the implementation of the flow values deriving from the use of these rating curves into the model, leads to a constant offset of the water stages between the HEC-RAS and the SIRMIP of about 50 cm. For this reason, another simulation characterized by the use of the May 23rd 2015 – March 7th 2017 rating curves for the entire event has been performed. The results of this simulation show a perfect matching between the simulated and the measured stages throughout the entire event, leading to the conclusion that for the period ranging from March 3rd – March 24th 2017 the only use of the May 23rd 2015 – March 7th 2017 rating curves is recommended.

Looking at the Ponte Garibaldi cross-section results, at the peak the stages coming from the simulations are lower than those measured by the SIRMIP. Also in this case, this behavior can be due to the lack of surface runoff implementation into the model. For what regards the remaining part of the graphs, the SIRMIP measured stages seem not to account for the negative tidal motion, showing an almost flat trend. Moreover, at the rightmost section of the graph, a sudden decrease in the SIRMIP measured stages occurred, probably because of a collapse of the riverbed in correspondence of the instrument linked to erosion phenomena. Considering the Ponte Garibaldi results coming from the

simulation performed by means of the same rating curves throughout the period, it is possible to notice a trend similar to that of the previous simulation. An aspect confirming that the gap at the peak is mainly provoked by the lack of the surface runoff lies on the fact that; the Ponte Garibaldi cross-section is located in a strongly urbanized environment with a high runoff coefficient, although this cannot be easily observed from the analysis of the specific discharge (Section 4.5). In addition to this, a significant amount of precipitation fell in a reduced period of time, this excluding a substantial water infiltration.

For the February 18th – March 5th 2018 event (Figure 94 and 95), the used Manning coefficients for the entire considered river stretch range between 0.025 and 0.15. The selected rating curves equations (4) and (5) cover the period March 7th 2017 – March 5th 2018 (Table 9 and 10).

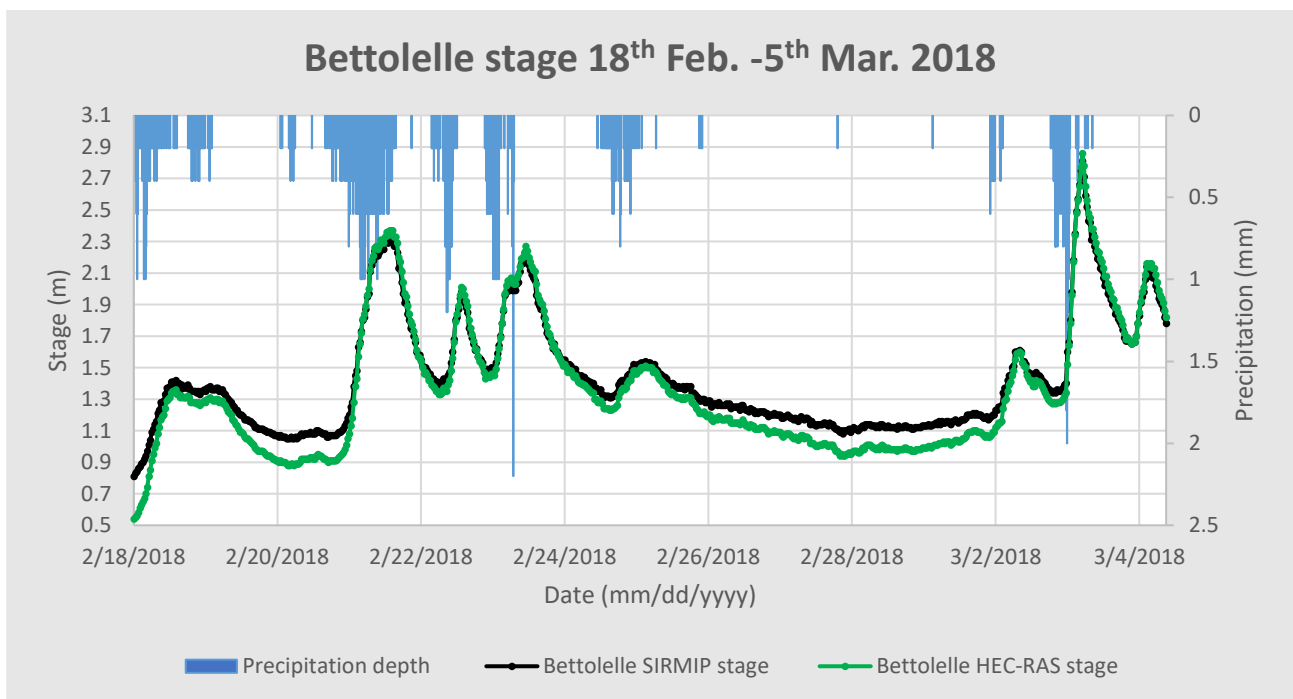


Figure 94. Simulation results at Bettollele cross-section for the February 18th – March 5th 2018 event

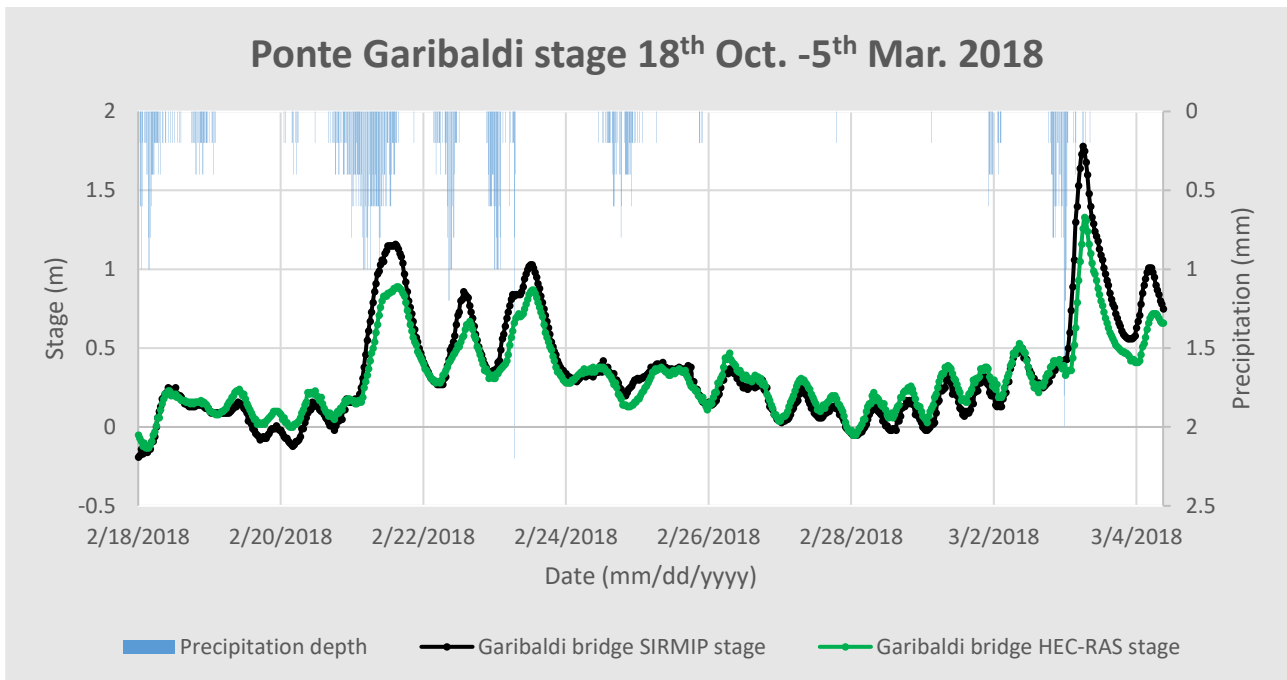


Figure 95. Simulation results at Ponte Garibaldi cross-section for the February 18th – March 5th 2018 event.

The Bettollelle graph displays a good matching between the measured and the simulated stage values, especially at the peaks. The differences between the HEC-RAS and the SIRMIP stages for low flow conditions can be address to the variations of either the lower part and/or the main channel of the Bettollelle cross-section.

Considering the Ponte Garibaldi cross-section, there is an overall good matching between the measured and the simulated water elevations. Nevertheless, the stages at the peak outcoming from the simulation are underestimated if compared to the SIRMIP ones. In this case an important amount of precipitation fell during the studied event making the soil in saturated conditions, thus enhancing the runoff contribution effect responsible to the differences at the peaks.

The last studied event (December 27th 2020 – December 31st 2020) has been performed with the purpose of calibrating the river model for events going from December 15th 2019 onwards (Tables 11 and 12), which characterize the period covered by the most updated Civil Protection Bettollelle rating curves (equations (6), (7), (8), (9)).

Start of validity					End of validity				
Year	Month	Day	Hour	Minute	Year	Month	Day	Hour	Minute
2019	12	15	0	0	2030	1	1	0	0
2019	12	15	0	0	2030	1	1	0	0
2019	12	15	0	0	2030	1	1	0	0
2019	12	15	0	0	2030	1	1	0	0

Table 11. Rating curves validity periods.

Range of validity
$0.85 \leq H \leq 1.03$
$1.04 \leq H \leq 2.1$
$2.11 \leq H \leq 3.8$
$3.81 \leq H \leq 5.5$

Table 12. Rating curves stage validity.

$$Q = 2.33 \cdot [H - (0.84)]^{0.79} \quad (6)$$

$$Q = 19.68 \cdot [H - (1.03)]^{1.24} + 0.6 \quad (7)$$

$$Q = 64.05 \cdot [H - (2.1)]^{1.26} + 22.01 \quad (8)$$

$$Q = 155.87 \cdot [H - (3.8)]^{1.16} + 146.7 \quad (9)$$

In order to carry out the calibration, the simulated stages have been compared to the SIRMIP stages for both the Bettolle (Figure 97) and the Ponte Garibaldi (Figure 99) cross-sections, while the results coming from the software in correspondence of the H-ADCP, which is installed at 21.1 meters upstream from SIRMIP hydrometer, have been compared with the data acquired by the river gauge (Figure 98). Since the H-ADCP requires relatively high water elevations to start gathering data, the only part of the event which has been registered by the instrument, is that corresponding to the peak.

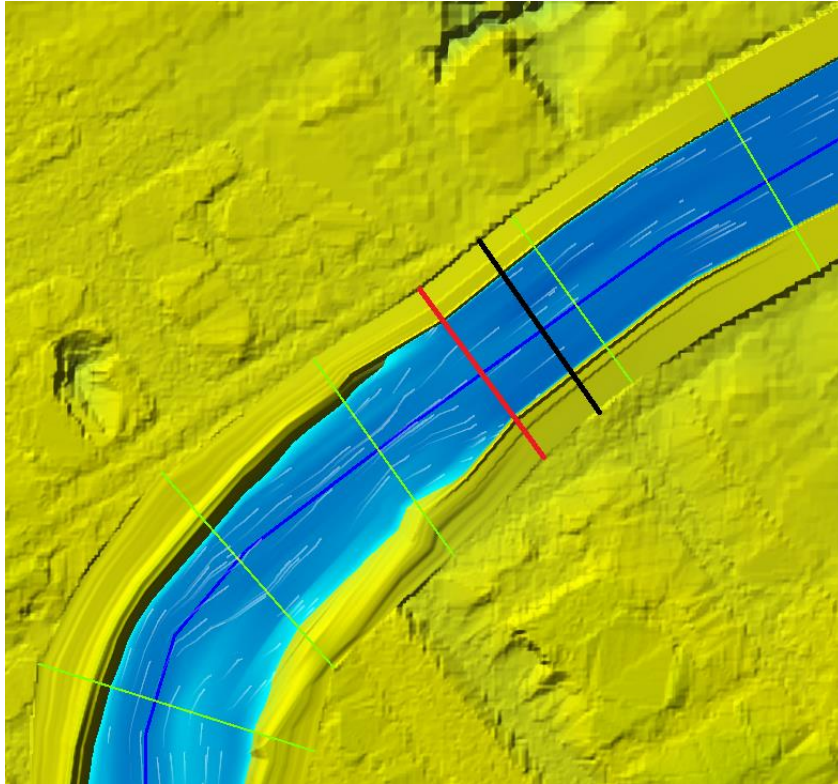


Figure 96. H-ADCP cross-section (in red) and Ponte Garibaldi cross-section (in black).

Since the data coming from the H-ADCP are characterized by one water elevation value every 2 minutes, both the HEC-RAS computation interval and the output interval have been lowered to 2 minutes as well. Moreover, the tidal ranges used in this simulation have been those related to the Senigallia tide gauge, which account for an interval time of 6 minutes.

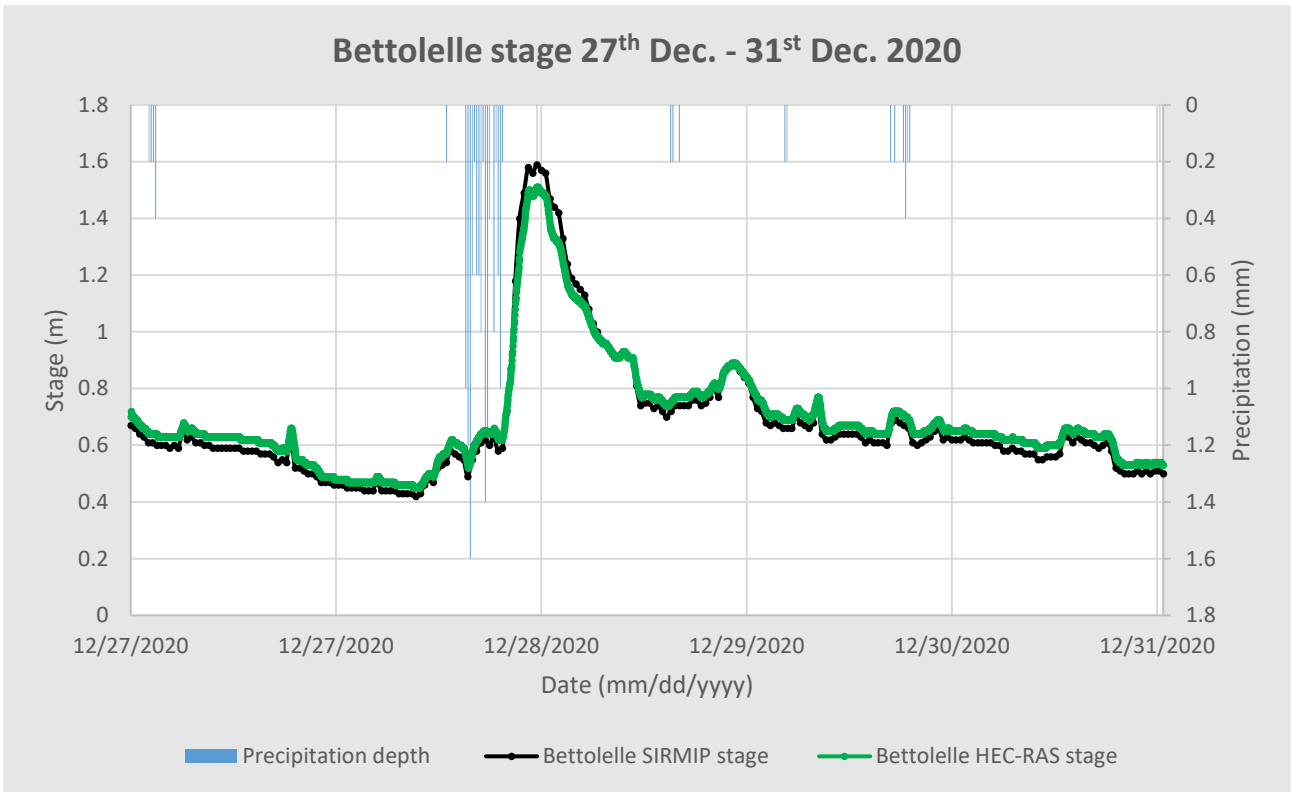


Figure 97. Simulation results at Bettolle cross-section for the December 27th – December 31st 2020 event.

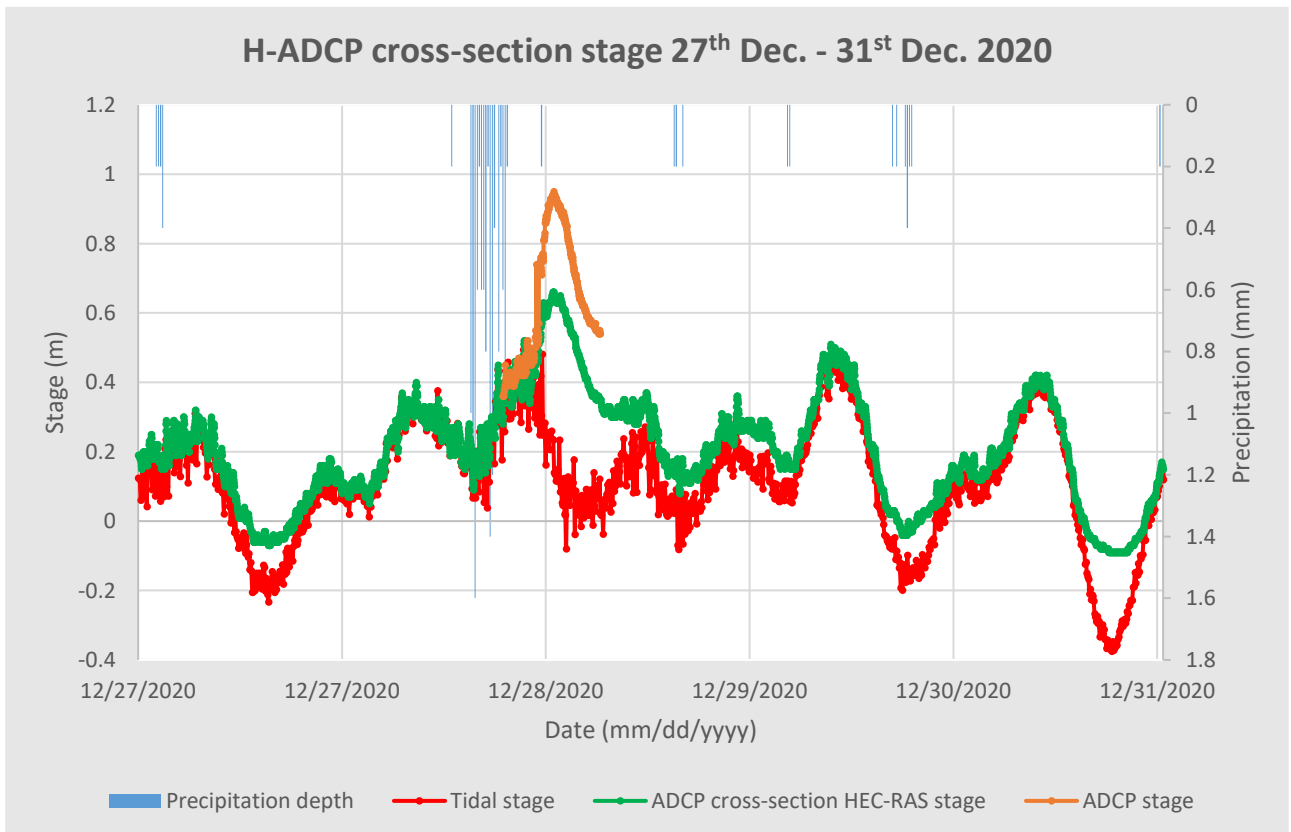


Figure 98. Simulation results at H-ADCP cross-section for the December 27th – December 31st 2020 event.

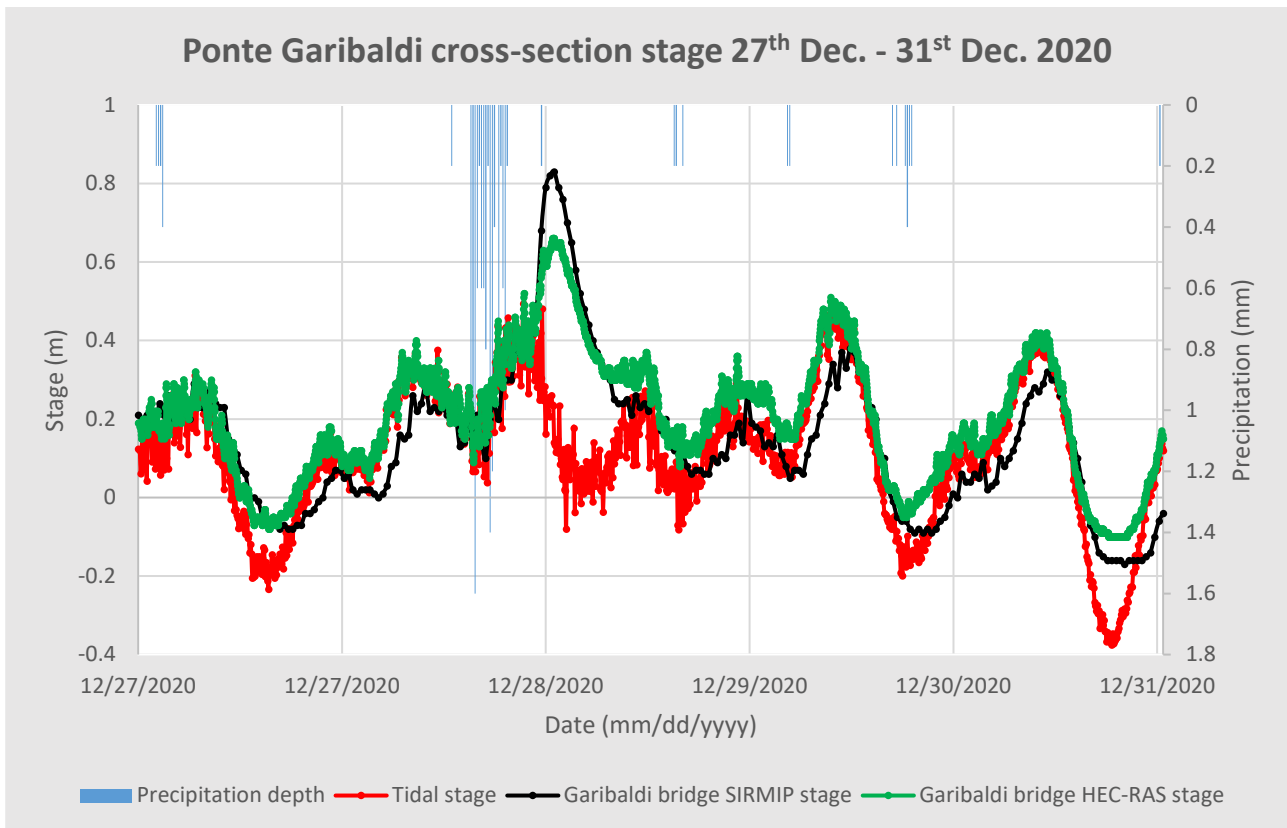


Figure 99. Simulation results at Ponte Garibaldi cross-section for the December 27th – December 31st 2020 event.

The simulations have been conducted by applying Manning coefficients ranging between 0.025 and 0.2. Analyzing the Bettollele cross-section, it is possible to notice a particularly good matching between the HEC-RAS and the SIRMIP stage for the entire event, meaning that the most updated Civil Protection rating curves well suit the cross-section used at Bettollele for the numerical simulations.

For what concerns the H-ADCP cross-section, as for the Ponte Garibaldi cross-section, all the results are referred to the average sea level. The solid orange line represents the data collected by the river gauge and from the graph, in correspondence of the rising limb, it is possible to notice an agreement between the H-ADCP and the HEC-RAS stages. However, at the peak the water stages acquired by the river gauge result to be higher than those coming from the simulation. Also in this case, this behavior may be addressed to a lack of runoff implementation into the software and to the uncertain validity of the rating curves used at Bettollele for large discharges.

At the Ponte Garibaldi cross-section, the data measured by the Civil Protection hydrometer show a water elevation trend similar to that acquired by the H-ADCP, with an overlap between the SIRMIP

and the HEC-RAS stage values at the rising limb and an underestimate of the latter in correspondence of the peak (29th December 2020, 12:26 AM). Anyway, a better agreement at the decreasing limb between the measured and simulated data is present.

From this analysis it is also possible to confirm that the tidal motion drives the water oscillations in case of low flow conditions, while for high flow its contribution can be considered as negligible.

6.1 Aggregated data comparison at Ponte Garibaldi

The following scatter plots (Figures 100 and 101) represent a comparison between the data coming from the simulations and the data measured by the SIRMIP hydrometer at both Bettollelle and Ponte Garibaldi cross-sections. The graphs have been realized by considering the data of all the tested events, with the exception of the March 3rd – April 24th 2017 event characterized by the use of the rating curves (4) and (5).

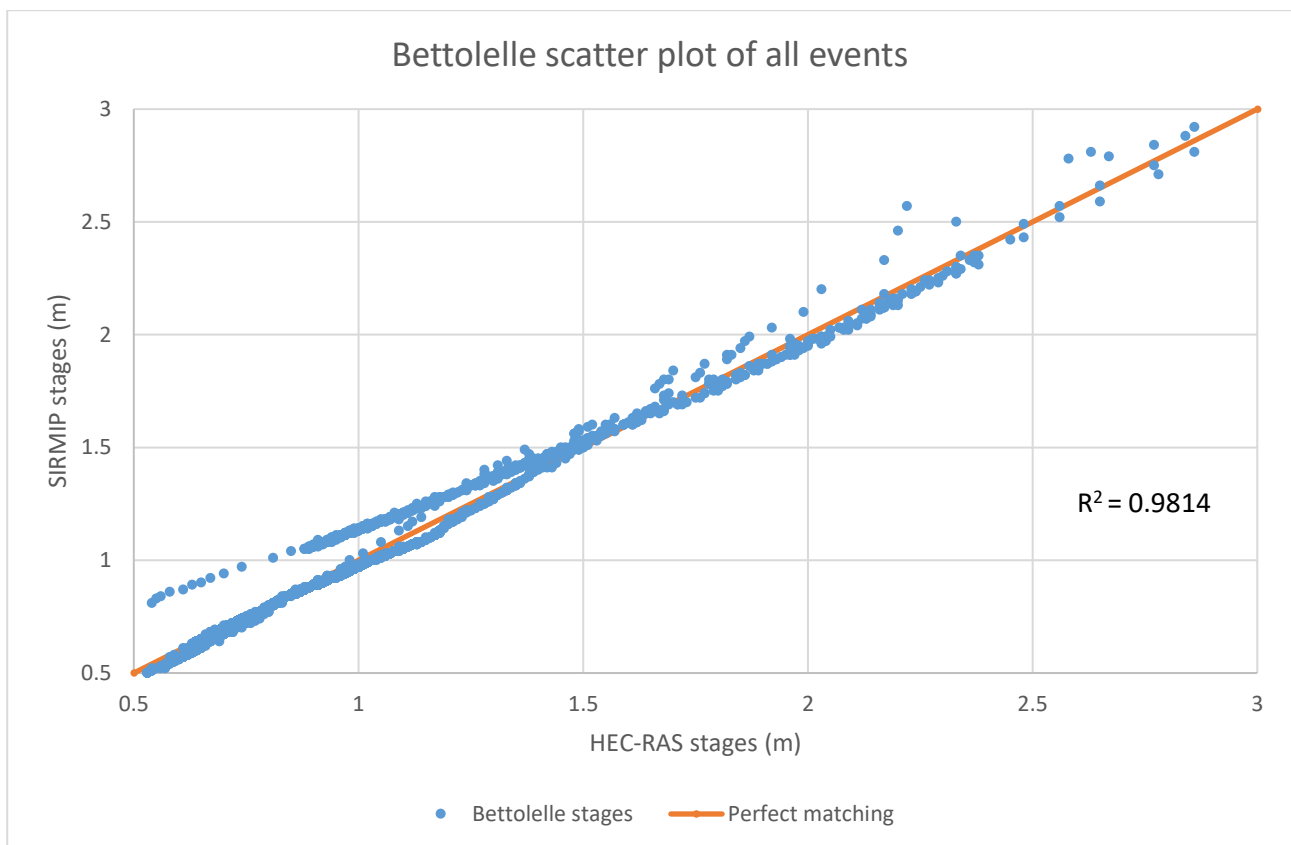


Figure 100. Scatter plot at Bettollelle cross-section for the tested events.

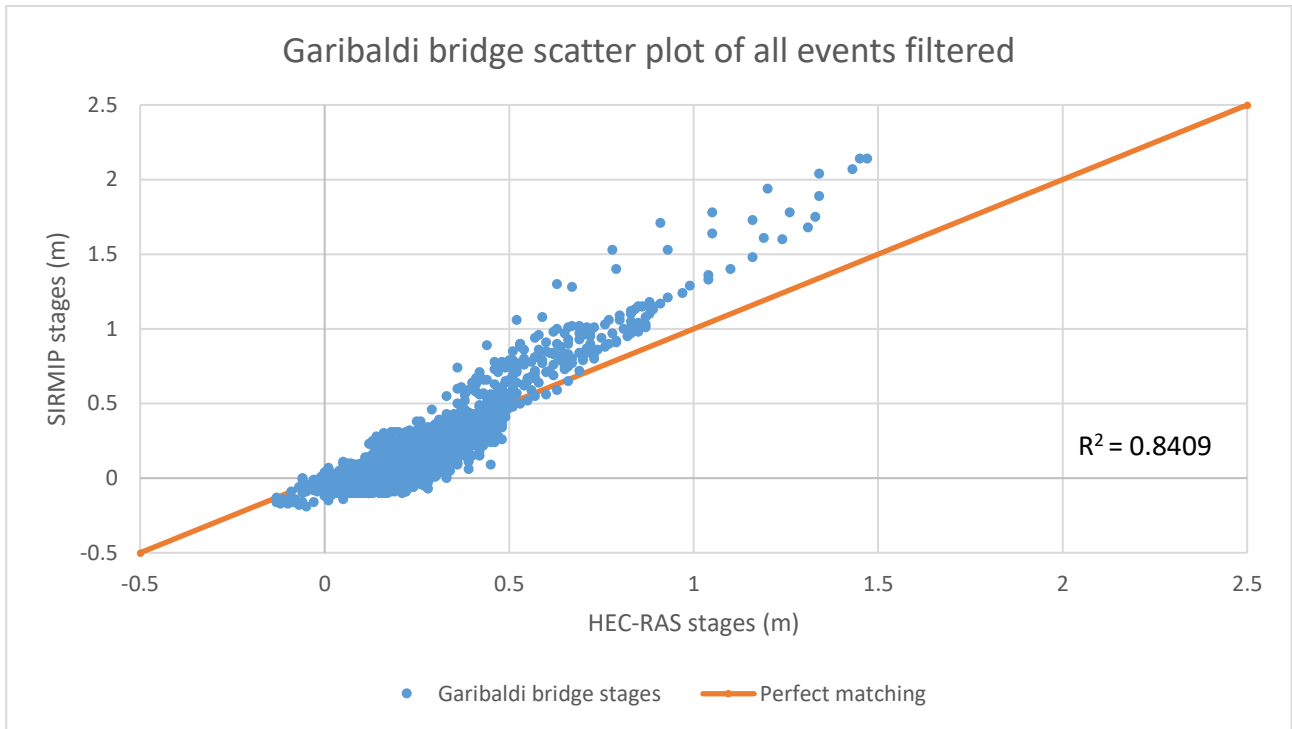


Figure 101. Scatter plot at Ponte Garibaldi cross-section for the tested events.

For what regards the Bettolle scatter plot, it is possible to notice a very good matching between the measured and the simulated water stages. Only the data belonging to low flow conditions deriving from the February 18th – March 5th 2018 event slightly differ from the SIRMIP stages, lowering the coefficient of determination which, in any case, presents a value close to 1.

The Ponte Garibaldi cross-section scatter diagram has been realized by removing the SIRMIP data characterized by a flat trend, being such data meaningless in this regard due to the probable presence of bed forms or submerged objects (e.g. branches) in correspondence of the sensor. The plot displays an overall good agreement between the measured and the simulated water elevations, although the coefficient of determination results to be lower than 1 mainly due to differences at the peak conditions provoked by the runoff contribution existing between Bettolle and Ponte Garibaldi and not accounted for by the software, as well as the uncertain validity of the rating curves used at Bettolle for large discharges.

7 CONCLUSIONS

This thesis focused on the construction and the subsequent calibration of a hydraulic model of the Misa River. To that end, a project characterized by the use of cross-sections belonging to the Civil Protection of the Marche Region dated back to 2001, was constructed with the aim at running a preliminary steady simulation, since this kind of analysis is the easiest to perform. Afterwards, in order to deal with a more reliable and updated project, more recent Bettollele and Ponte Garibaldi cross-sections dated back to 2019 were implemented into the software. Considering that the survey relative to the Bettollele 2019 cross-section was not complete, missing the levees, these have been reconstructed. With the updated river geometry, different simulations belonging to different time periods were performed by imposing a flow hydrograph as upstream boundary condition and a stage hydrograph representing the tidal motion, as downstream boundary condition. Since the data coming from the simulations showed a significant difference in correspondence of the peaks if compared to the SIRMIP ones, two “specific discharge vs area of the basin” graphs relative to both the annual average discharges and the maximum discharges of three river stations belonging to the same basin of the Misa River, were carried out. However, since the analyses were performed by accounting only for a limited number of years, the results deriving from these tests have provided just a rough estimation of the possible surface runoff, which therefore does not help in the interpretation of the comparison. Discharge data relative to the Senigallia wastewater treatment plant, received by the Viva Servizi S.P.A., were analyzed, showing a negligible contribution of the latter in increasing the river stages. In order to deal with a more robust hydraulic model, different digital terrain models dated back to 2008 coming from the Ministero dell’Ambiente e della Tutela del Territorio e del Mare were worked out with the goal of being implemented into the software. Considering that the Lidar technique was not capable of correctly identifying the bathymetry of the last stretch of the river, bathymetric surveys were employed. Given that the simulations results deriving from the 2D hydraulic model turned out to be the most accurate, the calibration procedure was conducted by relying on this model. Firstly, in order to compare the results coming from HEC-RAS with the SIRMIP ones, the thalweg of the cross-section was selected as reference system for the Bettollele cross-section while, for the Ponte Garibaldi cross-section, the selected reference system was the average sea level. The calibration was carried out by acting on different parameters, among which the Manning coefficients. To correctly implement these coefficients, the levees and the main channel banks were set for each simulation, since, characterizing the extension of both the main channel and the floodplains, they are linked to the roughness. In relation to both the period and the event, the Manning coefficients which provided the best correlation between the measured and the simulated stage values go from 0.025 to 0.2. Taking into account that the studied river stretch is characterized

by the presence of different bridges, the contraction/expansion coefficients were added into the model in correspondence of the latter, with a value of 0.3 for the contraction and 0.5 for the expansion. With the model calibrated, the results coming from the simulations show a very good agreement between the HEC-RAS and the SIRMIP stages which is highlighted by a correlation coefficient of 0.9814. For what concerns the Ponte Garibaldi cross-section, it is possible to notice a good matching between the measured and the simulated stage values in the case of low flow conditions, showing that in low-flow conditions the river dynamics are primarily driven by the tidal motion. In the presence of precipitations, however, the model provides results which are underestimated in correspondence of the peaks. This behavior may be justified by the potential unsuitability of the rating curve for large flow rates and by the lack of implementation of the surface runoff into the model, since the last stretch of the river is characterized by a strongly urbanized area which leads to high runoff coefficient values. In any case it is possible to confirm that for high flows the river discharges overwhelm the tidal motion. The calibrated model has been used in another thesis work to carry out an analysis relative to the influence of the sea actions on the river dynamics when river mouth bars exist, these being occasionally present within the estuarine region of the Misa River (Ilari, 2021).

8 REFERENCES

Anitori L., *Analysis of the Misa River watershed and numerical simulations of the river hydrodynamics during low – and high-flow conditions*, 2018/2019. Università Politecnica delle Marche.

Brocchini M., Calantoni J., Postacchini M., Sheremet A., Staples T., Smith J., Reed A., Edwards F., Braithwaite III, Lorenzoni C., Russo A., Corvaro S., Mancinelli A., Soldini L., 2017. *Comparison between the wintertime and summertime dynamics of the Misa River estuary*.

Consorzio di Bonifica delle Marche. *Relazione bacino idrografico del fiume Misa*. Dicembre 2019.

Ilari M., *Hydrodynamic modeling of the final reach of the Misa River (Senigallia, Italy): the role of sea action and bed forms*, 2020/2021. Università Politecnica delle Marche.

McLusky, D. S.; Elliott, M. (2004). *The Estuarine Ecosystem: Ecology, Threats and Management*. New York: Oxford University Press.

Melito L., Postacchini M., Sheremet A., Calantoni J., Zitti G., Darvini G., Penna P., Brocchini M., 2020. *Hydrodynamics at a microtidal inlet: Analysis of propagation of the main wave components*.

Newsletter bimestrale Cluster Big, 22 Febbraio 2021. *Il progetto MORSE a Senigallia: monitoraggio di lungo periodo della zona costiera-estuarina-fluviale*.

Postacchini M., Melito L., Sheremet A., Calantoni J., Darvini G., Corvaro S., Memmola F., Penna P., Brocchini M., 2020. *Upstream Propagating Long-Wave Modes at Microtidal River Mouth*.

Pritchard, D. W. (1967). "*What is an estuary: physical viewpoint*". In Lauf, G. H. (ed.). *Estuaries*. A.A.A.S. Publ. **83**. Washington, DC. pp. 3–5.

Regione Marche – Servizio Protezione Civile SIRMIP ON-LINE. *Sistema Informativo Regionale Meteo-Idro-Pluviometrico*.

Tratto da SIRMIP: <http://app.protezionecivile.marche.it/sol/indexjs.php?lang=it>.

US Army Corps of Engineers Institute for Water Resources Hydrologic Engineering centre, HEC-RAS Reference Manual, Version 5.0. February 2016.

US Army Corps of Engineers Institute for Water Resources Hydrologic Engineering centre, HEC-RAS User's Manual, Version 5.0. February 2016.

Wikipedia, The Free Encyclopedia, *Estuary*. <https://en.wikipedia.org/wiki/Estuary>.

9 ACKNOWLEDGEMENTS

I wish first of all to express my warmest thanks to my parents, Lorella and Claudio, and to my girlfriend Silvia, for always having supported me through my university course, trusted me and helped me to overcome all the difficult moments, making me believe in myself.

Special thanks go to my colleague Marco, with who I shared the realization of this work and to my professors, for having guided me in writing my thesis and for having succeeded in increasing my interest in the taught subjects.

Additional thanks are reserved to the Viva Servizi S.P.A. and in particular to Mr. Maurizio Pieroni for the willingness shown in sharing the wastewater treatment plant data, to the Civil Protection of the Marche Region and its referents for having provided cross-sections, discharge and stage data, and to the MORSE project for the data relative to the H-ADCP.